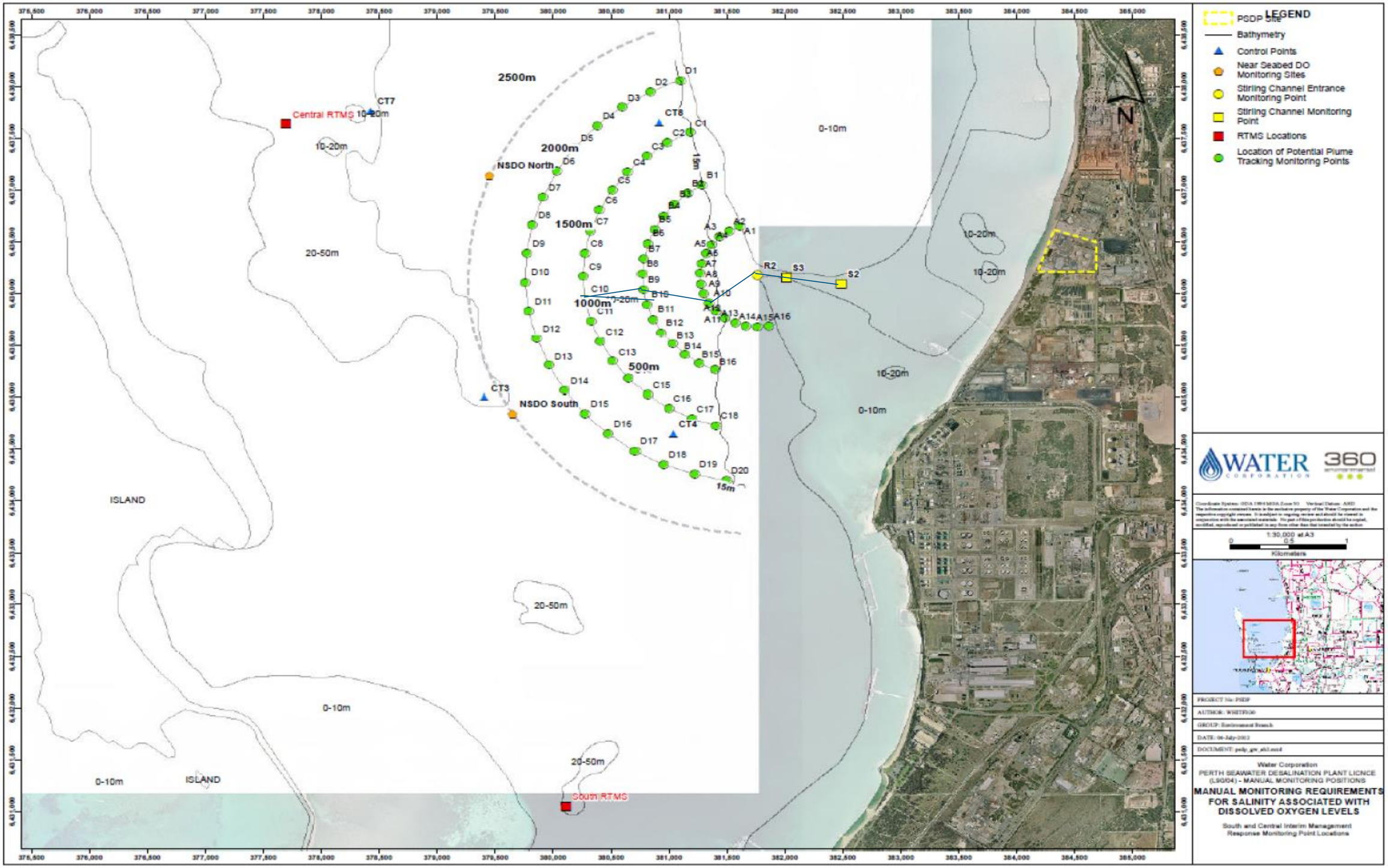

Figure 3-25 Locations at which simulated profile data were sampled to produce the curtain transects. Location were the same as the those identified in MMMP (Water Corporation 2013).

Discharge signatures

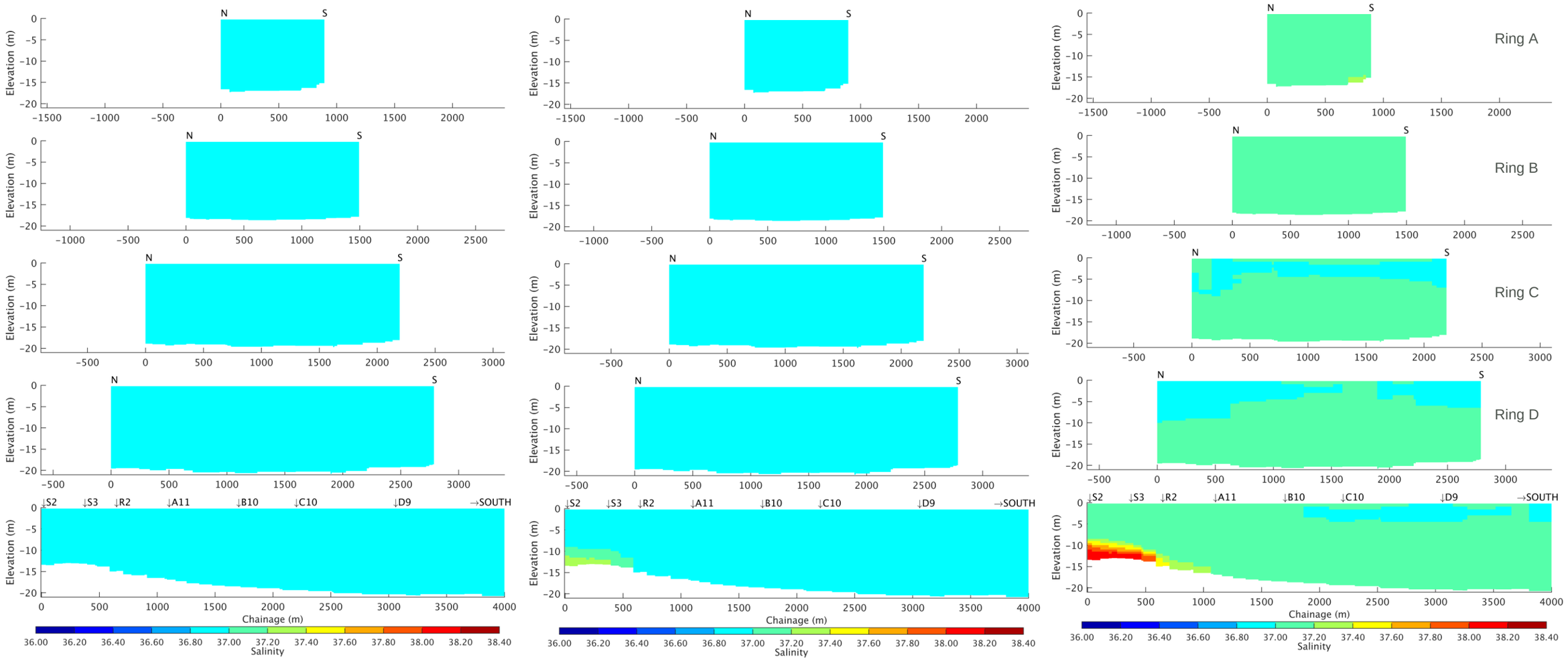

Figure 3-26 Curtain plots of median salinity at increasing distances from the discharge location for ambient conditions in Feb-Mar 2008. Left panel: Scenario 1A noDESAL. Centre panel: Scenario 1A. Right panel: Scenario 2A.

Discharge signatures

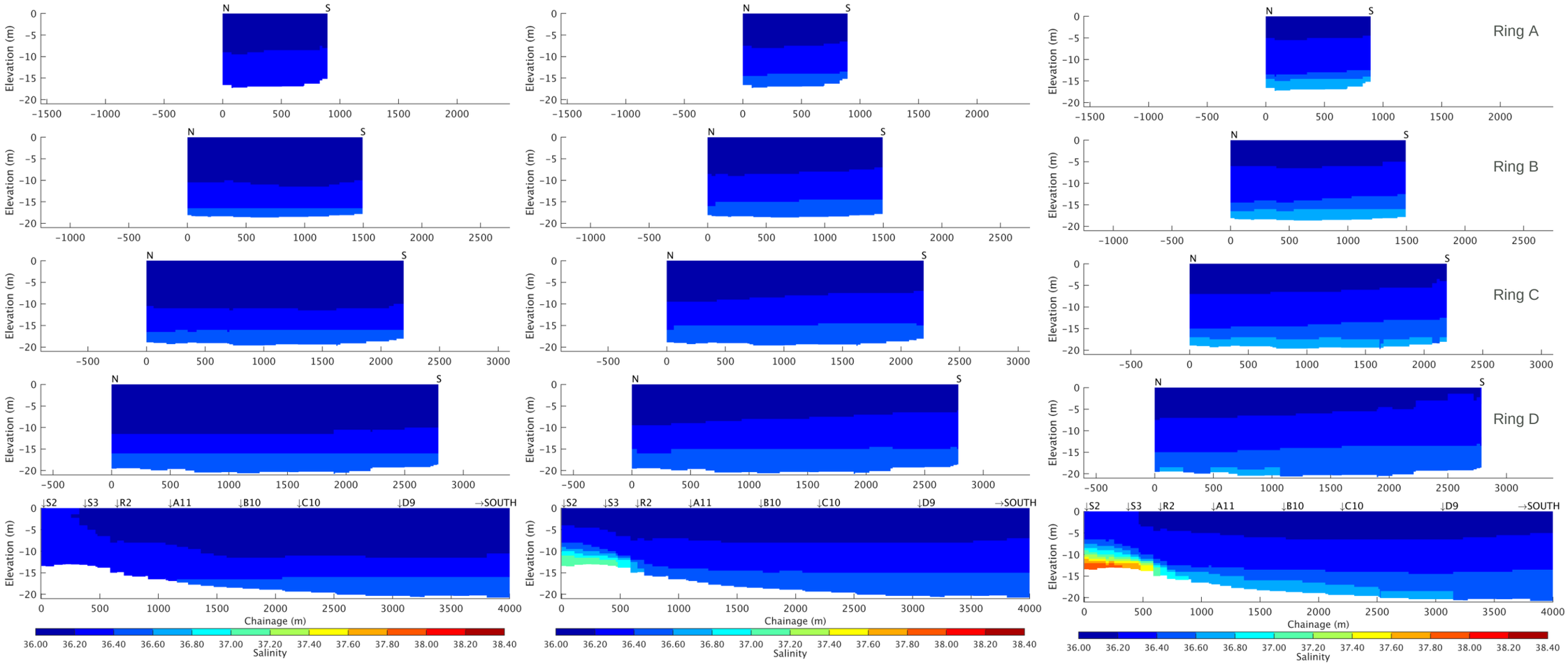

Figure 3-27 Curtain plots of median salinity at increasing distances from the discharge location for ambient conditions in Apr 2013. Left panel: Scenario 1A noDESAL. Centre panel: Scenario 1A. Right panel: Scenario 2A.

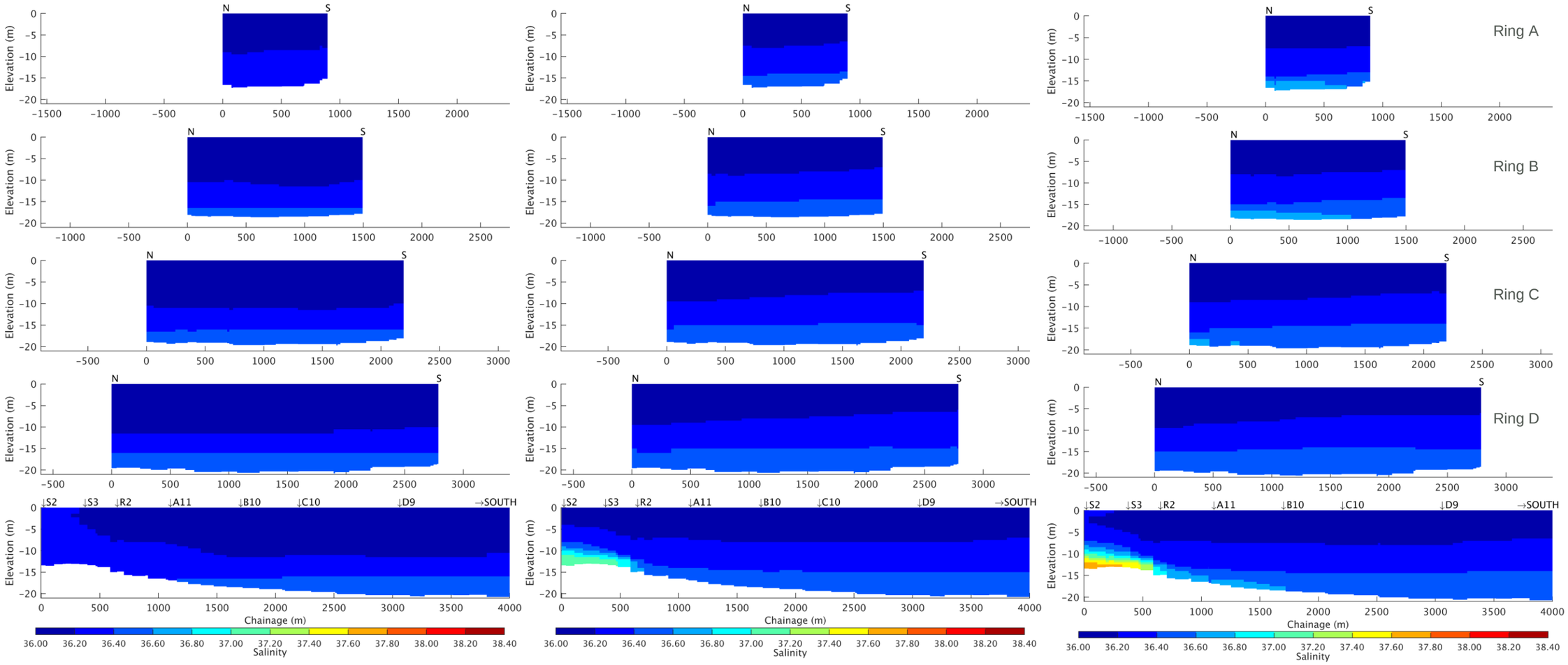

Figure 3-28 Curtain plots of median salinity at increasing distances from the discharge location for ambient conditions in Apr 2013. Left panel: Scenario 1A noDESAL. Centre panel: Scenario 1A. Right panel: Scenario 2C.

The median for scenario 1A noDESAL in Feb-Mar 2008 ambient condition presented no salinity stratification (Figure 3-26), whilst the Apr-2013 (Figure 3-26) displayed some level of salinity stratification, which reflects the less favourable mixing conditions over the periods. The 2013 period also showed relatively lower salinity in comparison to 2008.

For the desal scenarios (1A, 2A and 2C), the two simulated periods exhibited higher salinities within the confinements of Stirling Channel. Contrastingly, as the plumes inserted further into the deep basin, their salinity approached the scenario 1A noDESAL baseline levels. Inside the channel the thickness of the plume was between 5 and 6 metres. The interface at the plume was also much sharper for scenario 2A in comparison to scenarios 1A and 2C.

Differences between the simulated ambient conditions and desalination scenarios were at times marked. For example, once in the deep basin the thickness of the plumes, as displayed by the median salinity, reduced and indicated a shorter incursion into the deep basin with the improved mixing conditions in Feb-Mar 2008 (Figure 3-26). Whilst the median salinity plume was generally arrested within 1000 m of the channel exit (i.e. ~Ring B) for scenario 1A, conditions for Scenario 2A show the plume between 1500 m (Feb-Mar 2008, Figure 3-26) from the channel exit to approximately 2,300 m (Apr 2013, Figure 3-27). The salinity increases were however relatively small, of the order of 0.2 or less. Scenario 2C in April 2013 showed a less sharp interface and smaller incursions than Scenario 2A to approximately 800 m from the channel exit.

3.3.2 Temperature

To illustrate the temperature discharge signatures, the approach adopted was also to compare the results from simulations including the PSDP discharges (i.e. scenarios 1A, 2A and 2C) with simulations without any of the PSDP discharges (i.e. scenarios 1A noDESAL). To this effect, contour maps and timeseries are presented. Again, note that Scenario 2C results are only available for the Apr 2013 and Autumn 2008 simulation periods.

3.3.2.1 Contour Maps

Contour maps were based on point to point difference between the discharge scenario (1A, 2A and 2C) to the baseline (1A noDESAL) simulations. Similarly to salinity, the median depth-averaged temperatures were calculated between 0.0 and 0.5m from the seabed for all the scenarios. The differences between the discharge scenarios and the baseline were then mapped. Temperature increase contour lines (varying between each season) were then obtained and mapped where applicable. The maps for the different simulation periods are shown in Figure 3-29 to Figure 3-42.

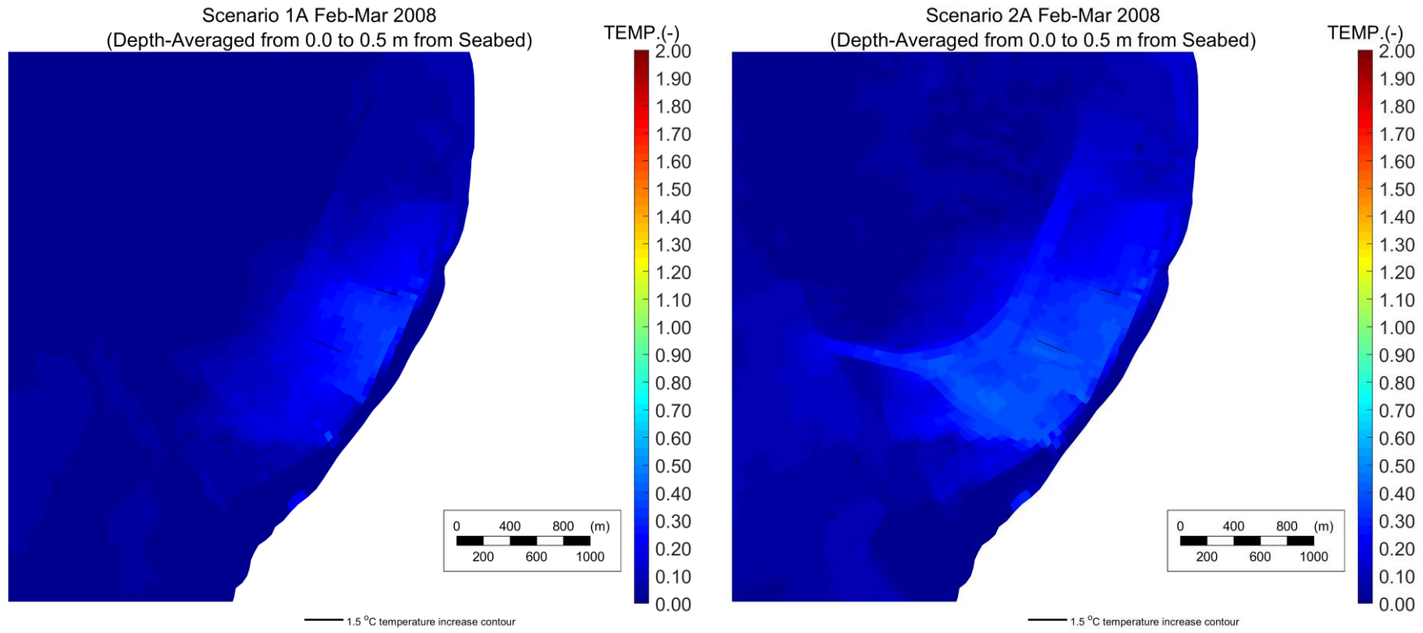

Figure 3-29 Median temperature increases with respect to the baseline (Scenario 1A noDESAL) for ambient conditions in Feb-Mar 2008. Left panel: Scenario 1A. Right panel: Scenario 2A. The thick black contour line (if applicable) shows the 1.5°C temperature increase contour. The thin black lines show the PSDP1 and PSDP2 diffuser locations.

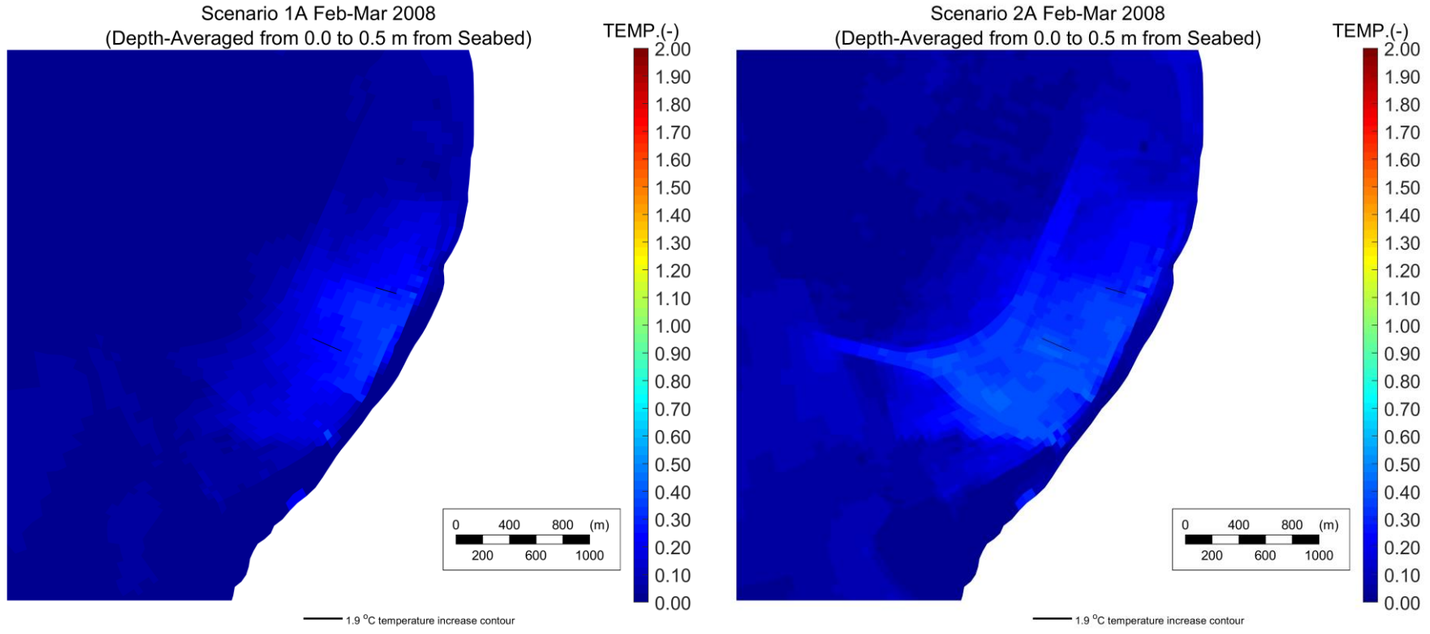

Figure 3-30 Median temperature increases with respect to the baseline (Scenario 1A noDESAL) for ambient conditions in Feb-Mar 2008. Left panel: Scenario 1A. Right panel: Scenario 2A. The thick black contour line (if applicable) shows the 1.9°C temperature increase contour. The thin black lines show the PSDP1 and PSDP2 diffuser locations.

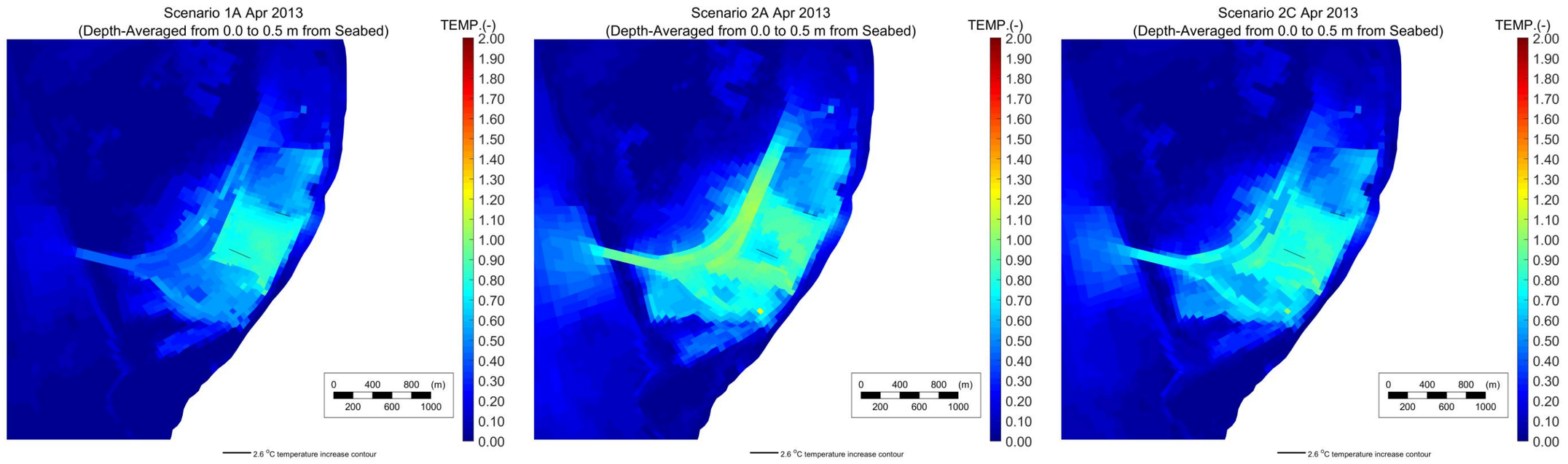

Figure 3-31 Median temperature increases with respect to the baseline (Scenario 1A noDESAL) for ambient conditions in Apr 2013. Left panel: Scenario 1A. Centre panel: Scenario 2A. Right panel: Scenario 2C. The thick black contour line (if applicable) shows the 2.6°C temperature increase contour. The thin black lines show the PSDP1 and PSDP2 diffuser locations.

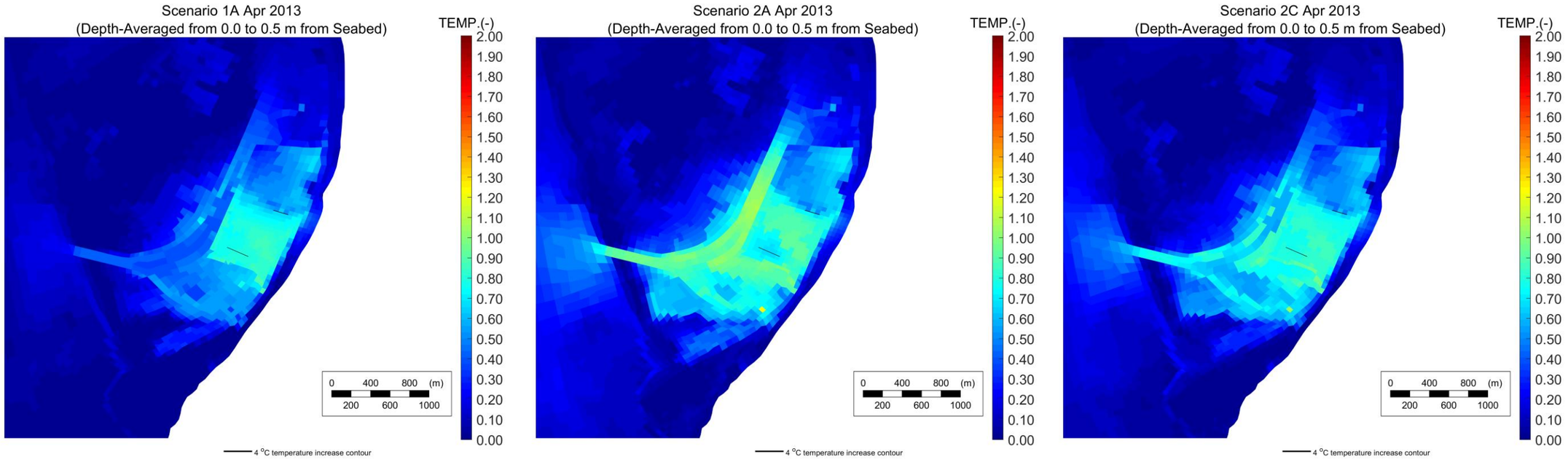

Figure 3-32 Median temperature increases with respect to the baseline (Scenario 1A noDESAL) for ambient conditions in Apr 2013. Left panel: Scenario 1A. Centre panel: Scenario 2A. Right panel: Scenario 2C. The thick black contour line (if applicable) shows the 4.0°C temperature increase contour. The thin black lines show the PSDP1 and PSDP2 diffuser locations.

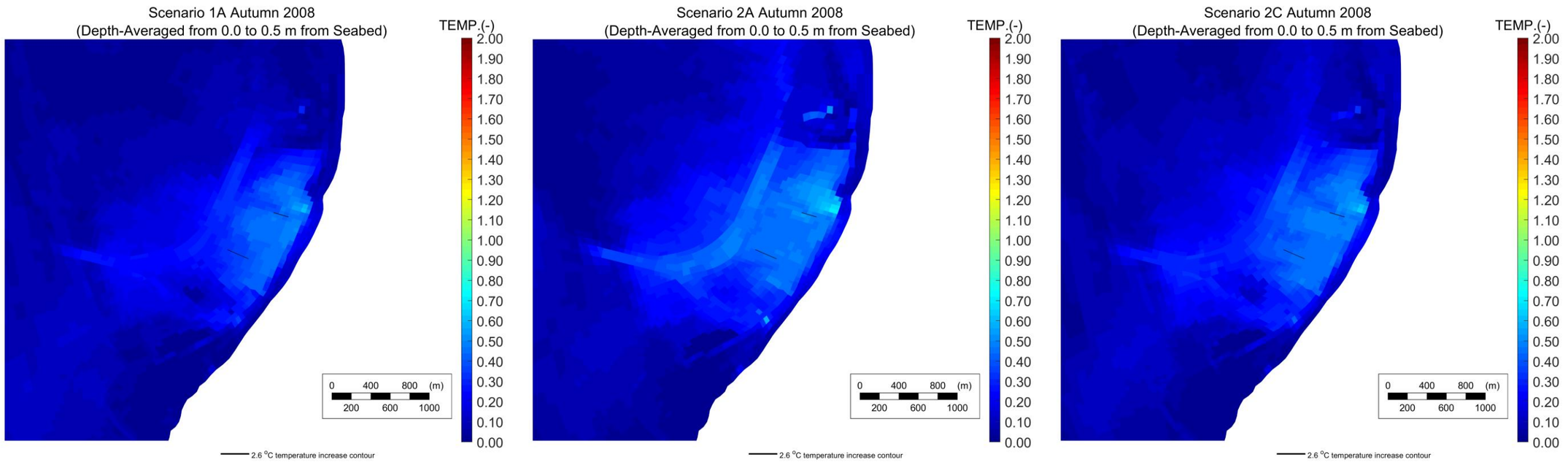

Figure 3-33 Median temperature increases with respect to the baseline (Scenario 1A noDESAL) for ambient conditions in Autumn 2008. Left panel: Scenario 1A. Centre panel: Scenario 2A. Right panel: Scenario 2C. The thick black contour line (if applicable) shows the 2.6°C temperature increase contour. The thin black lines show the PSDP1 and PSDP2 diffuser locations.

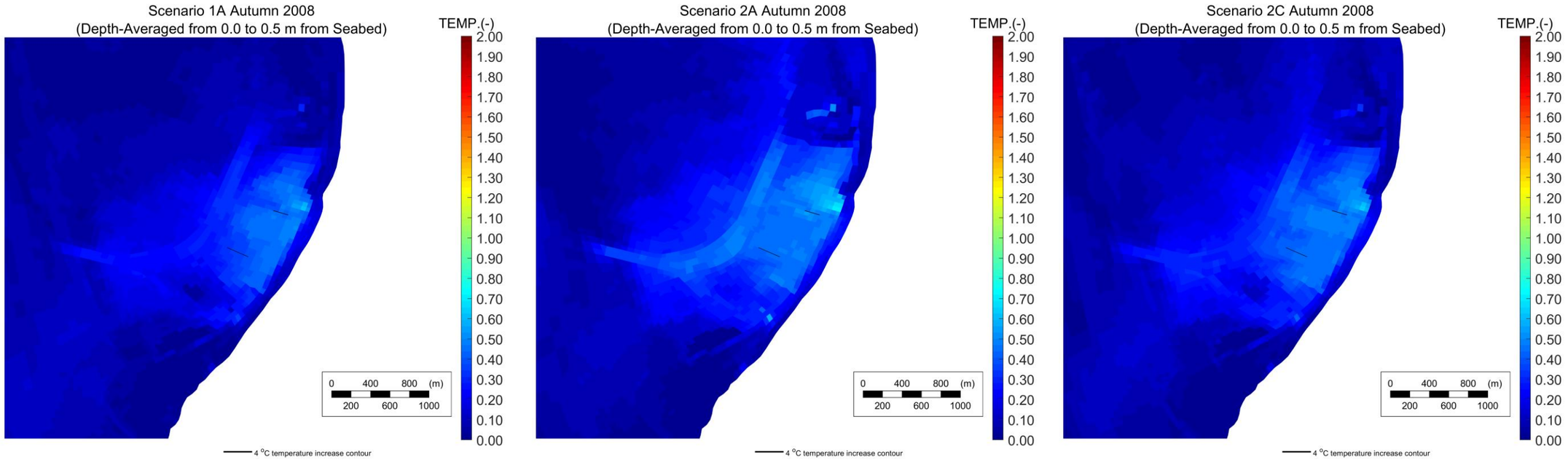

Figure 3-34 Median temperature increases with respect to the baseline (Scenario 1A noDESAL) for ambient conditions in Autumn 2008. Left panel: Scenario 1A. R Centre panel: Scenario 2A. Right panel: Scenario 2C. The thick black contour line (if applicable) shows the 4.0°C temperature increase contour. The thin black lines show the PSDP1 and PSDP2 diffuser locations.

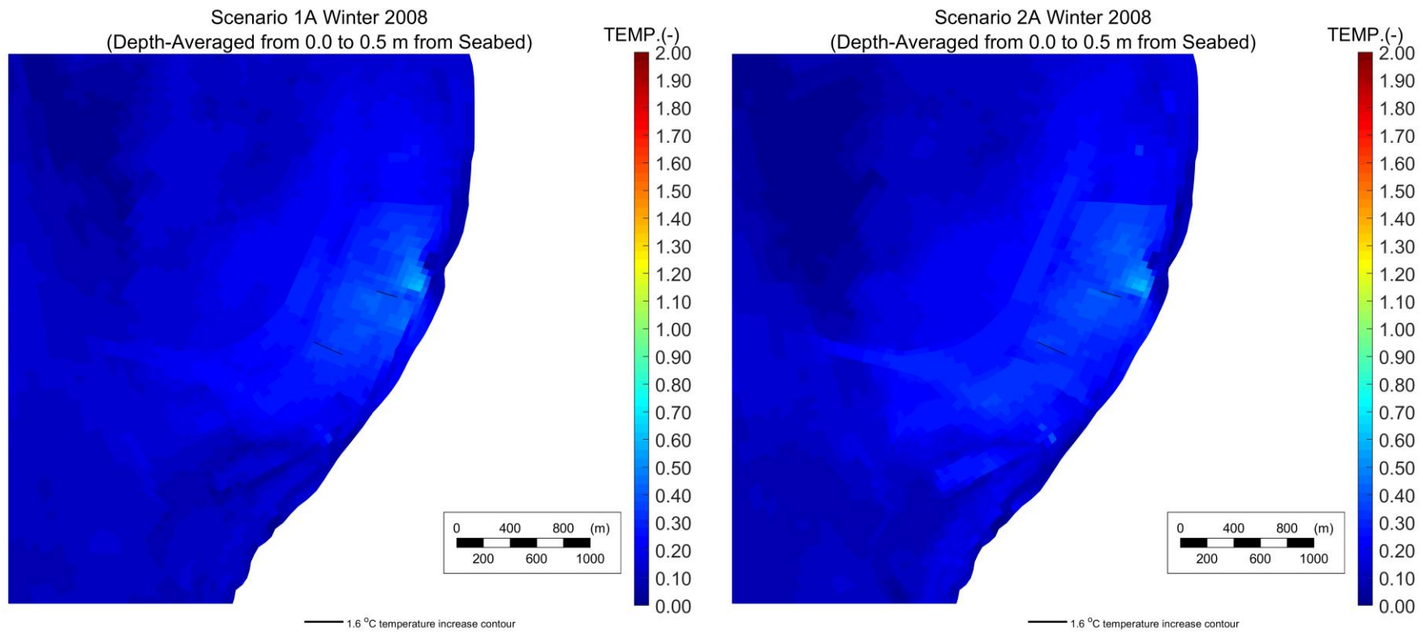

Figure 3-35 Median temperature increases with respect to the baseline (Scenario 1A noDESAL) for ambient conditions in Winter 2008. Left panel: Scenario 1A. Right panel: Scenario 2A. The thick black contour line (if applicable) shows the 1.6°C temperature increase contour. The thin black lines show the PSDP1 and PSDP2 diffuser locations.

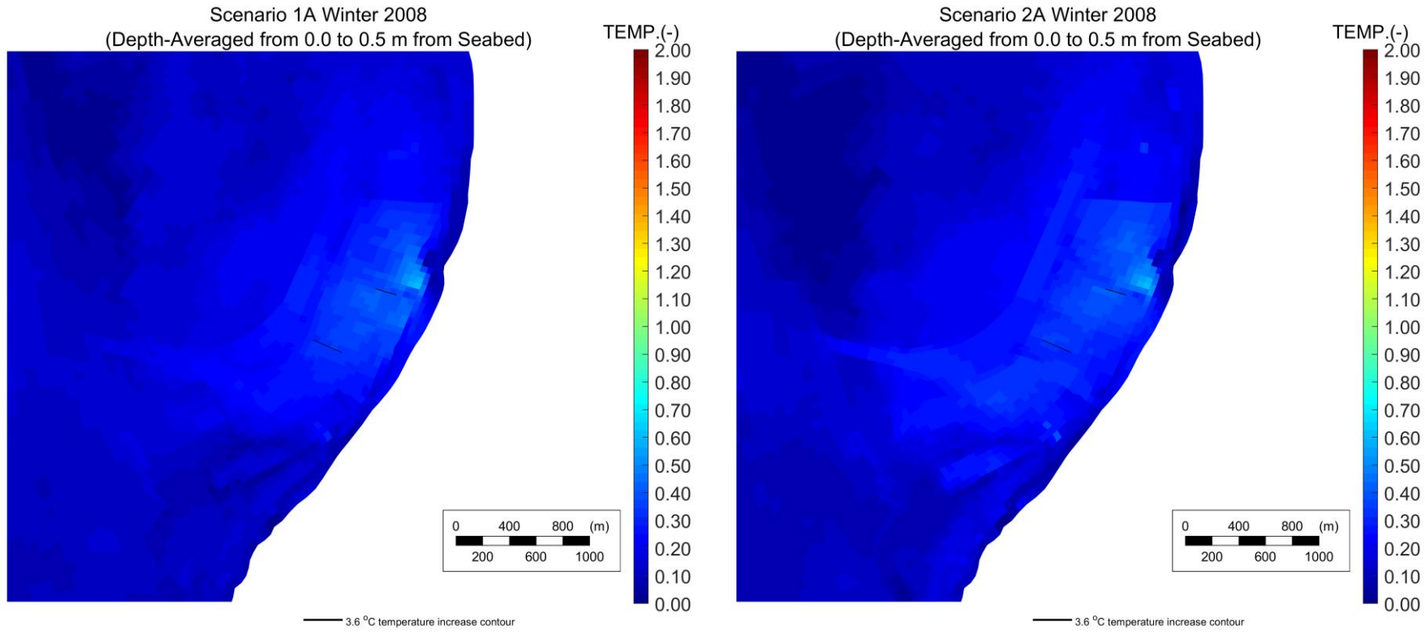

Figure 3-36 Median temperature increases with respect to the baseline (Scenario 1A noDESAL) for ambient conditions in Winter 2008. Left panel: Scenario 1A. Right panel: Scenario 2A. The thick black contour line (if applicable) shows the 3.6°C temperature increase contour. The thin black lines show the PSDP1 and PSDP2 diffuser locations.

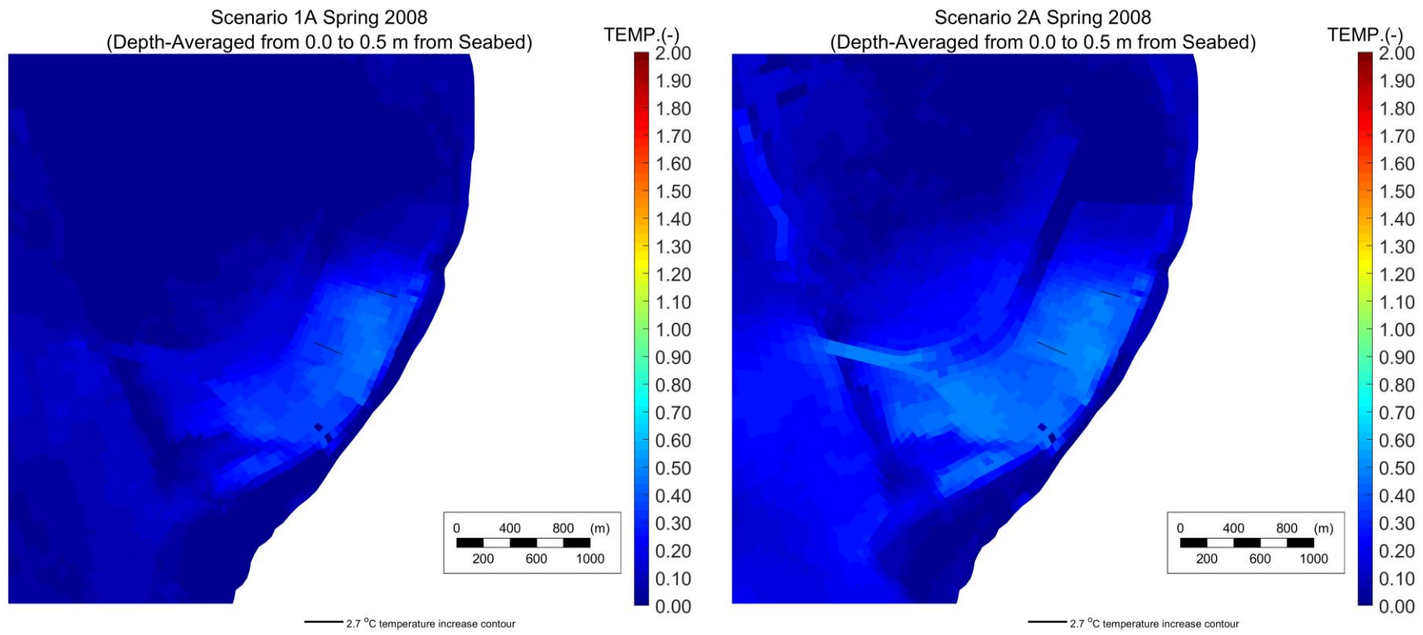

Figure 3-37 Median temperature increases with respect to the baseline (Scenario 1A noDESAL) for ambient conditions in Spring 2008. Left panel: Scenario 1A. Right panel: Scenario 2A. The thick black contour line (if applicable) shows the 2.7°C temperature increase contour. The thin black lines show the PSDP1 and PSDP2 diffuser locations.

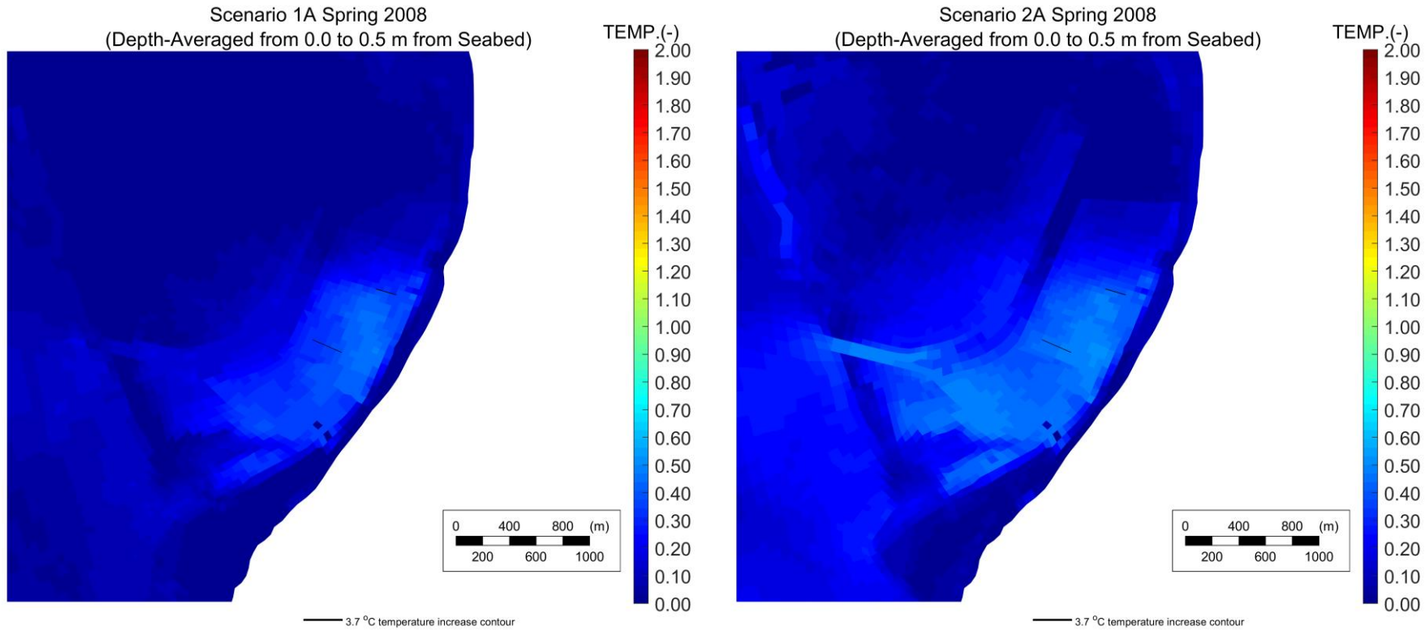

Figure 3-38 Median temperature increases with respect to the baseline (Scenario 1A noDESAL) for ambient conditions in Spring 2008. Left panel: Scenario 1A. Right panel: Scenario 2A. The thick black contour line (if applicable) shows the 3.7°C temperature increase contour. The thin black lines show the PSDP1 and PSDP2 diffuser locations.

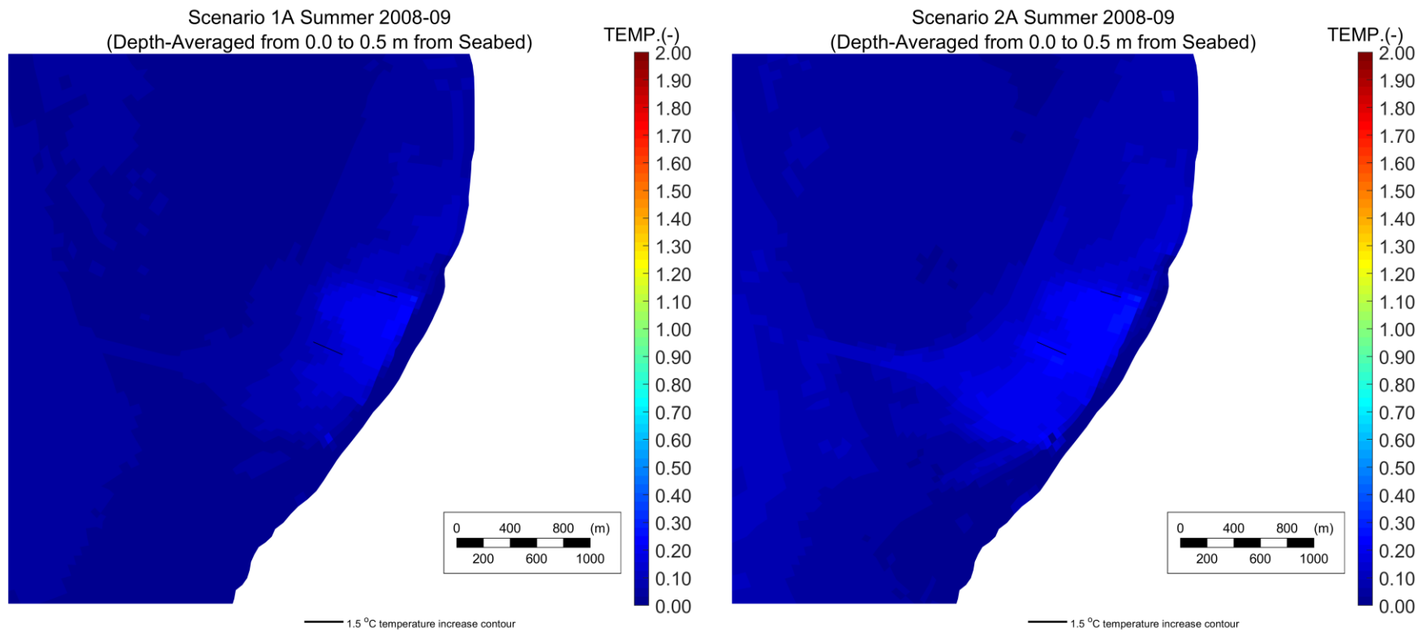

Figure 3-39 Median temperature increases with respect to the baseline (Scenario 1A noDESAL) for ambient conditions in Summer 2008. Left panel: Scenario 1A. Right panel: Scenario 2A. The thick black contour line (if applicable) shows the 1.5°C temperature increase. The thin black lines show the PSDP1 and PSDP2 diffuser locations.

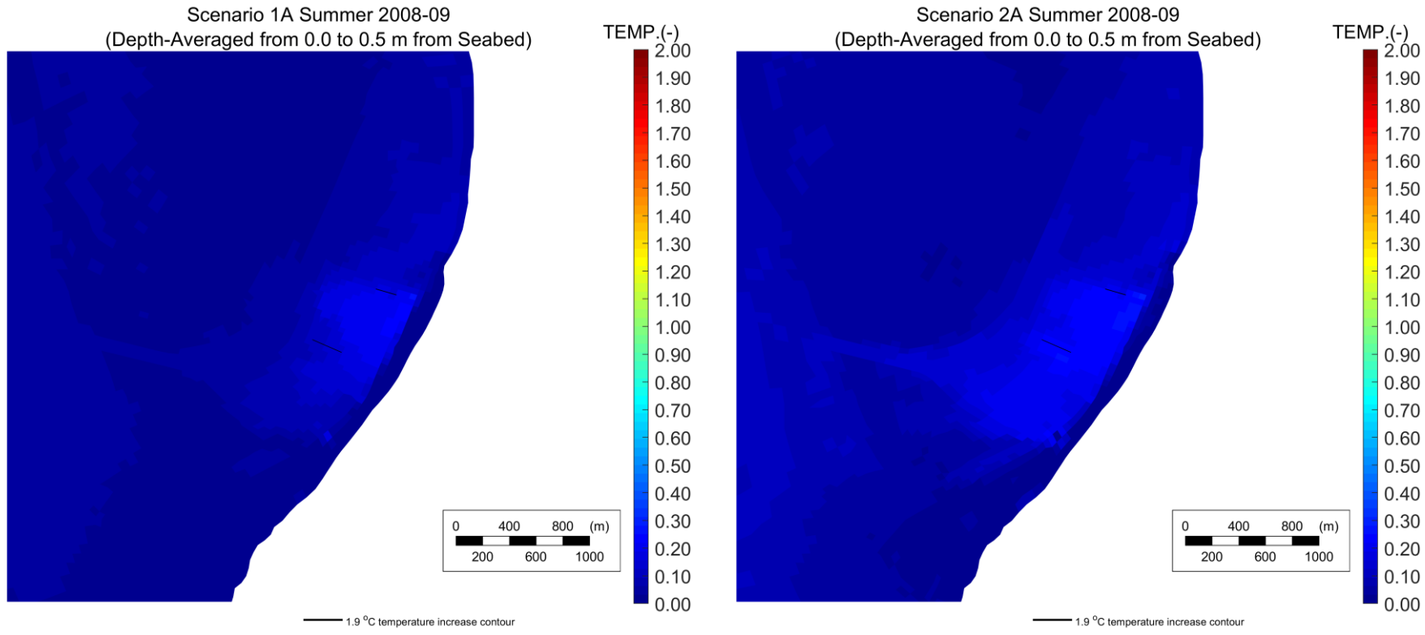

Figure 3-40 Median temperature increases with respect to the baseline (Scenario 1A noDESAL) for ambient conditions in Summer 2008. Left panel: Scenario 1A. Right panel: Scenario 2A. The thick black contour line (if applicable) shows the 1.9°C temperature increase contour. The thin black lines show the PSDP1 and PSDP2 diffuser locations.

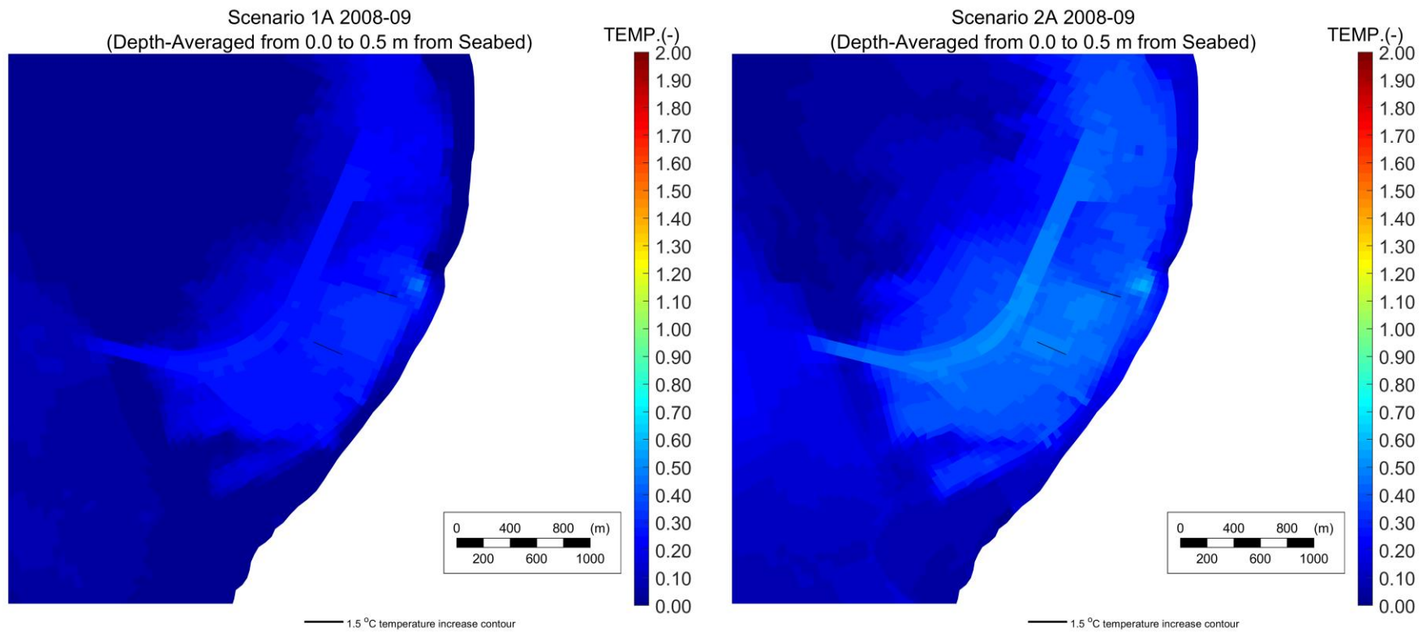

Figure 3-41 Median temperature increases with respect to the baseline (Scenario 1A noDESAL) for ambient conditions in Mar 2008 – Mar 2009. Left panel: Scenario 1A. Right panel: Scenario 2A. The thick black contour line (if applicable) shows the 1.5°C temperature increase contour. The thin black lines show the PSDP1 and PSDP2 diffuser locations.

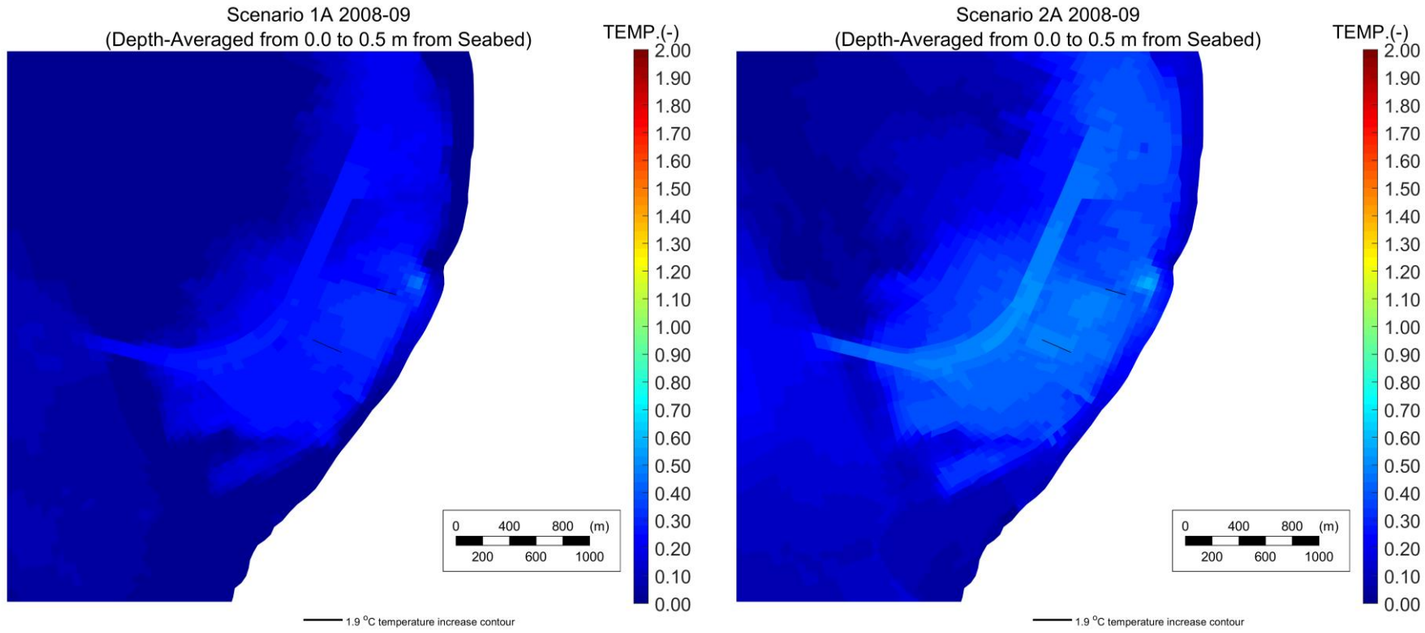

Figure 3-42 Median temperature increases with respect to the baseline (Scenario 1A noDESAL) for ambient conditions in Mar 2008 – Mar 2009. Left panel: Scenario 1A. Right panel: Scenario 2A. The thick black contour line (if applicable) shows the 1.9°C temperature increase contour. The thin black lines show the PSDP1 and PSDP2 diffuser locations.

From these contour maps, it was predicted that no significant increases to median temperature across the simulated periods and in general, median near bed temperature increases were below 1^{o}C across the entire model domain for all scenarios.

3.3.2.2 Timeseries

Similarly to salinity, near-surface (i.e. 0.5 m from the surface) and near bed (i.e. 0.5 m from the seabed) timeseries at the four locations in Figure 3-22 are presented to compare temporal variations in temperature across different scenarios. The difference between near surface and near bed temperature are also shown in these plots, so potential increases in temperature stratification duration and strength could be inspected.

Figure 3-43 Temperature timeseries comparisons for top and bottom waters at Perth Buoy North, Perth Buoy Central, Perth Buoy South and S2 (Feb-Mar 2008)

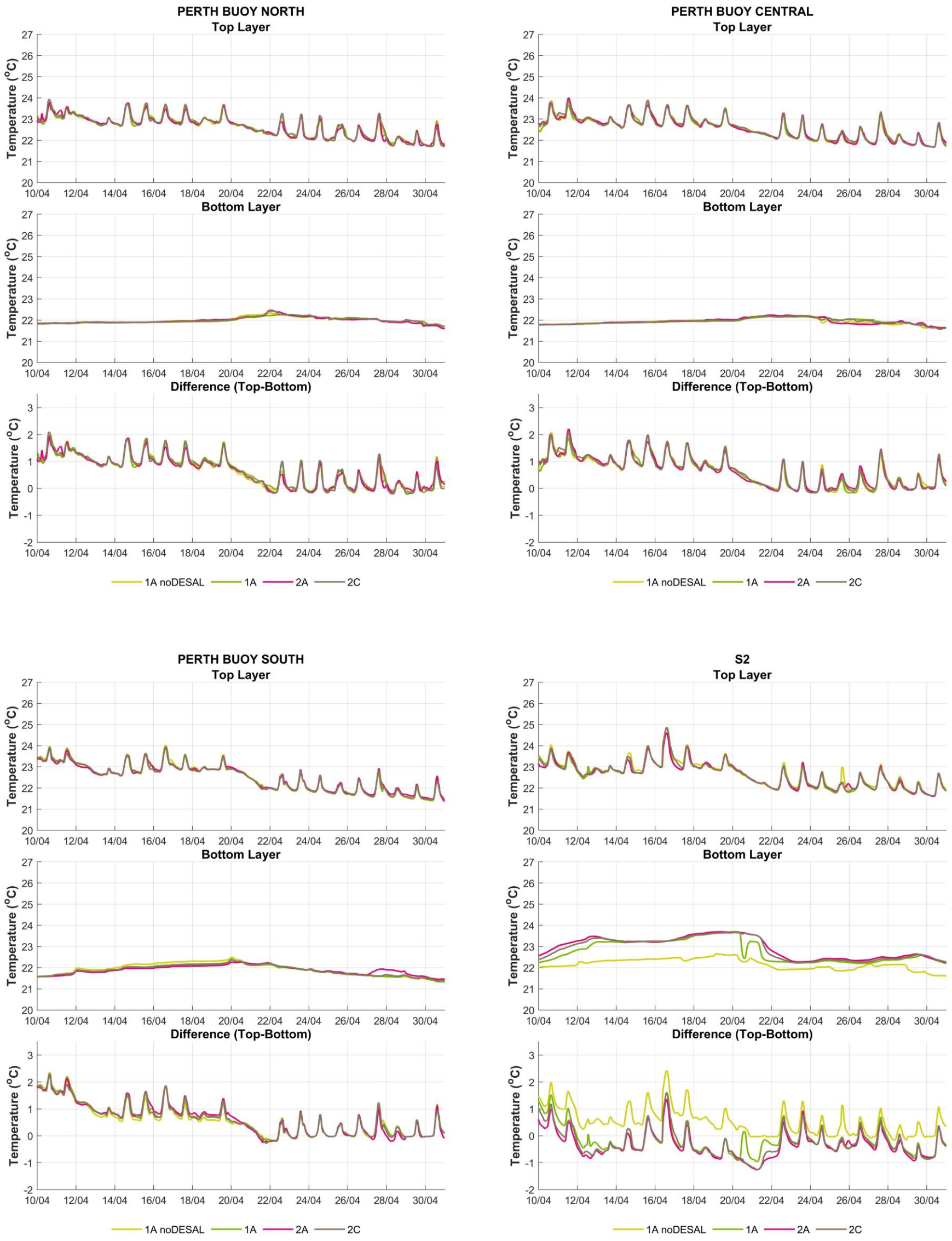

Figure 3-44 Temperature timeseries comparisons for top and bottom waters at Perth Buoy North, Perth Buoy Central, Perth Buoy South and S2 (Apr 2013)

3.3.2.2.1 February to March 2008

In the deep basin, increases in temperature were minimal in comparison to S2 and also between the discharge scenarios. As a result, the discharges induced little change to deep basin temperatures, resulting similarly in no appreciable changes to temperature stratification during this period.

S2 showed an increase in temperature above the baseline in the bottom waters for Scenario 1A (up to 0.8°C) and for Scenario 2A (up to 1.2°C). The increase in bottom temperature for both Scenario 1A and Scenario 2A resulted in periods where the temperature stratification was inverted (i.e. near bed temperatures higher than near surface temperatures). This occurred with more frequency and intensity in Scenario 2A, where salinity increases dominated density profiles (and allowed therefore temperature inversions to occur).

3.3.2.2.2 April 2013

In the deep basin, results were consistent with the Feb – Mar 2008 simulation showing modest temperature changes across discharge scenarios and sites. Results at S2 show an increase in bottom temperature for 1A, 2A and 2C in comparison to the baseline (up to 1°C). There was little difference in near bed temperatures for scenarios 1A, 2A and 2C. In some instances, an inversion in the temperature profile could again be observed at S2 (i.e. near bed temperatures higher than near surface temperatures), due to salinity dominating density.

3.3.2.2.3 March 2008 to March 2009

The temperature timeseries for each season are shown in Appendix B. Results for all periods were consistent with the results from the above simulations. The surface and near bed temperatures for Scenario 1A, 2A and 2C were comparable to the baseline for all deep basin locations.

Results at S2 showed there was little difference in surface water temperatures and some increases in near bed temperatures for both discharge scenarios in comparison to the baseline. The autumn and winter results showed a more substantial increase above the baseline for Scenario 1A and Scenario 2A (also Scenario 2C for autumn 2008) of up to 2°C. In comparison to the baseline, the near bed temperatures presented little increase for Spring and Summer 2008-09.

3.3.3 Effluent Tracer

The same numerical passive tracer was added to both PSDP1 and PSDP2 discharges at a concentration of 1 (arbitrary units). The tracer had no salinity, temperature or dissolved oxygen signature of its own, but simply acted as a tag to identify waters discharged from the PSDP1 and PSDP2 diffusers. The tracer was therefore distributed across the model domain around the diffuser along with the injected brine as a tag, using the nearfield linkage method described in BMT (2018a).

The tracer concentrations were then used for an analysis of the far field fate of the combined desalination plants' discharges and their potential for accumulation in Cockburn Sound. To this end, tracer fluxes across the northern entrance of the Sound and through the Causeway were extracted from model results along the lines shown in Figure 3-45. The fluxes were then integrated over time and compared to the total effluent fluxes from both diffusers. Doing so allowed an understanding of where the brine discharged from PSDP1 and PSDP2 travelled and its propensity, or otherwise, to accumulate within the Sound.

This analysis was undertaken for the simulation between March 2008 and March 2009 for Scenario 2A only.

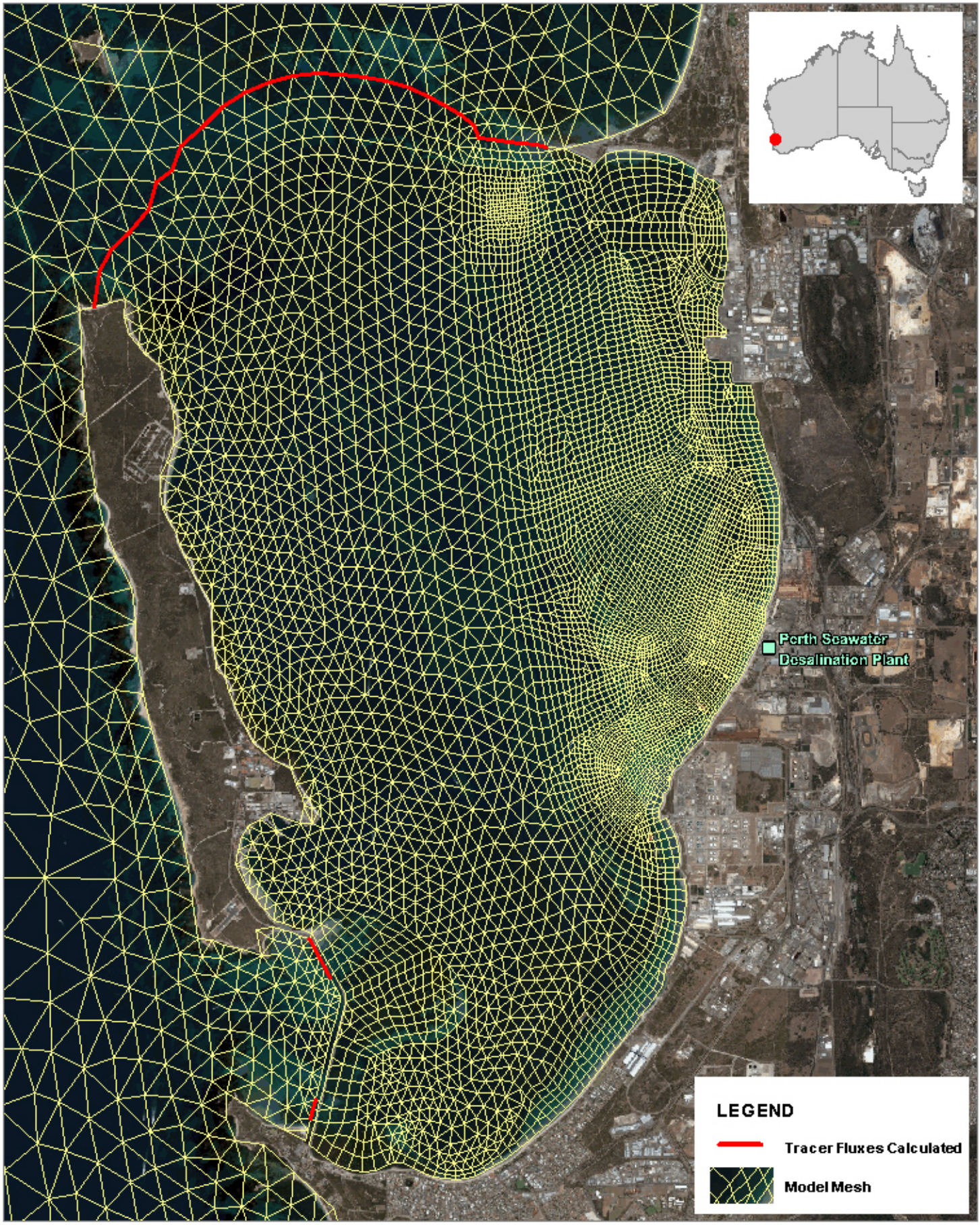

Title:

Lines across which tracer fluxes were calculated

Figure: 3-45

Rev: A

BMT endeavours to ensure that the information provided in this map is correct at the time of publication. BMT does not warrant, guarantee or make representations regarding the currency and accuracy of information contained in this map.

N

0 2 4km

Approx. Scale

BMT

www.bmt.org

Filepath: I:\B22253.I.meb.CockburnSound\DRG\CAR_062_181214_Lines_Tracer_Fluxes.wor

The mass flux across the northern entrance and the Causeway, as well as the corresponding combined mass exchange, are shown in Figure 3-46. The mass fluxes were also filtered using a 3-month moving-average window to remove the effect of short-term fluctuations and to therefore highlight seasonal trends.

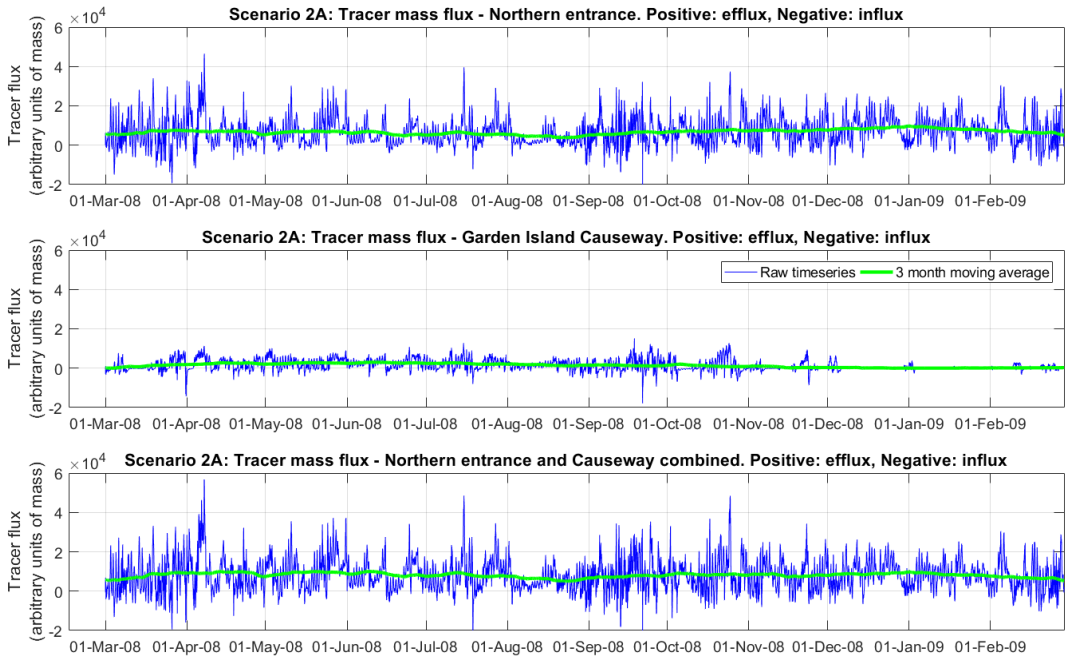

Figure 3-46 Tracer mass flux across Cockburn Sound boundaries

As expected, much of the tracer flux occurred across the northern entrance, as already highlighted in the previous work of DEP (1996) and D'Adamo (2002). Whilst the raw mass flux timeseries in Figure 3-46 shows short term instances in which they were negative (i.e. into the Sound), the fluxes were generally positive (i.e. out of the Sound). The 3-month moving-averaged series was always positive.

The combined mass flux across the Sound boundaries was also compared with the combined effluent mass flux from PSDP1 and PSDP2 (Figure 3-47). Note that the discharge flux was constant over the entire simulation period.

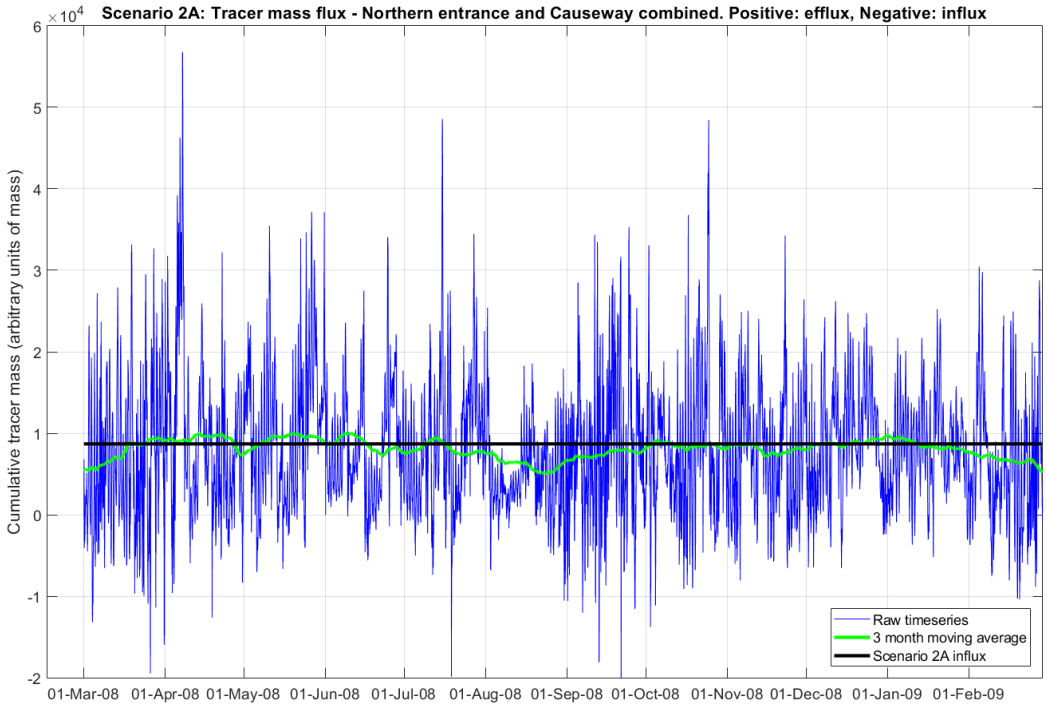

Figure 3-47 Combined tracer mass flux across Cockburn Sound boundaries and from PSDP1 and PSDP2 discharges

Whilst the combined raw flux timeseries at the Causeway and Northern entrance (blue line) fluctuated around the constant discharge fluxes, the moving average was generally approximately equal to the effluent flux. The reduced values in the tail ends of the moving average were not truly representative, as the averaging process was curtailed at both start and end of the series.

An exception to this approximate influx / efflux balance occurred around August 2008, where effluxes across the boundaries of Cockburn Sound were less than the combined PSDP influxes, for a sustained period. This was a period that coincided with the heaviest rainfall events in 2008 (see e.g. BMT 2018a). Thus, when rainfall is sufficiently large, freshwater flows are driven from the Swan River mouth towards Cockburn Sound (see e.g. D'Adamo 2002, BMT 2018a). As a result, these inflows momentarily arrest waters inside the Sound, and curtail efflux of the desalination plant brine.

The effect of this arrest on the cumulative tracer mass efflux (based on the raw time series) is illustrated in Figure 3-48. The figure shows that fluxes out of the Sound and from the desalination plant approximately balance each other throughout the simulation period (i.e. their cumulative totals overlay and are parallel). There is however, a brief reduction in the cumulative flux across the boundaries associated with the increased flows of the Swan River (as measured at Walyunga station in the figure) in August 2008. This is consistent with the Swan flows blanketing the Sound and constraining mixing and exchange. After approximately six weeks, the cumulative influx and efflux rates again align indicating a return to balance between the two (the red desalination plant cumulative influx line in the figure is duplicated and offset to illustrate this realignment). Therefore, with exception of times under increased influence of the Swan River flow, fluxes out of the Sound are predicted to balance the flux of effluent from the desalination plant discharges.

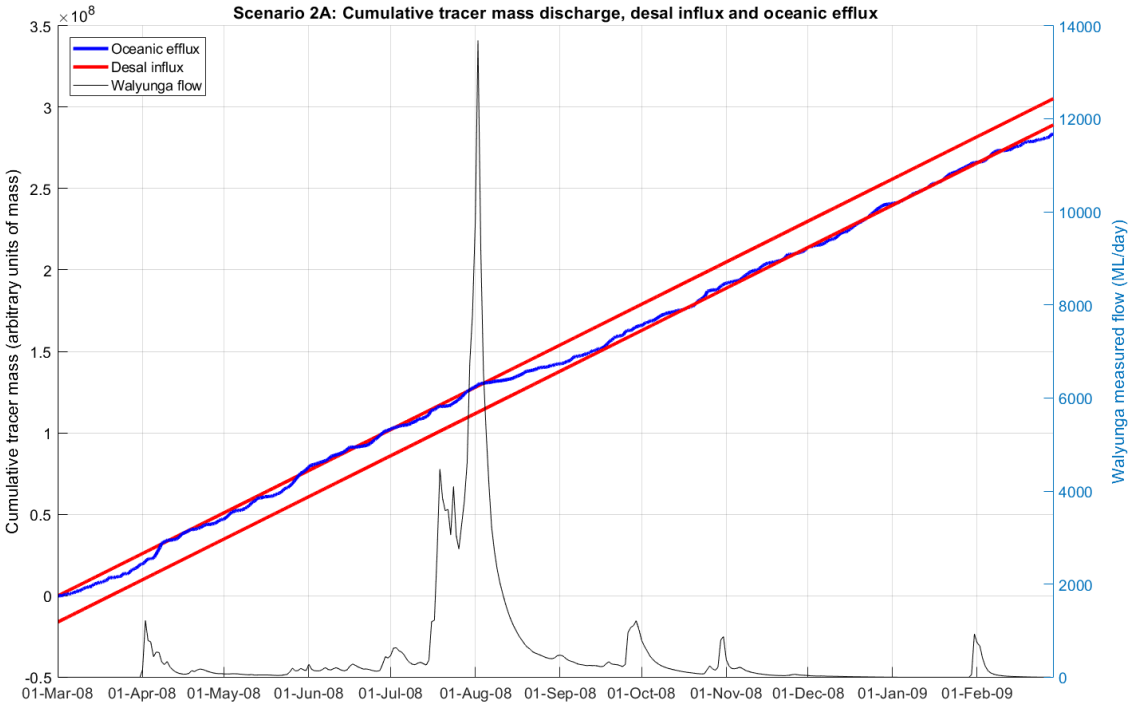

Figure 3-48 Cumulative tracer mass flux across Cockburn Sound boundaries and from PSDP1 and PSDP2 discharges. The lower desal influx line resets the effluent cumulative flux to same values of the boundary fluxes on 01 Dec 2008.

3.3.4 Dissolved Oxygen

To illustrate the discharges' DO signatures, maps of DO saturation and DO saturation occurrences were produced. In addition, timeseries of DO concentrations and DO saturation, as well as histograms of DO saturation occurrence were also prepared. Again, the processes adopted in the production of maps, timeseries and histograms were in line with requirements of environmental assessments. The production methods and results are presented below. Again, note that Scenario 2C results are only available for the Apr 2013 and Autumn 2008 simulation periods.

3.3.4.1 DO saturation contour maps

DO saturation contour maps were produced for both baseline and discharge scenarios. The maps were constructed to support environmental assessments according to the following procedure:

(1) The near bed (depth-averaged between 0 and 0.5 m from the bed) temperature, salinity and DO concentrations were obtained from the simulation results;

(2) DO saturation was then computed according to Riley and Skirrow (1974);

(3) Successive 7-day rolling medians were calculated for the DO saturation, discarding all DO saturation values between 18:00 and 06:00 of the subsequent day.

(4) The minimum of all the diurnal 7-day rolling medians (hereafter referred to as median only in the context of DO saturation) at each of the cell points was then mapped.

(5) Finally, contour lines were extracted for the 80% and 90% DO saturation levels.

The resultant median DO saturation maps are shown in Figure 3-49 to Figure 3-60 for each of the simulation periods.

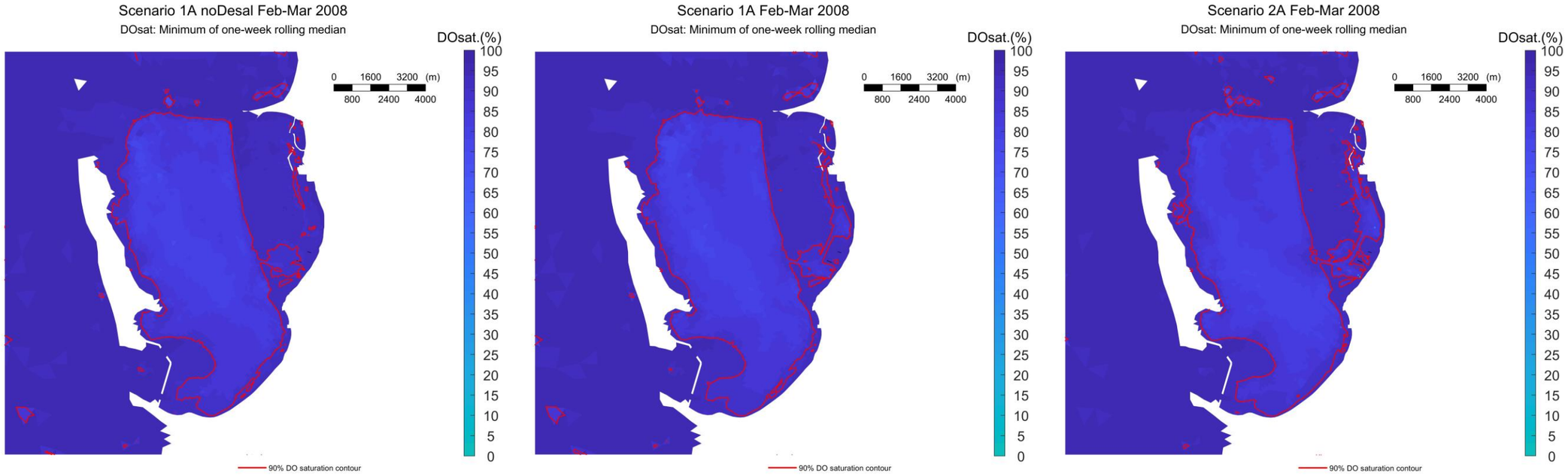

Figure 3-49 The minimum of the 7-day daylight near bed dissolved oxygen saturation rolling median for ambient conditions in Feb-Mar 2008. Left panel: Scenario 1A noDESAL. Centre panel: Scenario 1A. Right panel: Scenario 2A. The red line shows the median 90% DO saturation contour line. The black lines show the locations of PSDP 1and PASDP2 diffusers.

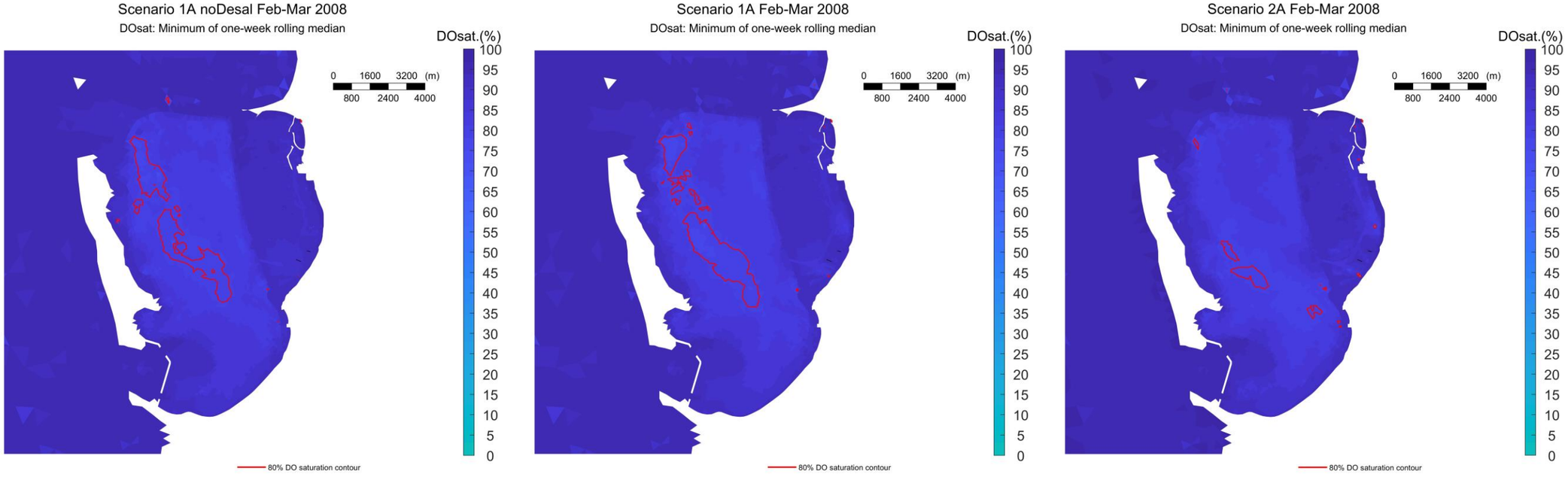

Figure 3-50 The minimum of the 7-day daylight near bed dissolved oxygen saturation rolling median for ambient conditions in Feb-Mar 2008. Left panel: Scenario 1A noDESAL. Centre panel: Scenario 1A. Right panel: Scenario 2A. The red line shows the median 80% DO saturation contour line. The black lines show the locations of PSDP 1and PASDP2 diffusers.

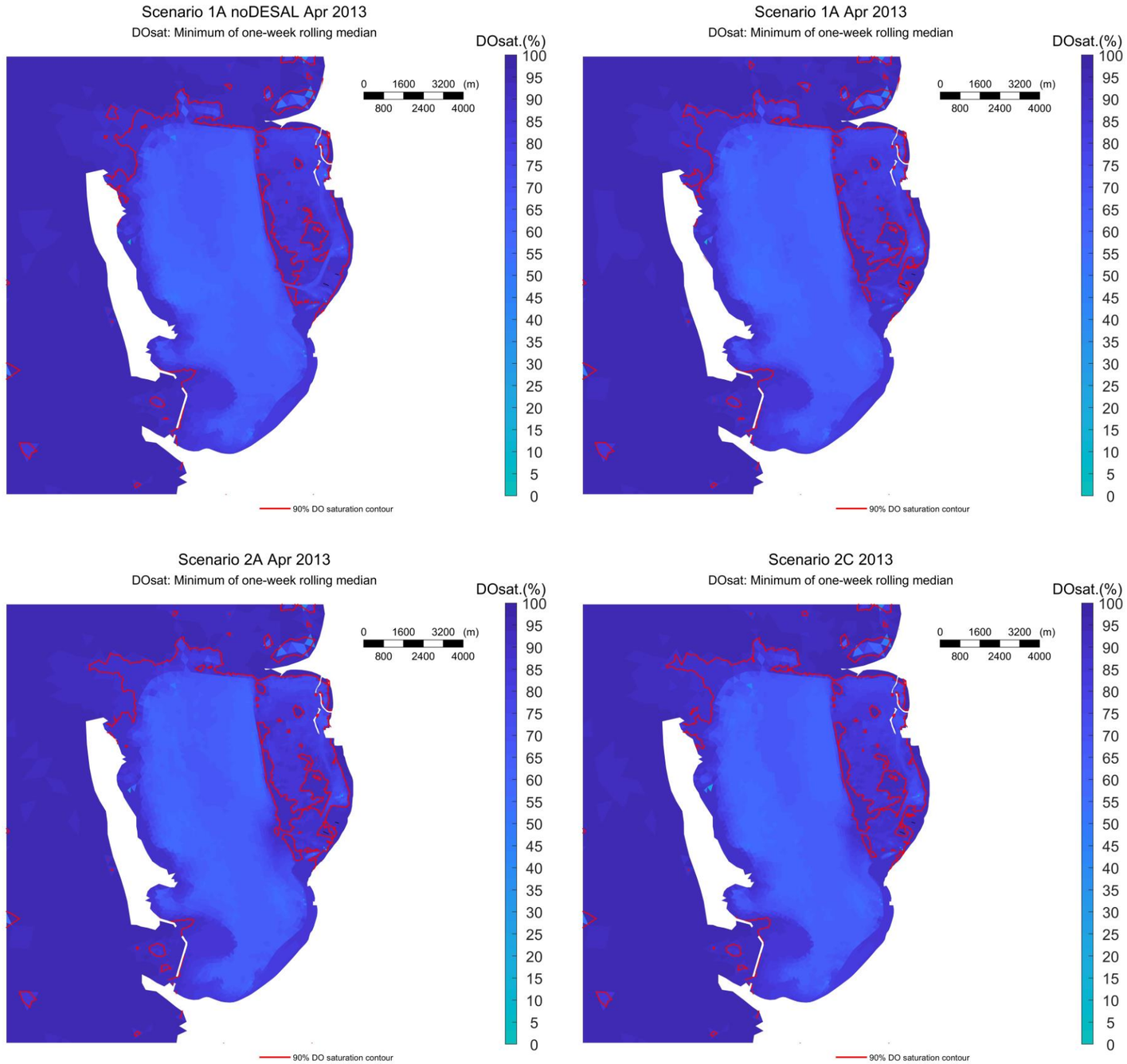

Figure 3-51 The minimum of the 7-day daylight near bed dissolved oxygen saturation rolling median for ambient conditions in Apr 2013. Top left panel: Scenario 1A noDESAL. Top right panel: Scenario 1A. Lower left panel: Scenario 2A. Lower right panel: Scenario 2C. The red line shows the median 90% DO saturation contour line. The black lines show the locations of PSDP 1and PASDP2 diffusers.

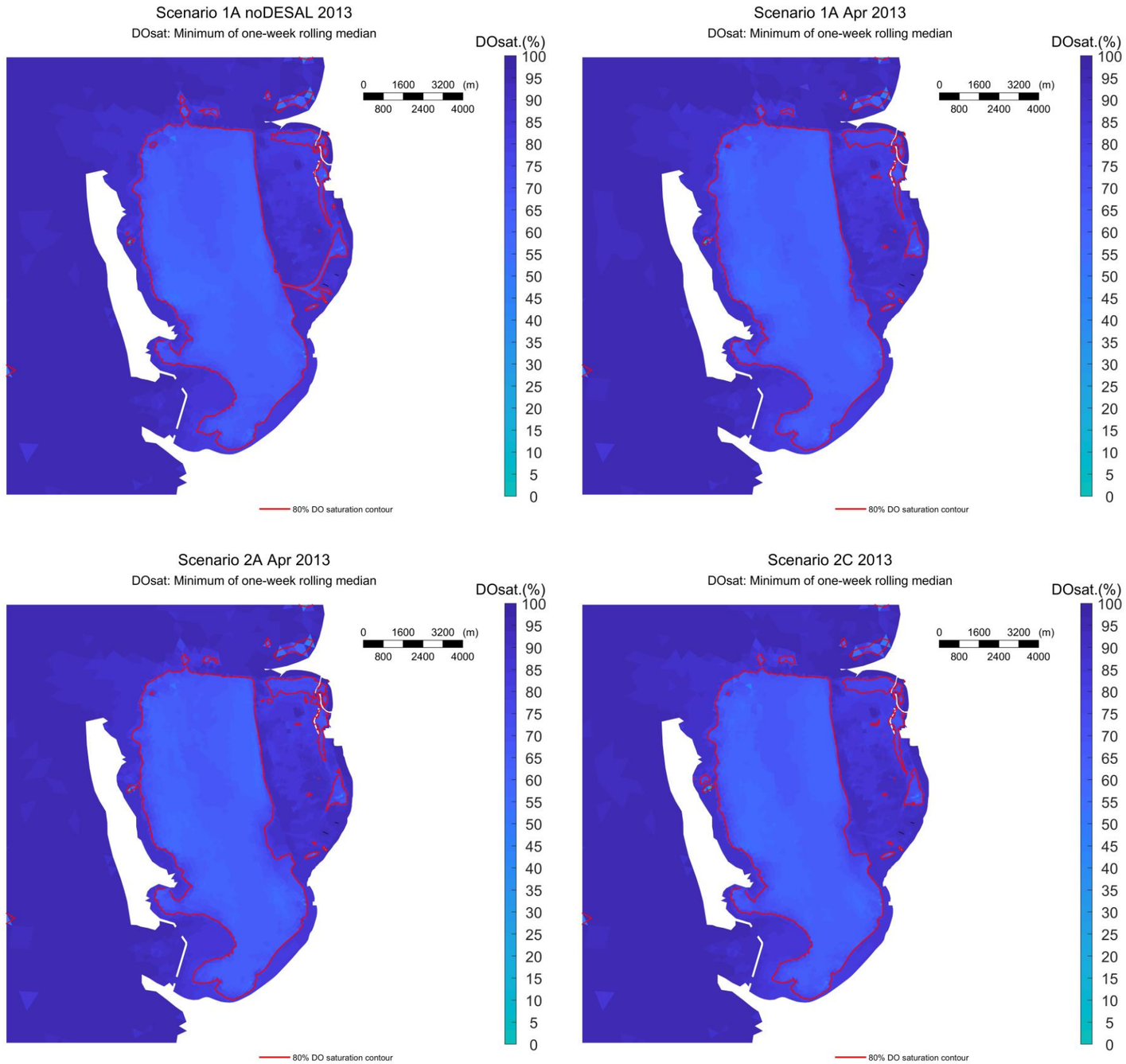

Figure 3-52 The minimum of the 7-day daylight near bed dissolved oxygen saturation rolling median for ambient conditions in Apr 2013. Top left panel: Scenario 1A noDESAL. Top right panel: Scenario 1A. Lower left panel: Scenario 2A. Lower right panel: Scenario 2C. The red line shows the median 80% DO saturation contour line. The black lines show the locations of PSDP 1and PASDP2 diffusers.

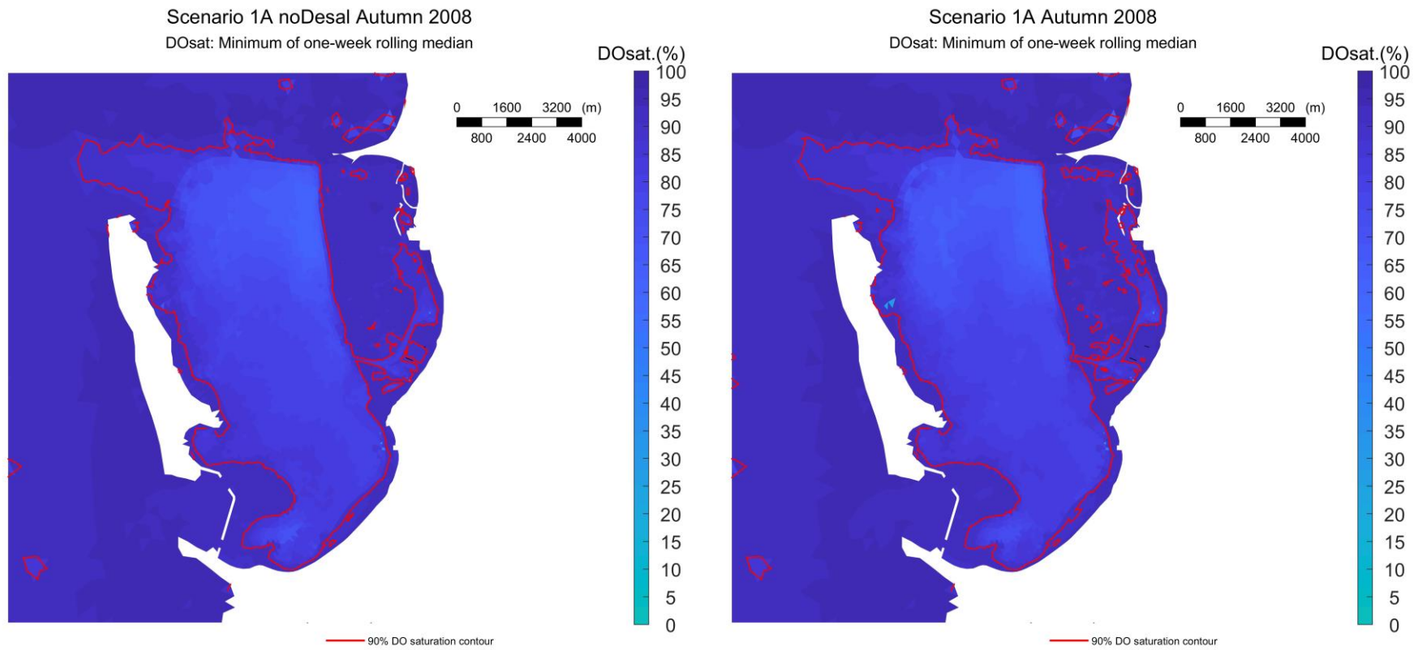

Figure 3-53 The minimum of the 7-day daylight near bed dissolved oxygen saturation rolling median for ambient conditions in Autumn 2008. Top left panel: Scenario 1A noDESAL. Top right panel: Scenario 1A. Lower left panel: Scenario 2A. Lower right panel: Scenario 2C. The red line shows the median 90% DO saturation contour line. The black lines show the locations of PSDP 1and PASDP2 diffusers.

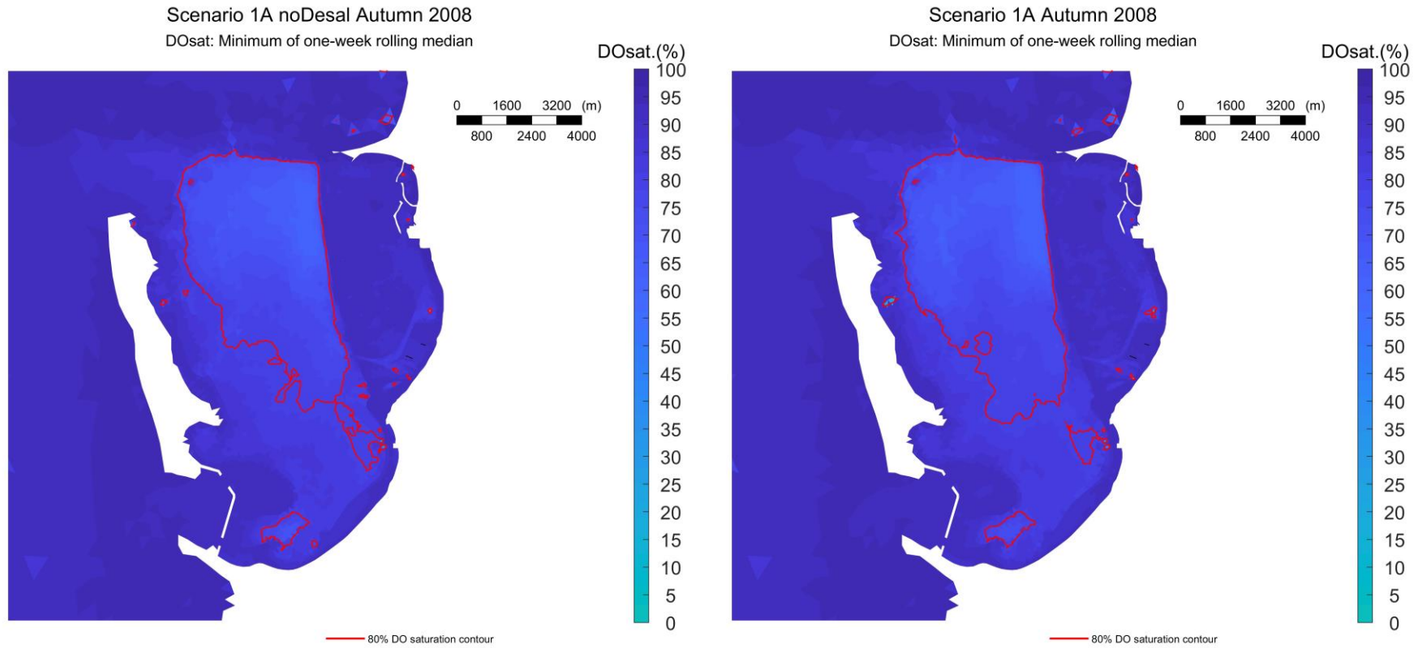

Figure 3-54 The minimum of the 7-day daylight near bed dissolved oxygen saturation rolling median for ambient conditions in Autumn 2008. Top left panel: Scenario 1A noDESAL. Top right panel: Scenario 1A. Lower left panel: Scenario 2A. Lower right panel: Scenario 2C. The red line shows the median 80% DO saturation contour line. The black lines show the locations of PSDP 1and PASDP2 diffusers.

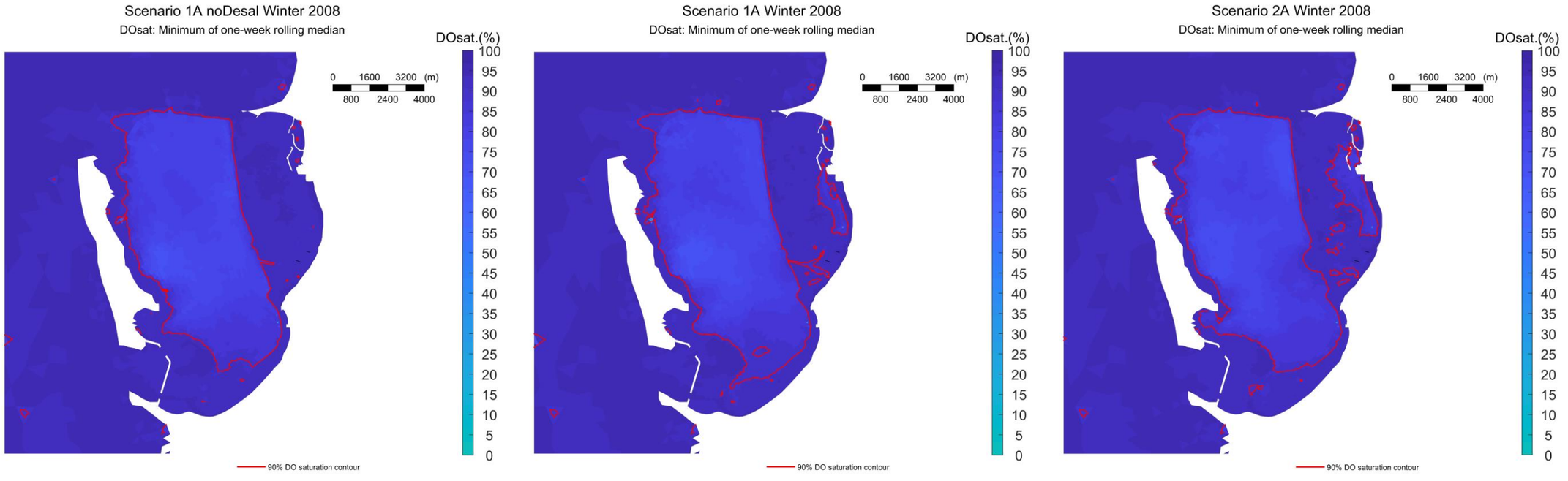

Figure 3-55 The minimum of the 7-day daylight near bed dissolved oxygen saturation rolling median for ambient conditions in Winter 2008. Left panel: Scenario 1A noDESAL. Centre panel: Scenario 1A. Right panel: Scenario 2A. The red line shows the median 90% DO saturation contour line. The black lines show the locations of PSDP 1and PASDP2 diffusers.

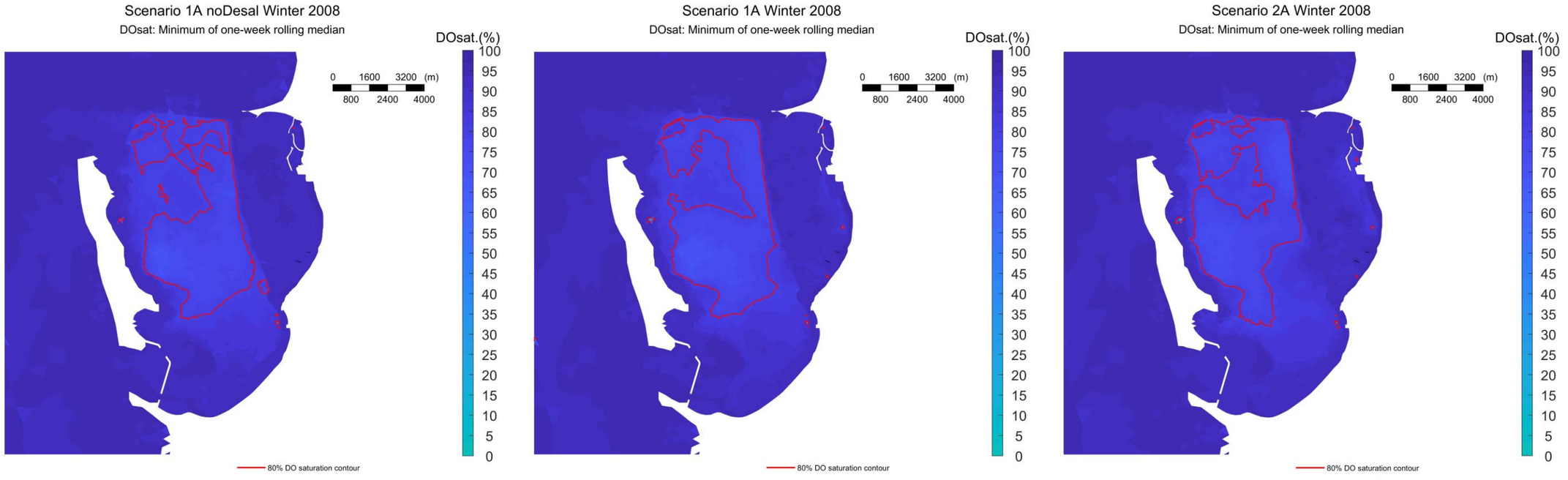

Figure 3-56 The minimum of the 7-day daylight near bed dissolved oxygen saturation rolling median for ambient conditions in Winter 2008. Left panel: Scenario 1A noDESAL. Centre panel: Scenario 1A. Right panel: Scenario 2A. The red line shows the median 80% DO saturation contour line. The black lines show the locations of PSDP 1and PASDP2 diffusers.

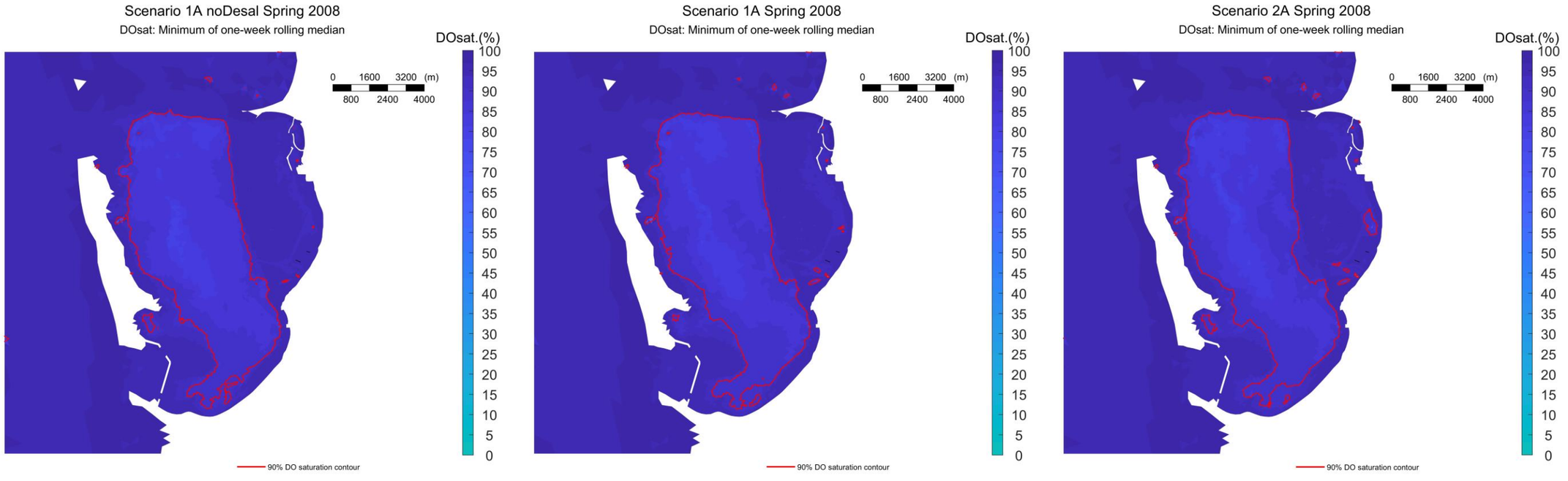

Figure 3-57 The minimum of the 7-day daylight near bed dissolved oxygen saturation rolling median for ambient conditions in Spring 2008. Left panel: Scenario 1A noDESAL. Centre panel: Scenario 1A. Right panel: Scenario 2A. The red line shows the median 90% DO saturation contour line. The black lines show the locations of PSDP 1and PASDP2 diffusers.

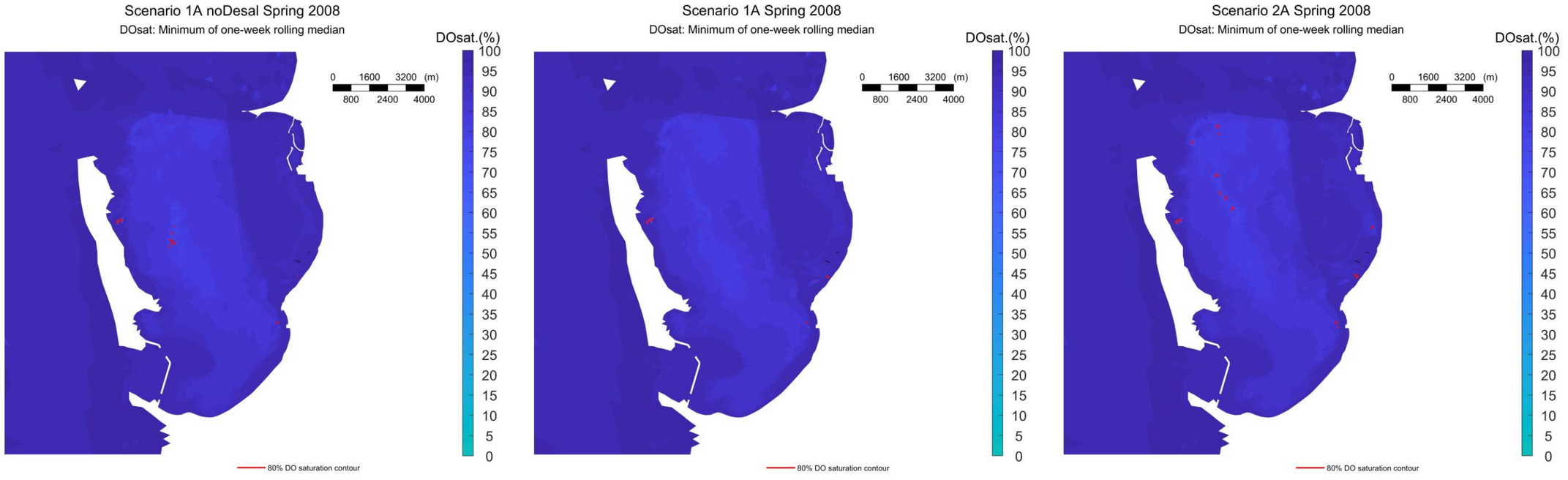

Figure 3-58 The minimum of the 7-day daylight near bed dissolved oxygen saturation rolling median for ambient conditions in Spring 2008. Left panel: Scenario 1A noDESAL. Centre panel: Scenario 1A. Right panel: Scenario 2A. The red line shows the median 80% DO saturation contour line. The black lines show the locations of PSDP 1and PASDP2 diffusers.

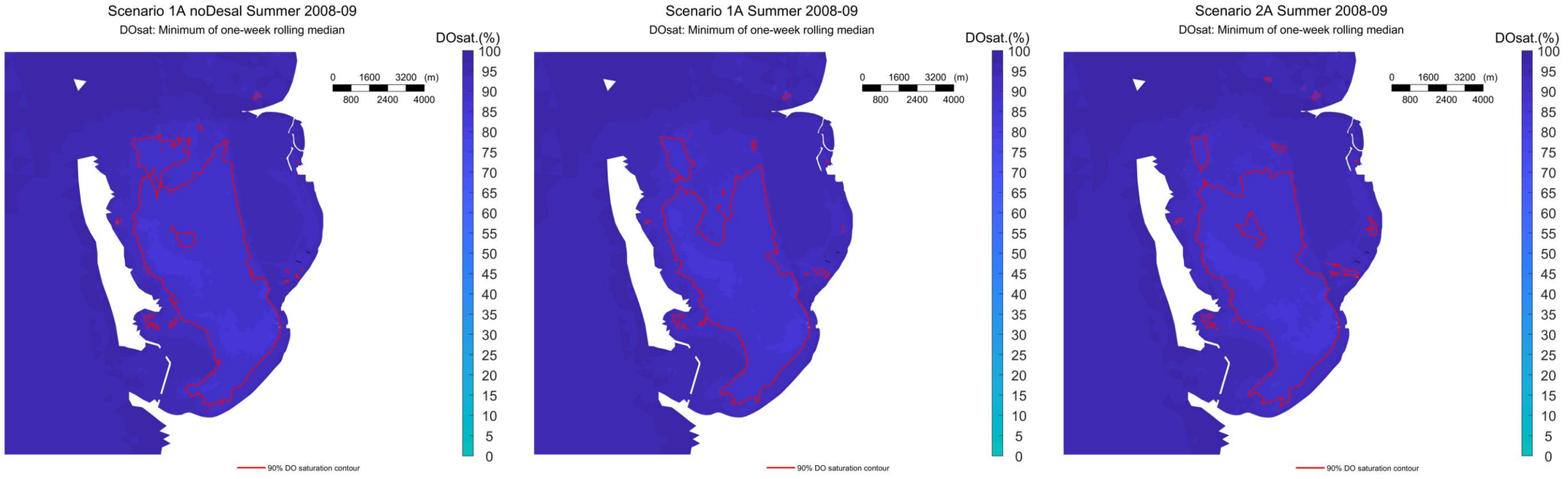

Figure 3-59 The minimum of the 7-day daylight near bed dissolved oxygen saturation rolling median for ambient conditions in Summer 2008-09. Left panel: Scenario 1A noDESAL. Centre panel: Scenario 1A. Right panel: Scenario 2A. The red line shows the median 90% DO saturation contour line. The black lines show the locations of PSDP 1and PASDP2 diffusers.

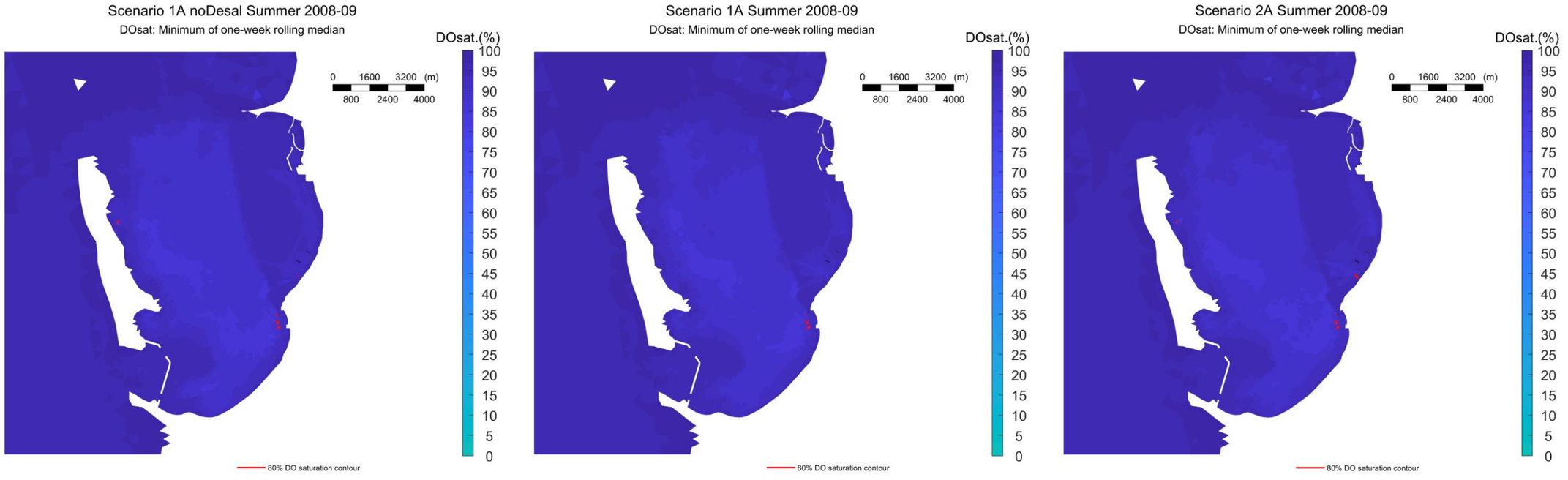

Figure 3-60 The minimum of the 7-day daylight near bed dissolved oxygen saturation rolling median for ambient conditions in Summer 2008-09. Left panel: Scenario 1A noDESAL. Centre panel: Scenario 1A. Right panel: Scenario 2A. The red line shows the median 80% DO saturation contour line. The black lines show the locations of PSDP 1and PASDP2 diffusers.

Common to all median DO saturation contour maps was the similarity between scenario 1A noDesal, and the discharge scenarios (1A, 2A and 2C), particularly throughout the deep basin. The desalination plant discharge cases also generally presented higher DO saturation in the shallow basin, particularly within the channels and the KBT swing basin, as well as in the transition between the basins at the exit of the Stirling Channel. This was an effect of the discharge saturation levels (see e.g. BMT 2018a) and is particularly evident in the 80% DO saturation contour line in Figure 3-52.

In the shorter simulations and autumn period (and to a lesser extent winter) (Figure 3-49 to Figure 3-56), however, scenarios 1A, 2A and 2C, in comparison to the baseline, presented larger areas with DO below 80% and 90% towards the northern end of the shallow basin, more prominently in the navigation channels (Jervoise and Medina), and in the AMC harbours and swing basin. Note the case without desal also presented low DO around those areas. The area enclosed by the 80% saturation contour lines in the Feb-Mar 2008 period (Figure 3-50) did not cover the entire deep basin as in Apr 2013.

As expected, the largest areas with low DO concentrations were in autumn. These low DO conditions were driven by the reduced wind stress exacerbating density stratification and curbing DO re-aeration below the pycnoclines (see e.g. BMT 2018a).

3.3.4.2 DO Concentration Timeseries

DO concentration near-surface (i.e. 0.5 m from the surface) and near bed (i.e. 0.5 m from the seabed) timeseries at the four locations are presented in Figure 3-61 to Figure 3-62 and in Appendix C. The results compare temporal variations in DO concentration across different scenarios (1A no Desal, 1A, 2A, 2C). The difference between near surface and near bed DO concentrations are also shown in Figure 3-61 to Figure 3-62.

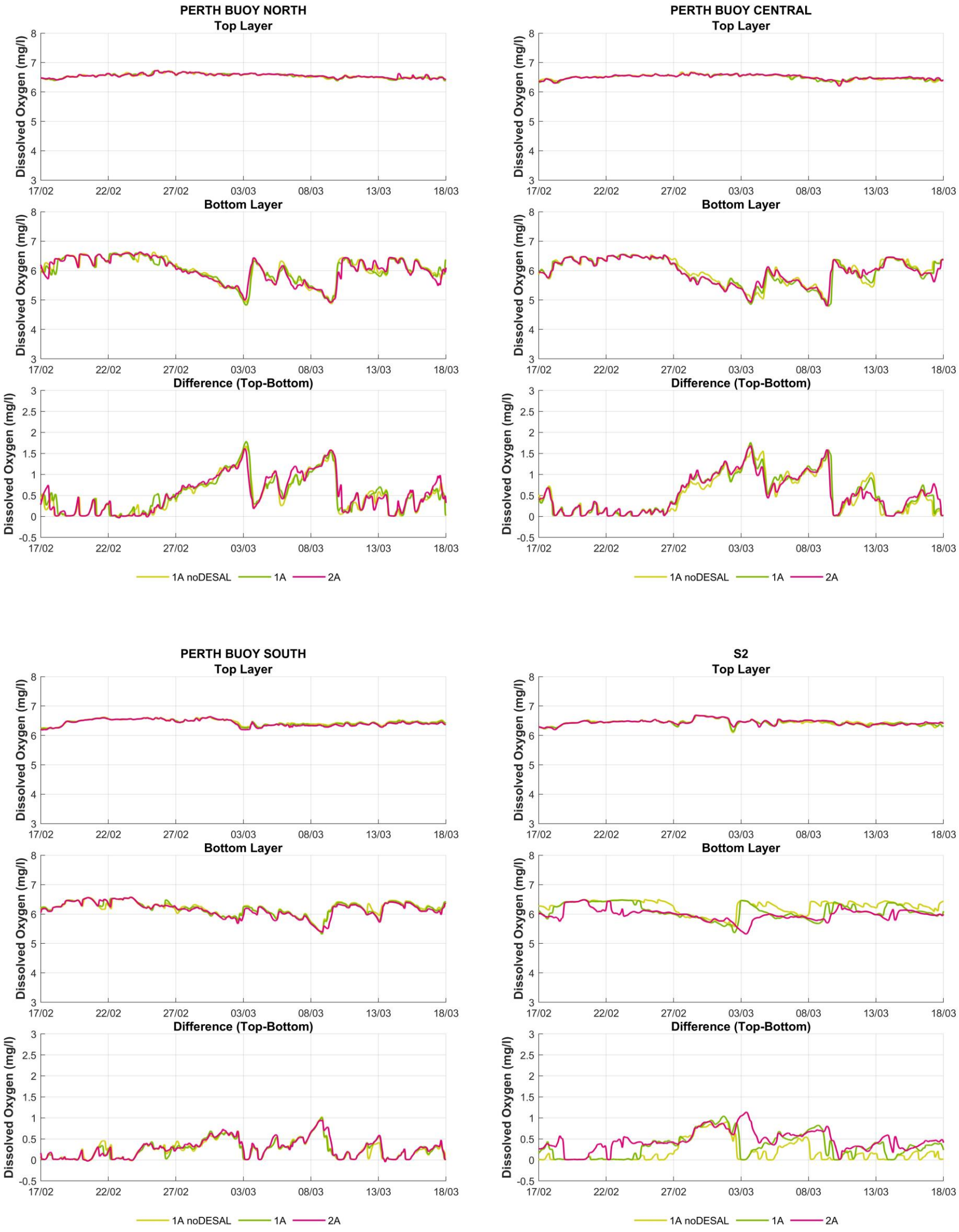

Figure 3-61 Dissolved Oxygen concentration timeseries comparisons for top and bottom waters at Perth Buoy North, Perth Buoy Central, Perth Buoy South and S2 (Feb-Mar 2008)

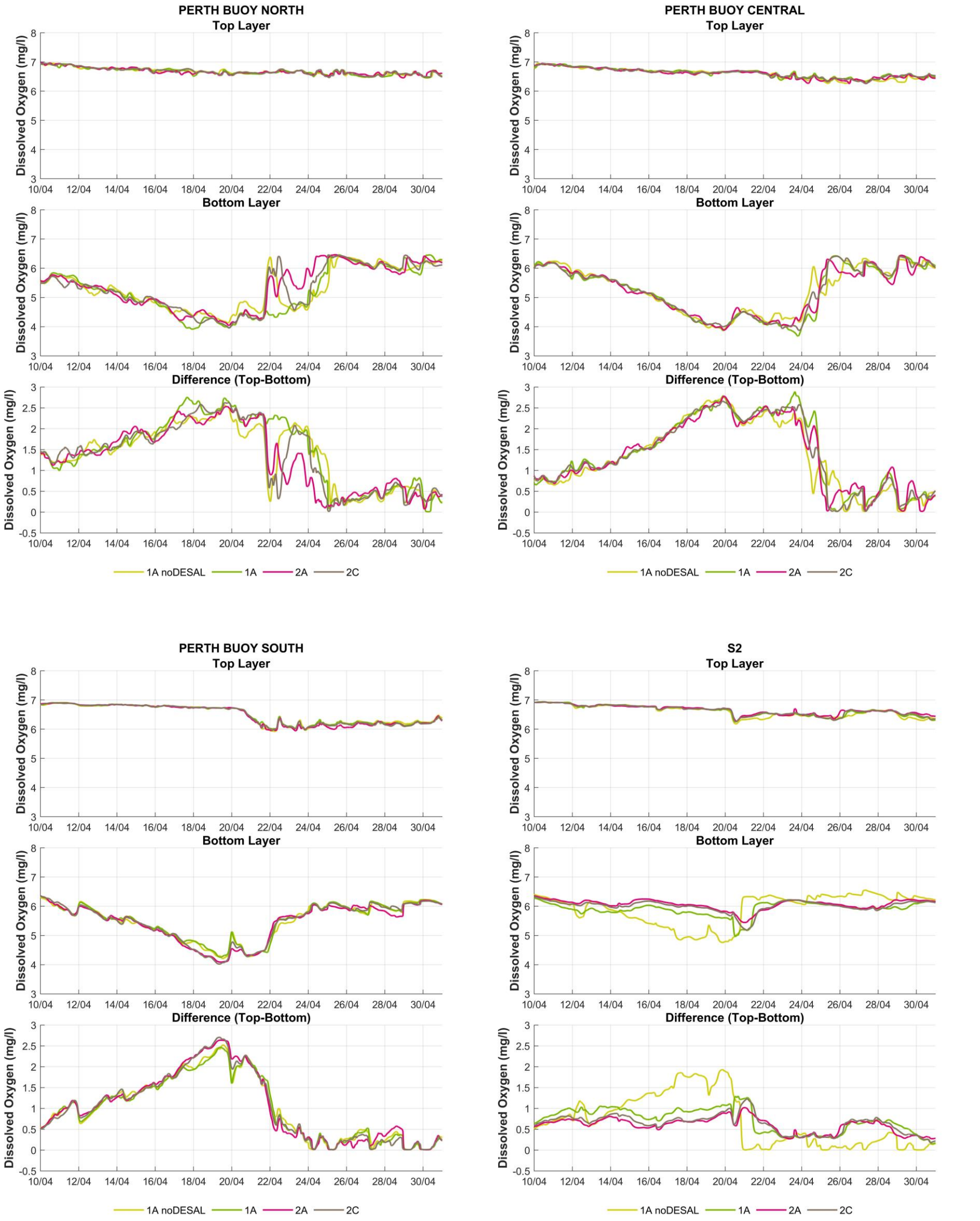

Figure 3-62 Dissolved Oxygen concentration timeseries comparisons for top and bottom waters at Perth Buoy North, Perth Buoy Central, Perth Buoy South and S2 (Apr 2013)

3.3.4.2.1 February to March 2008

Near-surface and near-bed DO concentrations in the deep basin (North Buoy, Central Buoy and South Buoy) were predicted to be very similar across the different simulations (Figure 3-61). There were some short periods (1-2 days) where scenario 2A presented near bed DO concentrations above both the baseline and 1A (up to 0.3mg/L).

At S2, near surface DO concentrations were similar across all scenarios. Near bed DO concentrations for scenarios 1A and 2A had extended periods of concentrations lower than the baseline (up to 3 days), with 2A results showing instances of lower DO concentrations than 1A (up to 1.2 mg/L on 03 March, but generally not significantly lower).

3.3.4.2.2 April 2013

Similar near surface DO concentrations were observed for all sites, with some small fluctuations between scenarios (Figure 3-62).

At the deep basin sites, the decreasing near bed DO concentration for the discharge scenarios were similar to the baseline during the first 10 days of the simulation. The subsequent periods, however, DO concentrations for both baseline and discharge scenarios increased, responding to more favourable wind-mixing conditions (Figure 3-62). On 22 Apr, at Perth Buoy North and Central, the discharge Scenarios 2A and 2C presented a higher rate of concentrations recovery than the baseline and by 23 Apr DO conditions considerably improved at these stations, particularly for Scenario 2A. At Perth Buoy South, very similar behaviour of DO recovery was observed between scenarios.

At S2, the near bed DO concentrations for the discharge scenarios remained above that of the baseline for the initial 10 days and resumed to similar levels following the re-aeration period around 20 April.

Over the Apr 2013 period, which is representative of low DO conditions, the simulated DO concentrations in the discharge scenarios alternated between higher and lower concentrations in comparison to the baseline. When lower concentrations were observed, these were typically less than 0.5 mg/L lower than the baseline.

3.3.4.2.3 March 2008 to March 2009

Appendix C shows the DO concentration results from the seasonal simulations over Mar 2008 to Mar 2009. The deep basin (North, Central and South Buoy) showed little variation of DO concentrations between scenarios for each of the seasons. The near bed DO concentrations were also similar across all simulations during the spring and summer periods.

The autumn and winter periods, however, showed more variability between discharge and baseline scenarios (variation at the peaks ranged from 0.2 up to 2.0 mg/L). In the final month of the winter period (August), reduced near bed DO concentrations occurred in response to the stratification imposed by Swan River flows associated with a substantial rainfall event (see BMT 2018a, also Figure 3-48). As a result, simulations provided differences in DO concentrations between the noDesal and discharge scenarios across the different locations. For example, the responses at Perth Buoy North was similar across all scenarios, whilst at both Perth Buoy South and Central, DO recovery for scenario 2A was not observed on 15 August. As a result, low DO conditions persisted

for approximately 2 to 3 days longer than those of scenarios 1A noDesal and 1A. Despite the more persistent low DO, concentrations did not decrease below 5 mg/L for any of the scenarios.

At S2, the near surface DO concentrations was similar across all seasons. The near bed DO concentration, however, presented more accentuated seasonal variations between scenarios. In autumn the results for 1A, 2A and 2C were predominantly below that of the baseline (up to 0.7 mg/L), with scenario 1A responding more rapidly to mixing events, and then returning to the same DO levels as the baseline. In winter, results for scenario 2A were below the baseline throughout the period, with the exception of the inflow event in early August. Whilst the less dense inflow inhibited near bed re-aeration at S2, the DO in the discharge produced conditions that fluctuated much less in comparison to the baseline. During spring and summer, scenario 2A presented instances of lower near bed DO concentrations in comparison to both the baseline and scenario 1A. These differences were however modest, with maximum differences approximately equal to 0.5 mg/L. During Autumn, scenario 2C remained consistent with the results from scenario 2A with brief periods of increased mixing occurring for 2 to 3 days in the last week of March (i.e. differences between top and bottom reducing to approximately 0 mg/L in Scenario 2C, whereas remaining at approximately 0.5 mg/L in Scenario 2A).

3.3.4.3 DO saturation timeseries

DO saturation time series are also presented (Figure 3-63 to Figure 3-64, with results from the seasonal simulations presented in Appendix D). In this case, DO saturation was produced from the temperature, salinity and DO concentrations, following Riley and Skirrow (1974). The 7-day rolling median saturations were then calculated. Again, the results show DO saturation timeseries for each of the scenarios (1A no Desal, 1A, 2A, 2C) across the different locations in Figure 3-22.

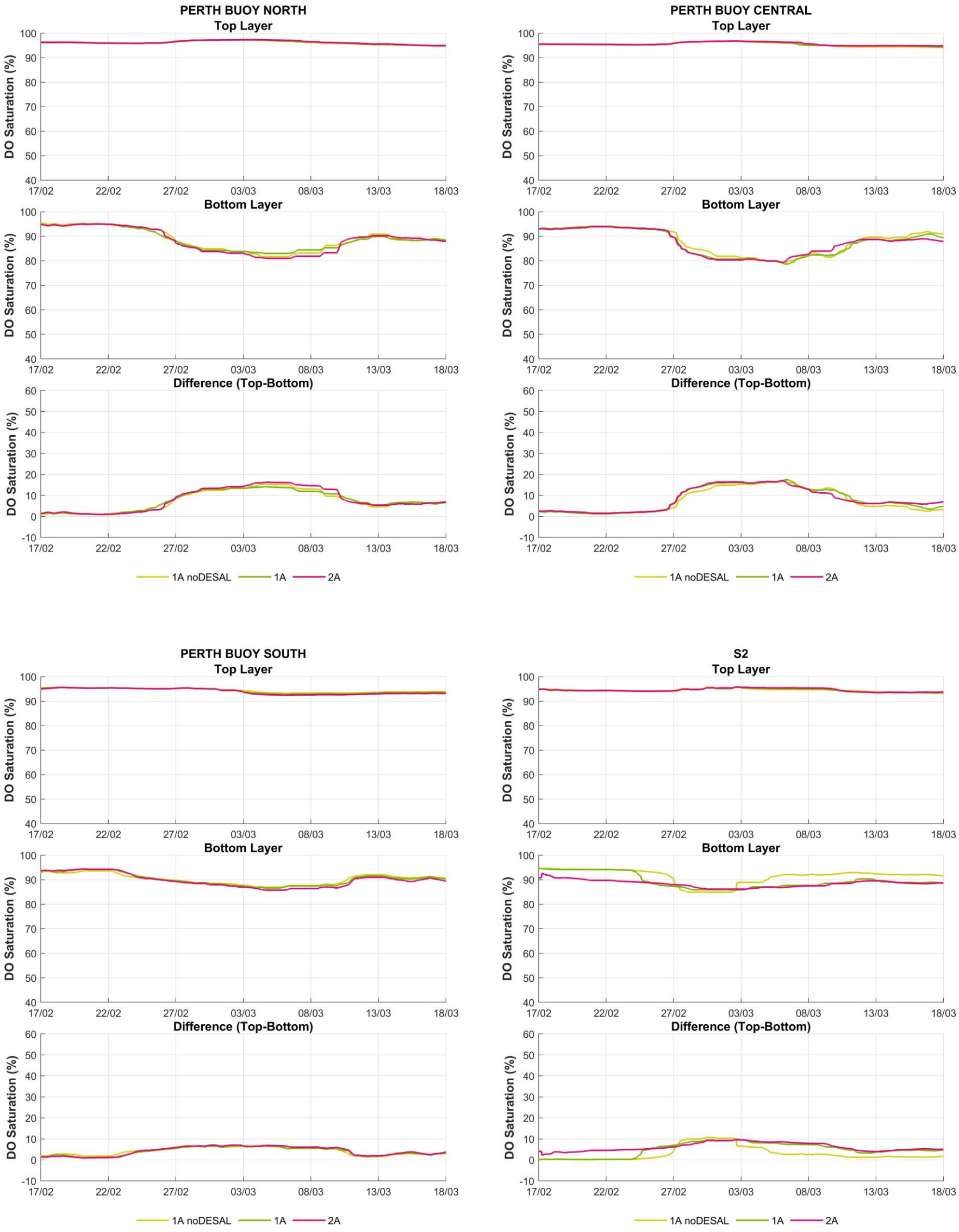

Figure 3-63 Dissolved Oxygen saturation timeseries comparisons for top and bottom waters at Perth Buoy North, Perth Buoy Central, Perth Buoy South and S2 (Feb to Mar 2008)

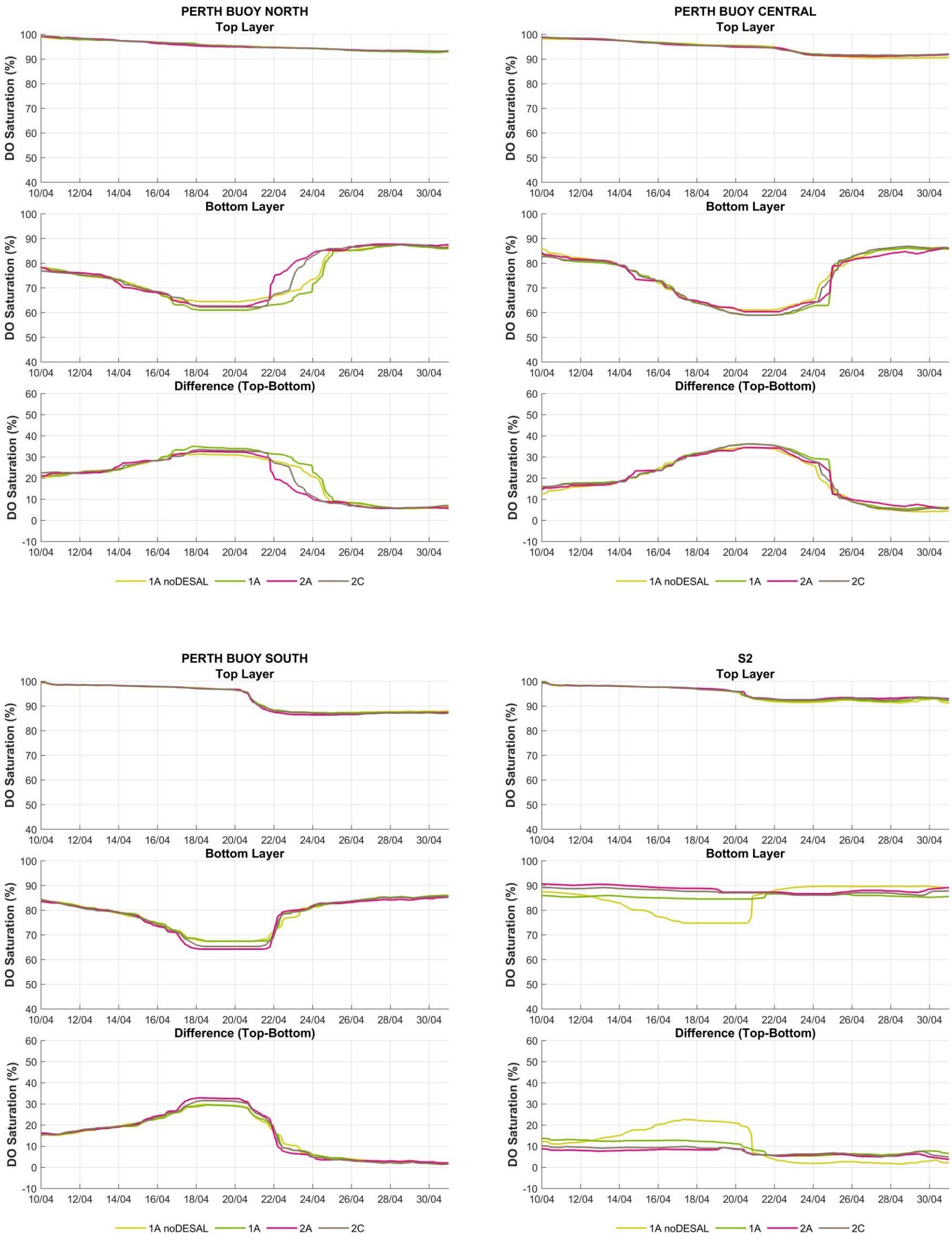

Figure 3-64 Dissolved Oxygen saturation timeseries comparisons for top and bottom waters at Perth Buoy North, Perth Buoy Central, Perth Buoy South and S2 (Apr 2013)

3.3.4.3.1 February to March 2008

In this simulation period, near bed DO saturation for all simulations were similar across all deep basin sites, showing initially high values at around 92% followed by sustained period of decline over the first two weeks of March that saw values as low as 80% (Perth Buoy North and Central) and 85% (Perth Buoy South).

At S2, the median near-surface DO saturation was similar across all scenarios, whereas for the near bed, scenario 2A presented saturation below the baseline (up to 3%) for most of the simulation. Scenario 1A, on the other hand, remained at baseline levels for the initial 10 days, before it decreased to similar saturation levels to scenario 2A.

3.3.4.3.2 April 2013

The near bed DO saturation for the Apr 2013 period reflected the DO concentration results presented earlier. At all deep basin sites, saturation was as low as 60% for Perth Buoy North and Perth Buoy Central, and as low as 65% for Perth Buoy South. Whilst the discharge scenarios presented lower DO at Perth Buoy North, the baseline presented lower DO saturation at the other deep basin locations. These differences were however lower than 5%.

The discharge scenarios also presented a quicker recovery from the DO depletion period at both Perth Buoy North and South (particularly scenario 2A and 2C). At S2, the DO saturation remained near constant for 1A, 2A and 2C, compared to the baseline which indicated reduced DO saturation levels (up to 20% between 16 and 20 April). Subsequent to the depletion period, DO saturation levels were as high as 90% for the baseline whereas for the discharge scenarios recovery increased to approximately 85%.

3.3.4.3.3 March 2008 to March 2009

The DO saturations over the year-long simulation are presented in Appendix D. Generally, all deep basin sites showed similar results between scenarios, following similar seasonal variations across the different locations. Median near bed DO saturation differences between the scenarios were generally less than 5%. Reductions in DO saturation were more obvious for autumn and winter than spring and summer. As discussed in BMT (2018a), poor mixing conditions and ingress of less saline water leads to the DO depletion events in autumn, whereas in winter, stratification induced by the Swan River flows creates conditions for dissolved oxygen depletion. Near bed DO saturation during the Swan River flow events in winter could be as low as 75% (Perth Buoy North), whilst in autumn they were as low as 65% (desal cases). For spring and summer, median near bed DO saturation remained always above 90%.

At S2, the median DO saturation levels were generally slightly lower than the baseline for scenario 2A, 2C and 1A (less than 5% DO saturation difference between the scenarios). The periods associated with inflow events, however, showed lower DO saturation levels in the baseline. These were generally of relatively short duration, depending on the magnitude and duration of the event. For example, for the sustained event early in August, DO saturation in the baseline was lower than the desal scenarios for up to approximately 14 days. Again, these differences were generally below 5%. Median near bed DO saturation levels at S2 were nevertheless always above 85%.

3.3.4.4 DO saturation occurrence maps

The proportion of time over the simulation period at which the median DO saturation (depth-averaged between 0 and 0.5 m from the seabed) remained below 80% and 90% was also calculated and mapped. These maps are shown in Figure 3-65 to Figure 3-76.

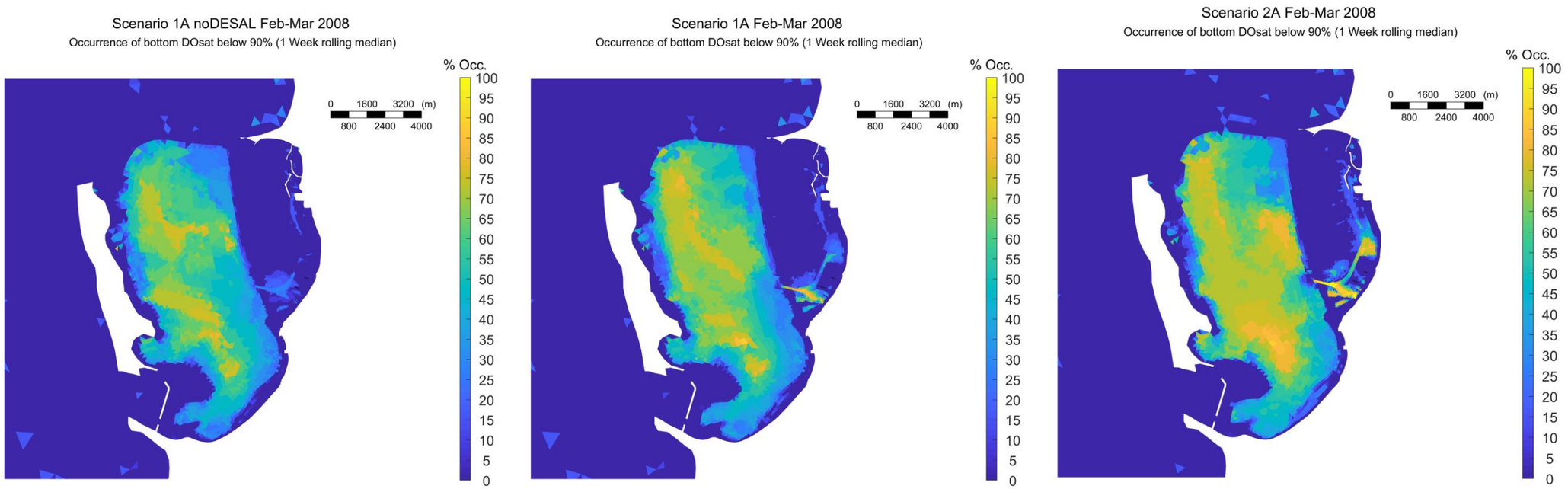

Figure 3-65 Percentage of occurrence of near bed DO saturation median below 90% for ambient conditions in Feb-Mar 2008. Left panel: Scenario 1A noDESAL. Centre panel: Scenario 1A. Right panel: Scenario 2A. Thin black lines show the locations of PSDP1 and PSDP2 diffusers.

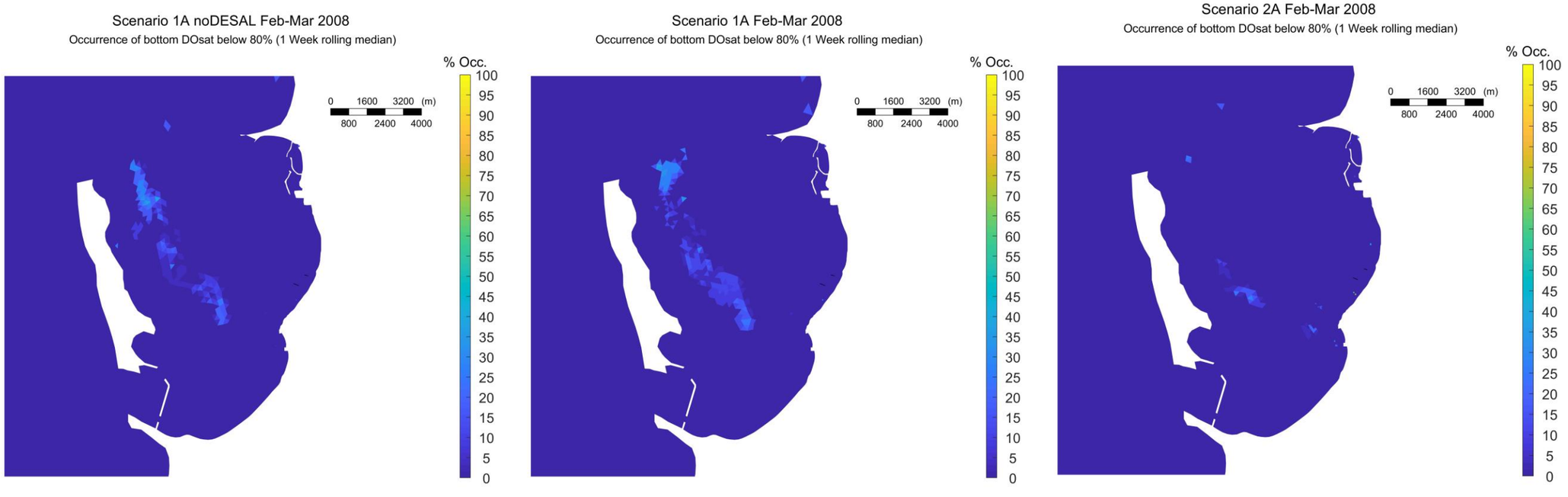

Figure 3-66 Percentage of occurrence of near bed DO saturation median below 80% for ambient conditions in Feb-Mar 2008. Left panel: Scenario 1A noDESAL. Centre panel: Scenario 1A. Right panel: Scenario 2A. Thin black lines show the locations of PSDP1 and PSDP2 diffusers.

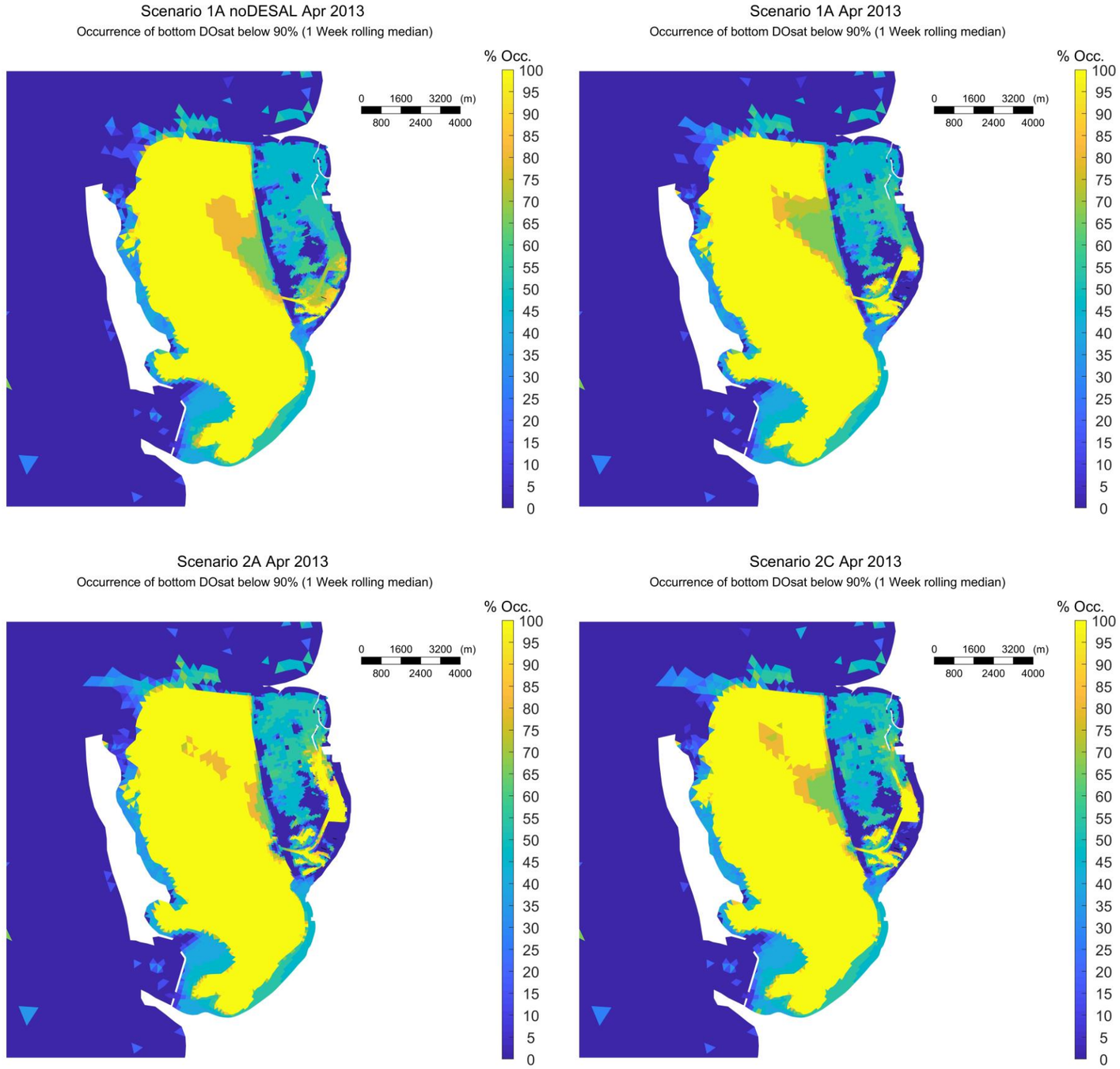

Figure 3-67 Percentage of occurrence of near bed DO saturation median below 90% for ambient conditions in Apr 2013. Top left panel: Scenario 1A noDESAL. Top right panel: Scenario 1A. Lower left panel: Scenario 2A. Lower right panel: Scenario 2C. Thin black lines show the locations of PSDP1 and PSDP2 diffusers.

Discharge signatures

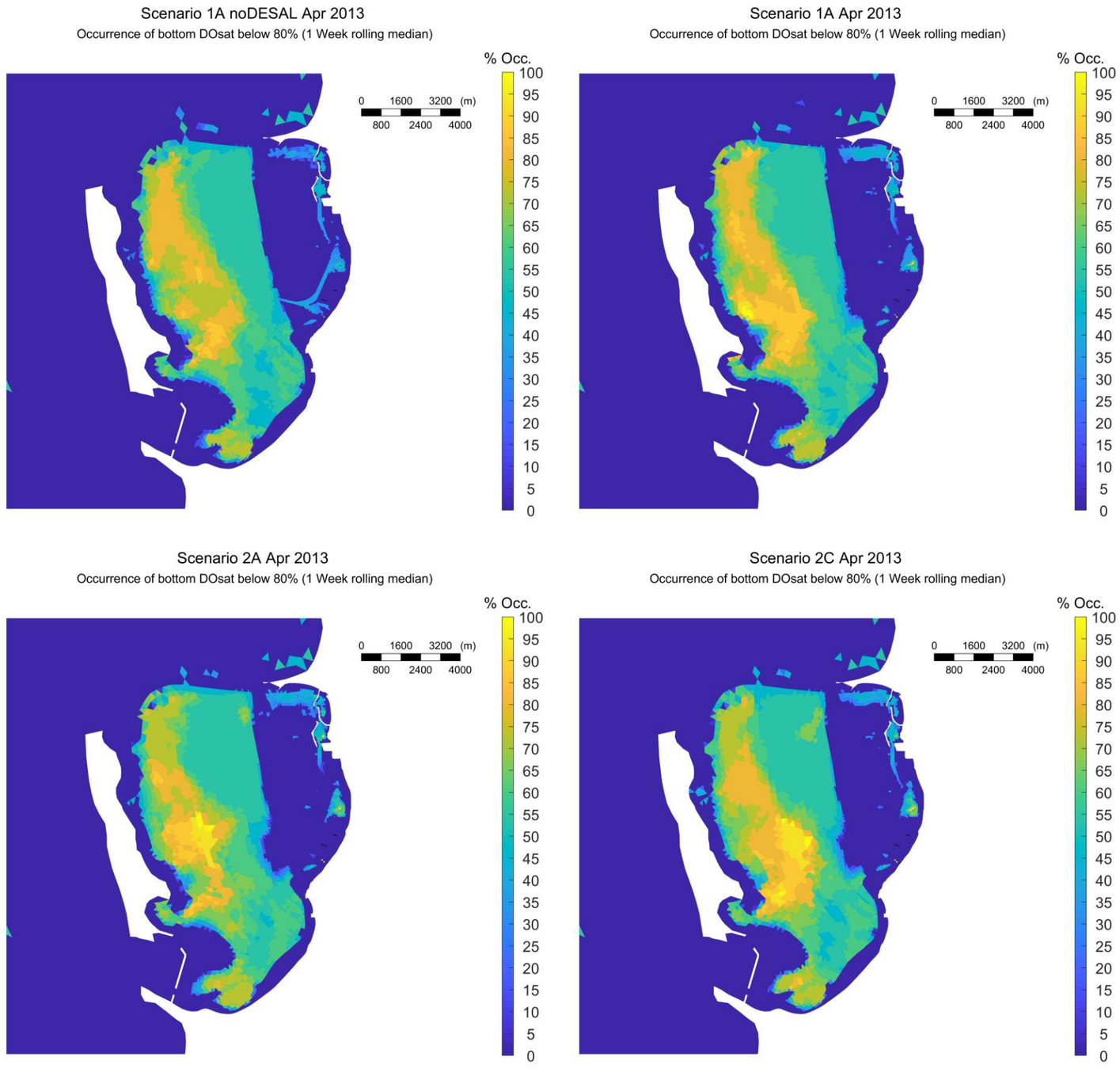

Figure 3-68 Percentage of occurrence of near bed DO saturation median below 80% for ambient conditions in Apr 2013. Top left panel: Scenario 1A noDESAL. Top right panel: Scenario 1A. Lower left panel: Scenario 2A. Lower right panel: Scenario 2C. Thin black lines show the locations of PSDP1 and PSDP2 diffusers.

Discharge signatures

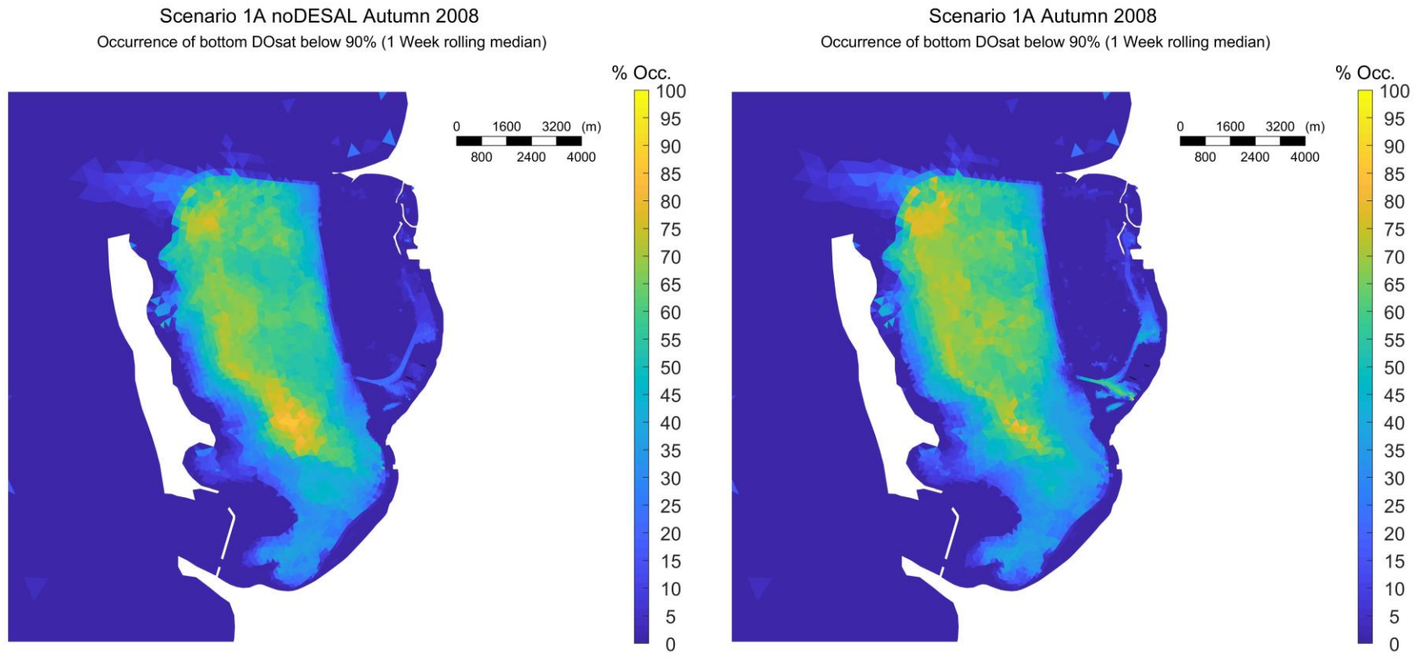

Figure 3-69 Percentage of occurrence of near bed DO saturation median below 90% for ambient conditions in Autumn 2008. Top left panel: Scenario 1A noDESAL. Top right panel: Scenario 1A. Lower left panel: Scenario 2A. Lower right panel: Scenario 2C. Thin black lines show the locations of PSDP1 and PSDP2 diffusers.

Discharge signatures

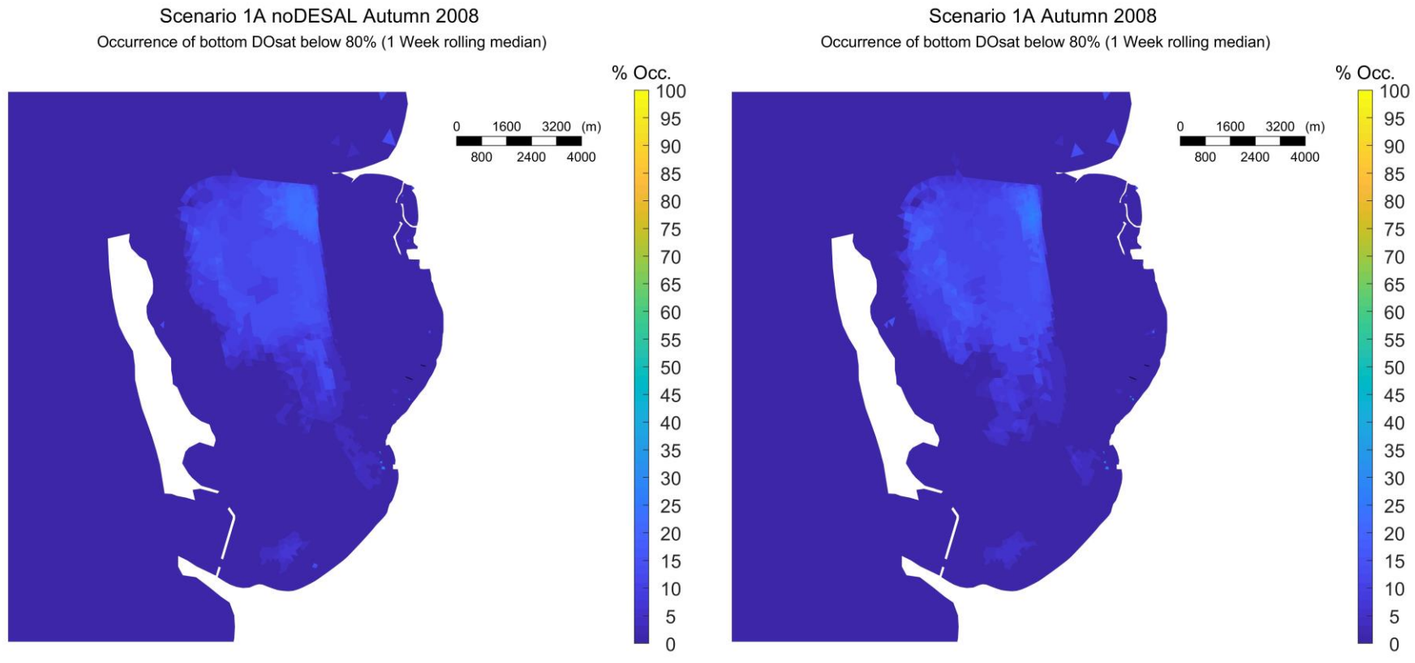

Figure 3-70 Percentage of occurrence of near bed DO saturation median below 80% for ambient conditions in Autumn 2008. Top left panel: Scenario 1A noDESAL. Top right panel: Scenario 1A. Lower left panel: Scenario 2A. Lower right panel: Scenario 2C. Thin black lines show the locations of PSDP1 and PSDP2 diffusers.

Discharge signatures

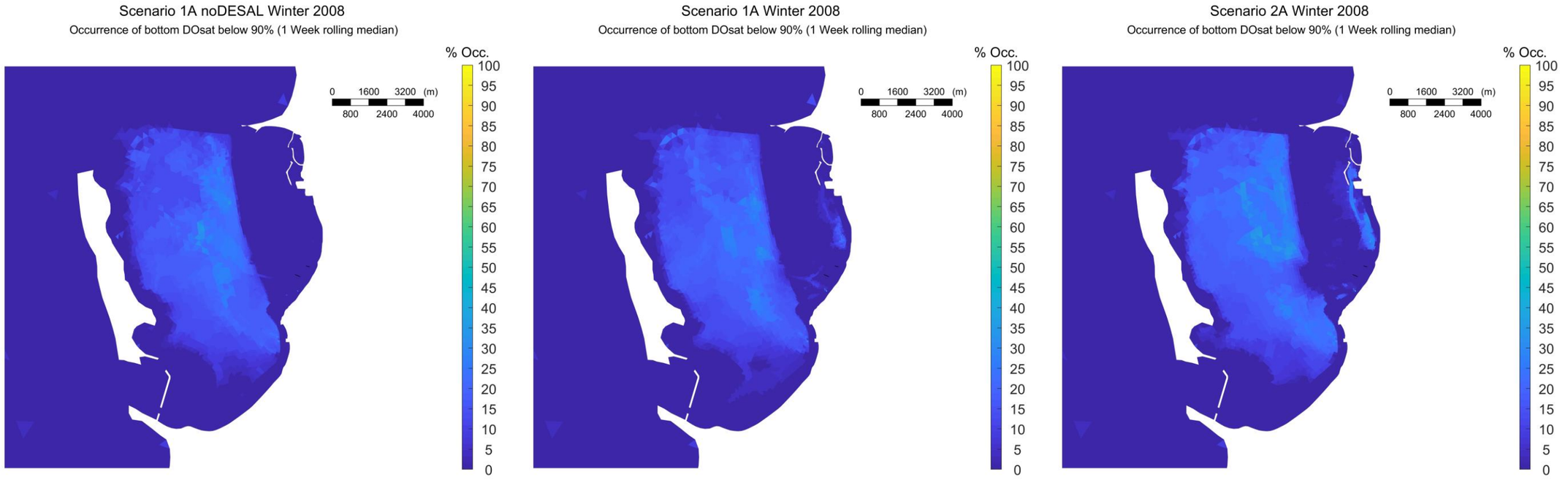

Figure 3-71 Percentage of occurrence of near bed DO saturation median below 90% for ambient conditions in Winter 2008. Left panel: Scenario 1A noDESAL. Centre panel: Scenario 1A. Right panel: Scenario 2A. Thin black lines show the locations of PSDP1 and PSDP2 diffusers.

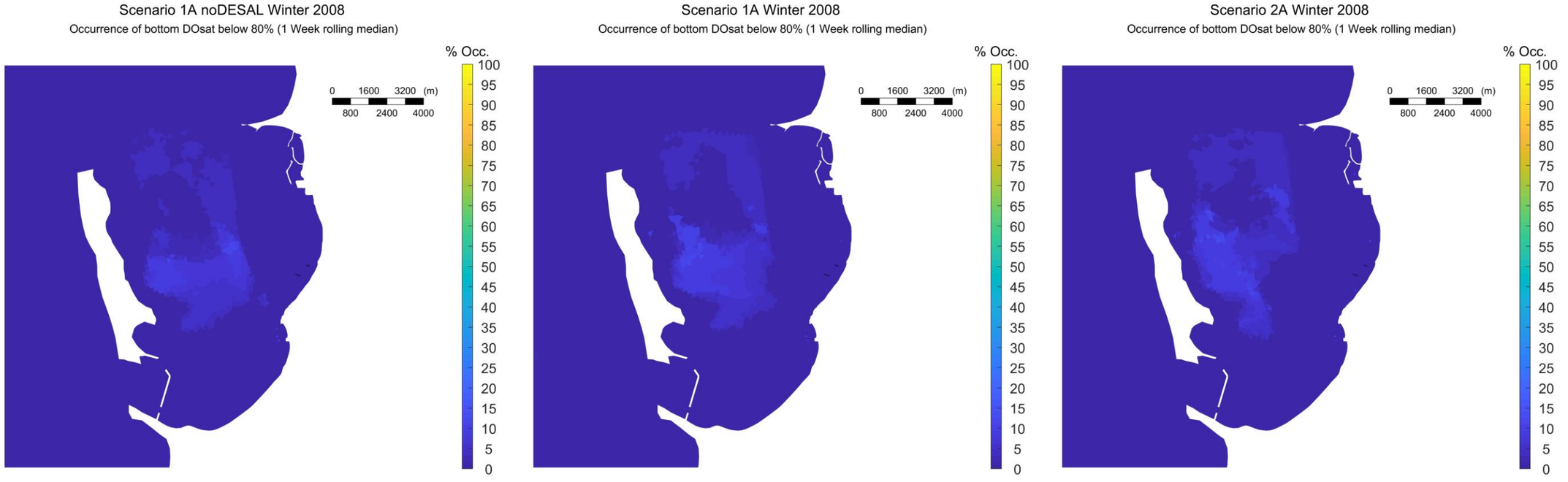

Figure 3-72 Percentage of occurrence of near bed DO saturation median below 80% for ambient conditions in Winter 2008. Left panel: Scenario 1A noDESAL. Centre panel: Scenario 1A. Right panel: Scenario 2A. Thin black lines show the locations of PSDP1 and PSDP2 diffusers.

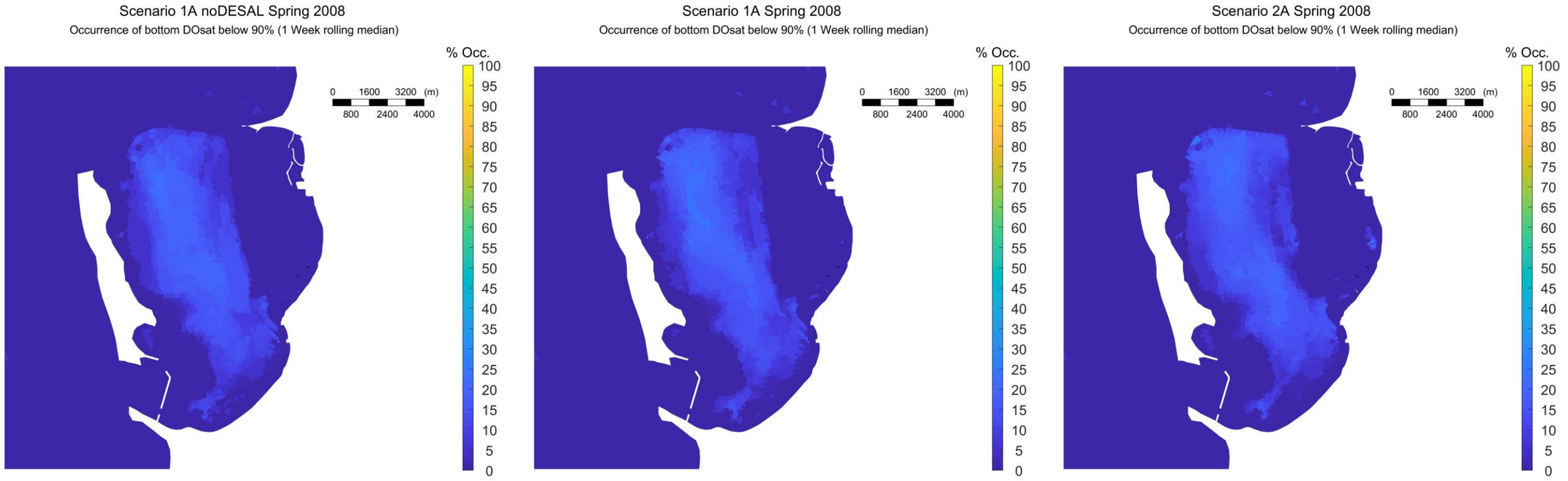

Figure 3-73 Percentage of occurrence of near bed DO saturation median below 90% for ambient conditions in Spring 2008. Left panel: Scenario 1A noDESAL. Centre panel: Scenario 1A. Right panel: Scenario 2A. Thin black lines show the locations of PSDP1 and PSDP2 diffusers.

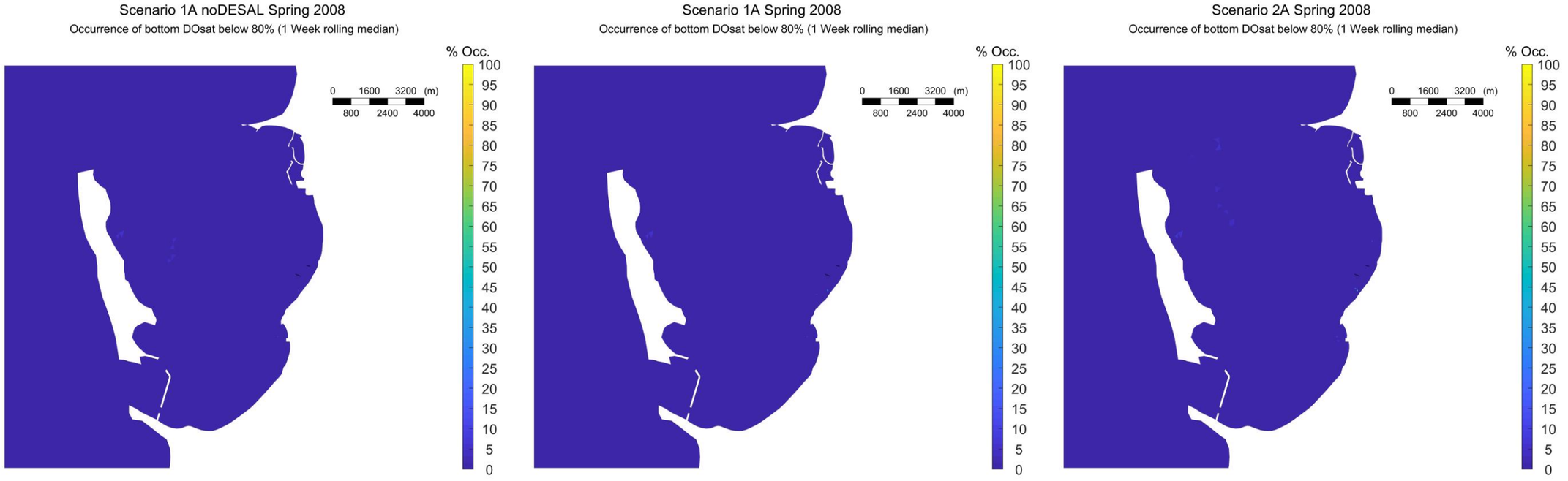

Figure 3-74 Percentage of occurrence of near bed DO saturation median below 80% for ambient conditions in Spring 2008. Left panel: Scenario 1A noDESAL. Centre panel: Scenario 1A. Right panel: Scenario 2A. Thin black lines show the locations of PSDP1 and PSDP2 diffusers.

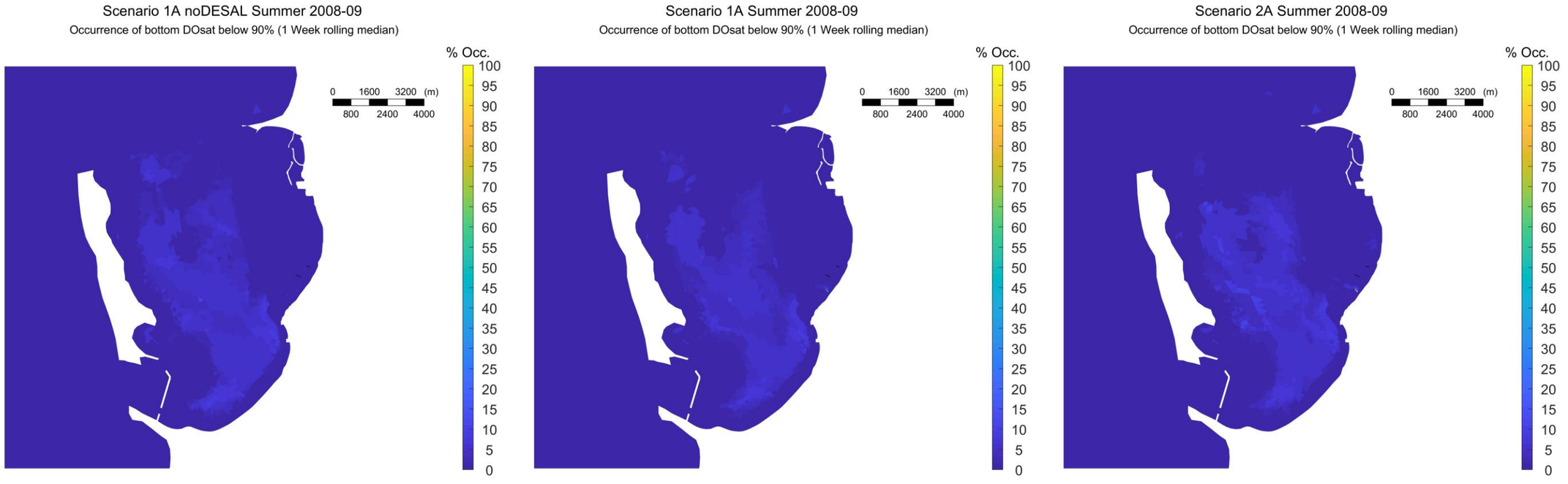

Figure 3-75 Percentage of occurrence of near bed DO saturation median below 90% for ambient conditions in Summer 2008-09. Left panel: Scenario 1A noDESAL. Centre panel: Scenario 1A. Right panel: Scenario 2A. Thin black lines show the locations of PSDP1 and PSDP2 diffusers.

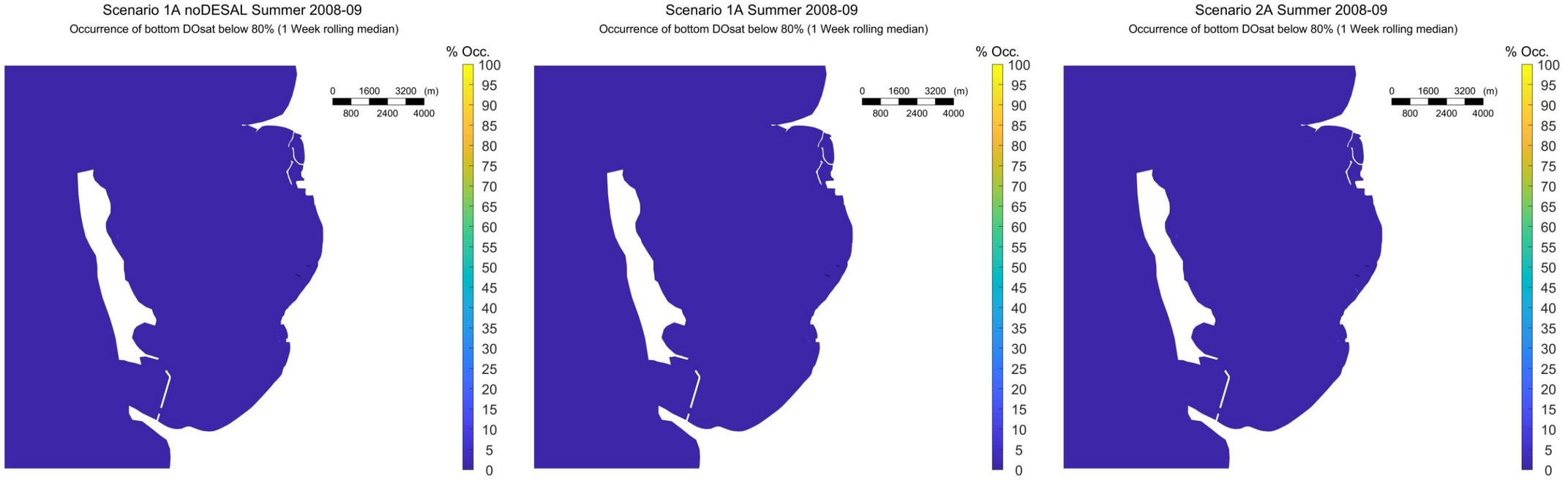

Figure 3-76 Percentage of occurrence of near bed DO saturation median below 80% for ambient conditions in Summer 2008-09. Left panel: Scenario 1A noDESAL. Centre panel: Scenario 1A. Right panel: Scenario 2A. Thin black lines show the locations of PSDP1 and PSDP2 diffusers.

As expected, the occurrence maps mimic the median DO saturation maps by displaying close similarity between the scenarios within each of the simulated periods. Also, and again as expected, the Feb-Mar 2008, April 2013 and Autumn 2008 periods, in comparison to the other seasons, showed relatively longer occurrences of DO below the 80% and 90% saturation levels (Figure 3-65 to Figure 3-70). An exception (i.e. relatively small areas), as also show in the median DO saturation contours, were the occurrences of DO saturation below 80% for the Feb-Mar 2008 (Figure 3-66). For all other seasons the median DO saturation was below 80% less than 20% of the time (Figure 3-71 to Figure 3-76).

The 2013 conditions produced the longest occurrences of DO saturation below 80% and 90% with most of the deep basin below 90% DO saturation for the entire time (Figure 3-67). The larger areas with 100% occurrences of DO saturation below 90% were observed for the desalination scenarios (1A, 2A and 2C), with larger areas for scenario 2A (Figure 3-67). Interestingly, however, areas with 100% occurrences of DO saturation below 80% were smaller for the discharge scenarios (Figure 3-68).

3.3.4.5 DO saturation histograms

Histograms of the median near bed DO saturation occurrences were computed from the timeseries at the four representative locations in Figure 3-22. Figure 3-76 to Figure 3-82 show the occurrences in different bands of DO saturation (<50%, 50% to 60%, 60% to 70%, 70% to 80%, 80 to 90% and >90%).

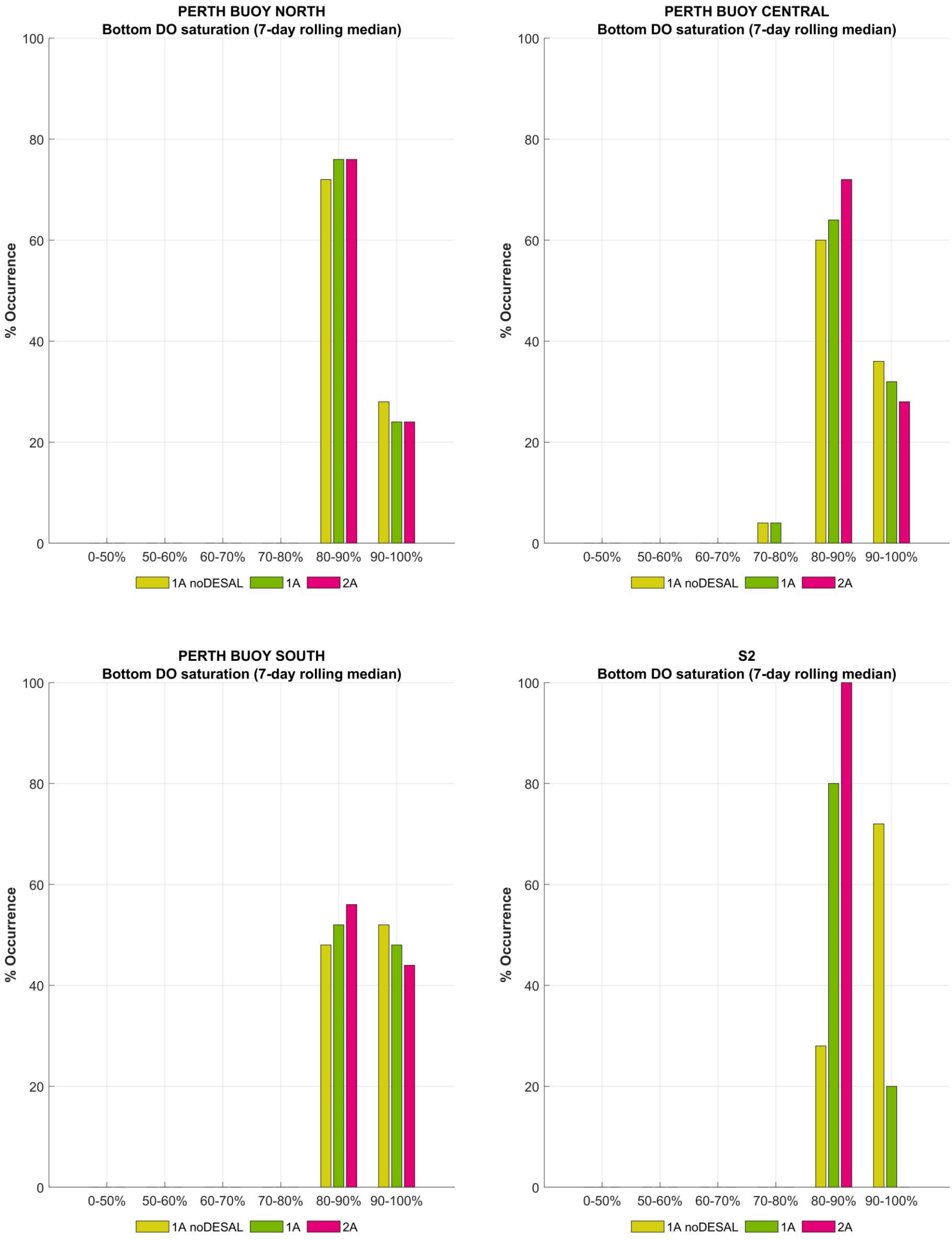

Figure 3-77 Histograms of median near bed DO saturation occurrence across different DO saturation bands in Feb-Mar 2008

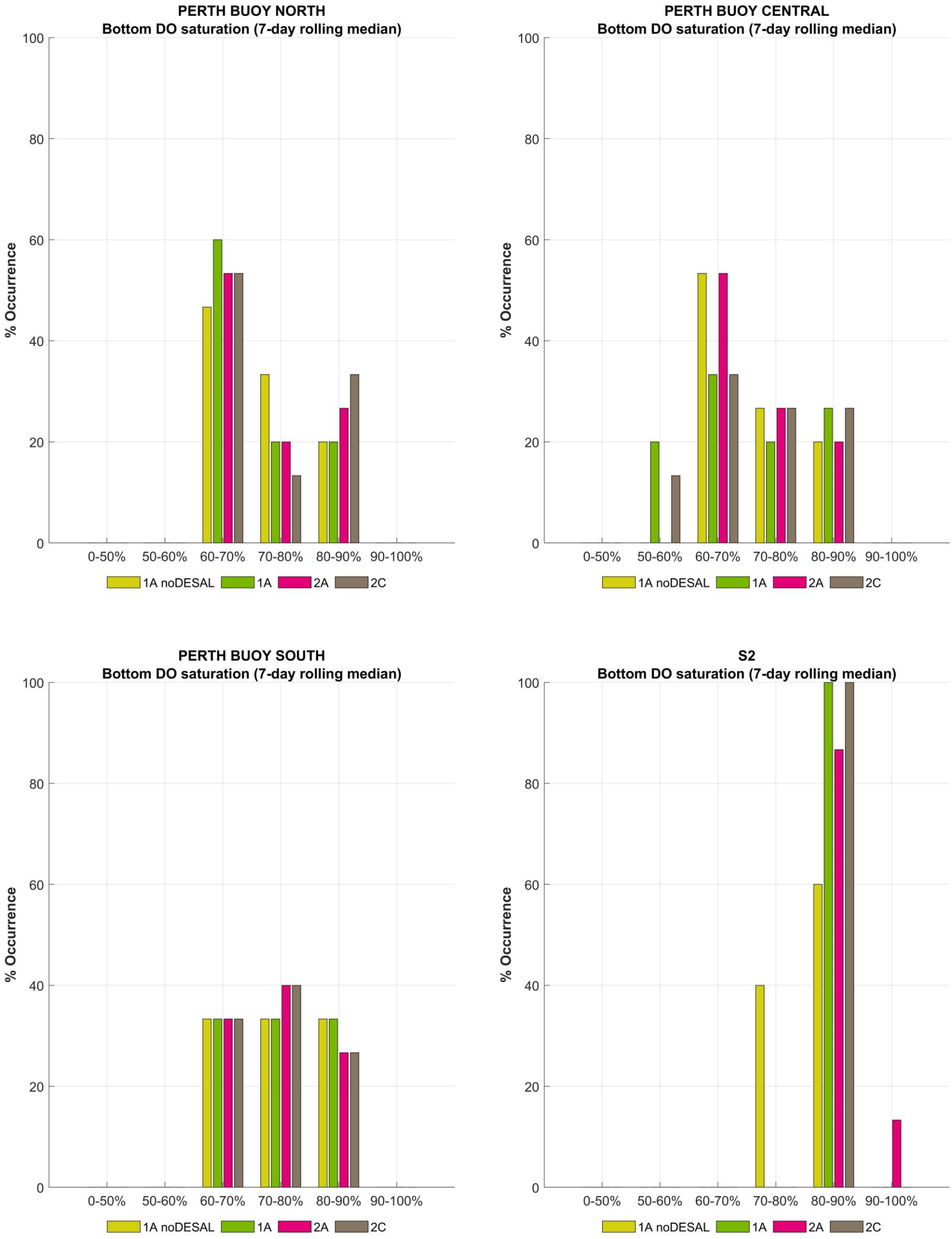

Figure 3-78 Histograms of median near bed DO saturation occurrence across different DO saturation bands in Apr 2013

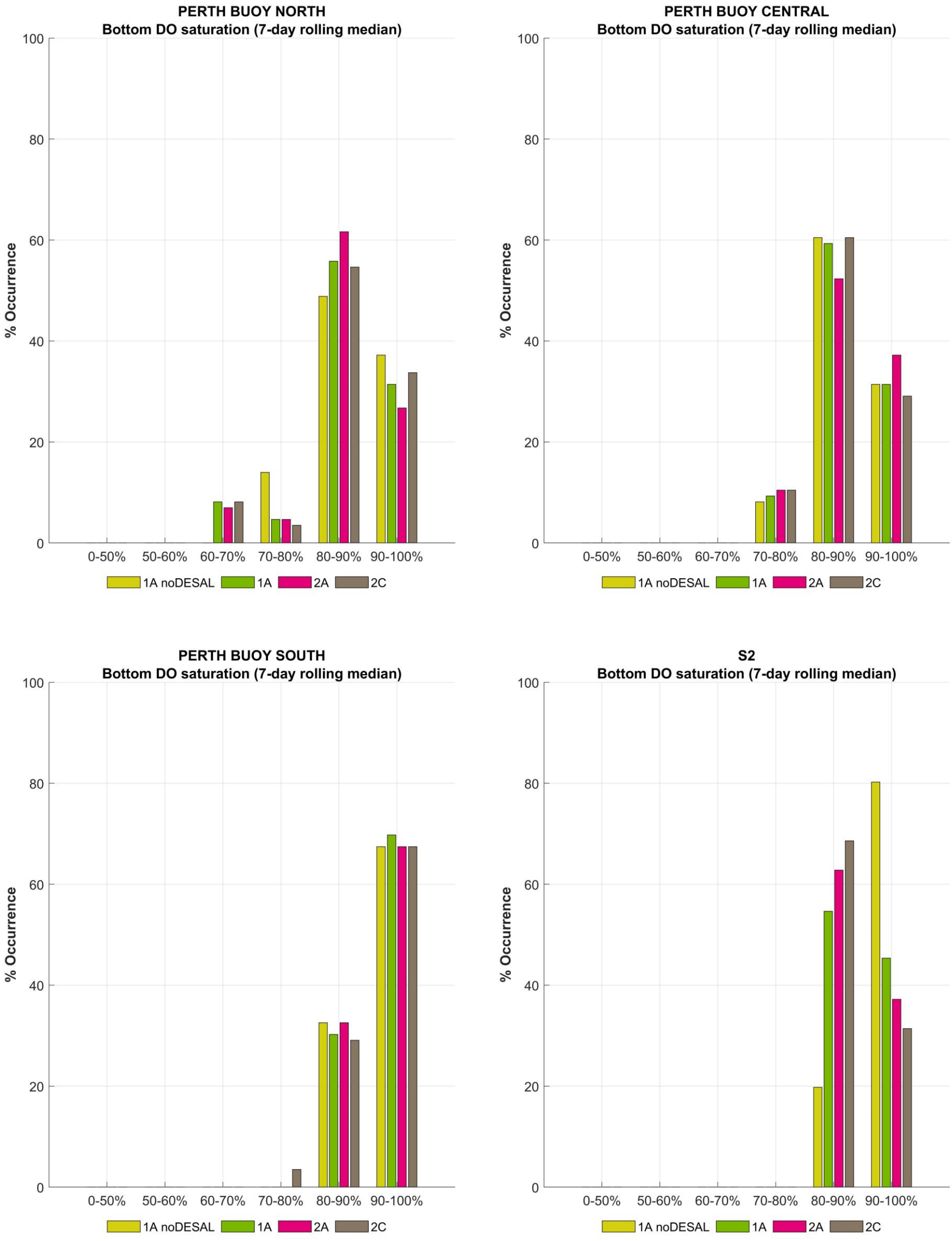

Figure 3-79 Histograms of median near bed DO saturation occurrence across different DO saturation bands in Autumn 2008

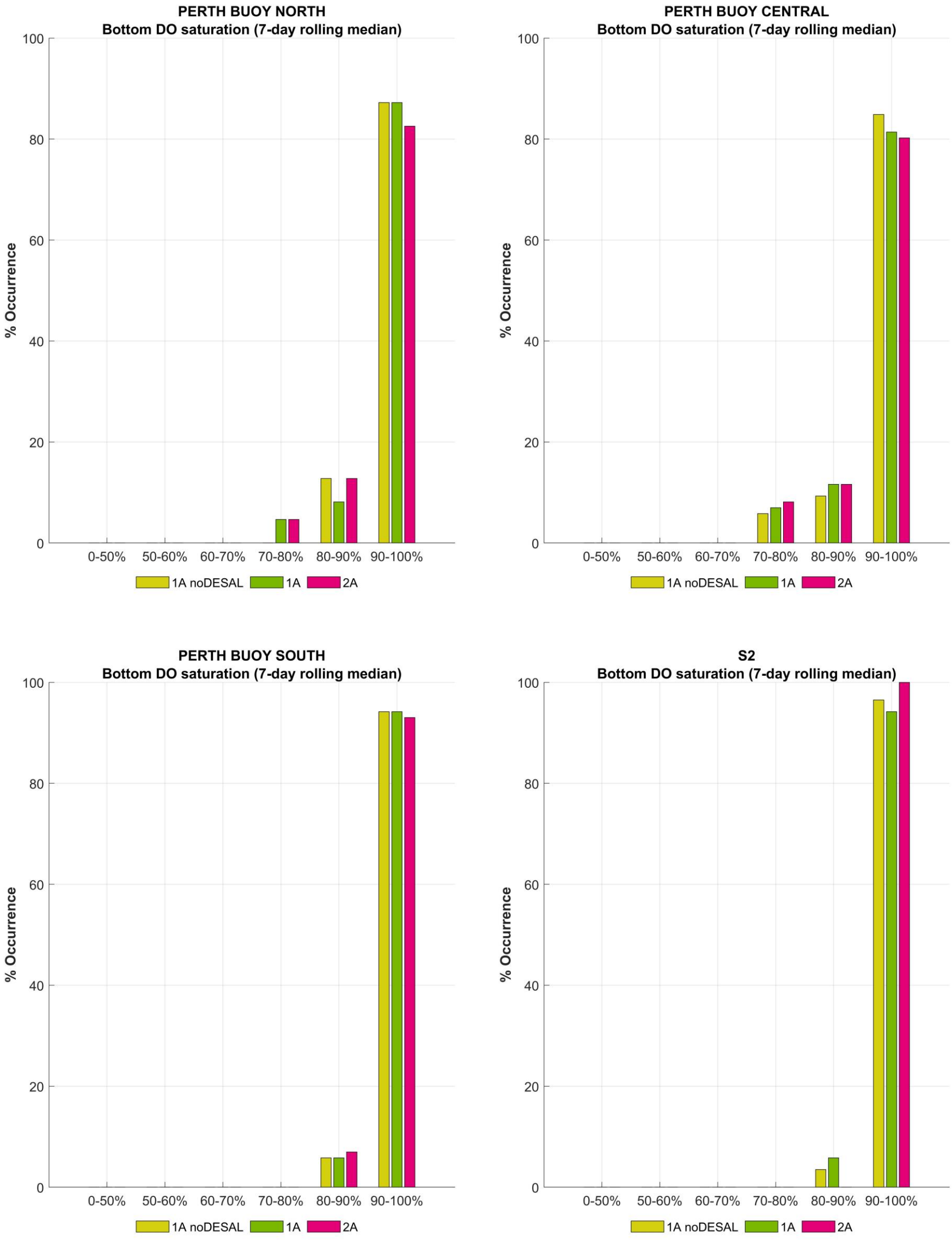

Figure 3-80 Histograms of median near bed DO saturation occurrence across different DO saturation bands in Winter 2008

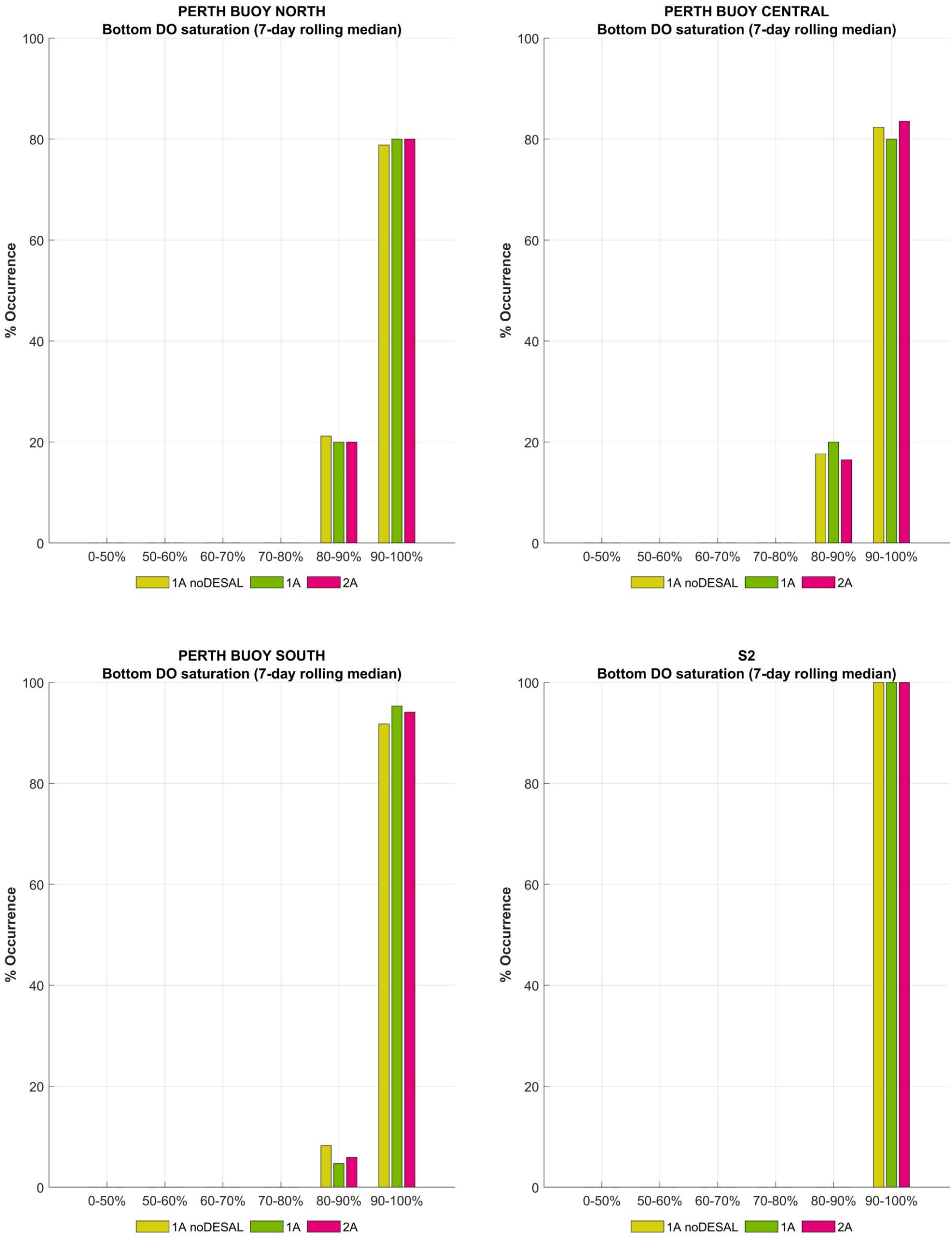

Figure 3-81 Histograms of median near bed DO saturation occurrence across different DO saturation bands in Spring 2008

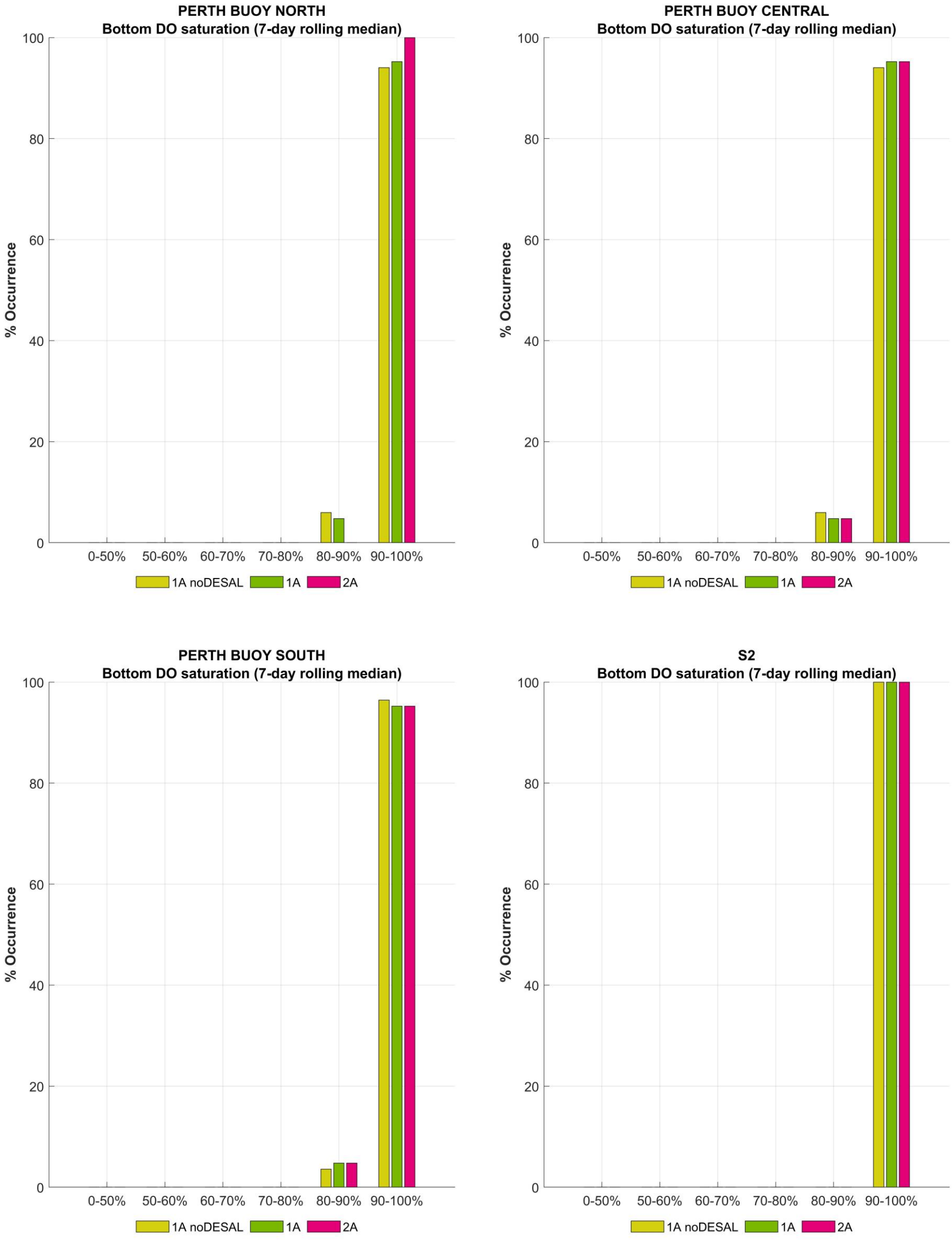

Figure 3-82 Histograms of median near bed DO saturation occurrence across different DO saturation bands in Summer 2008-09

Discharge signatures

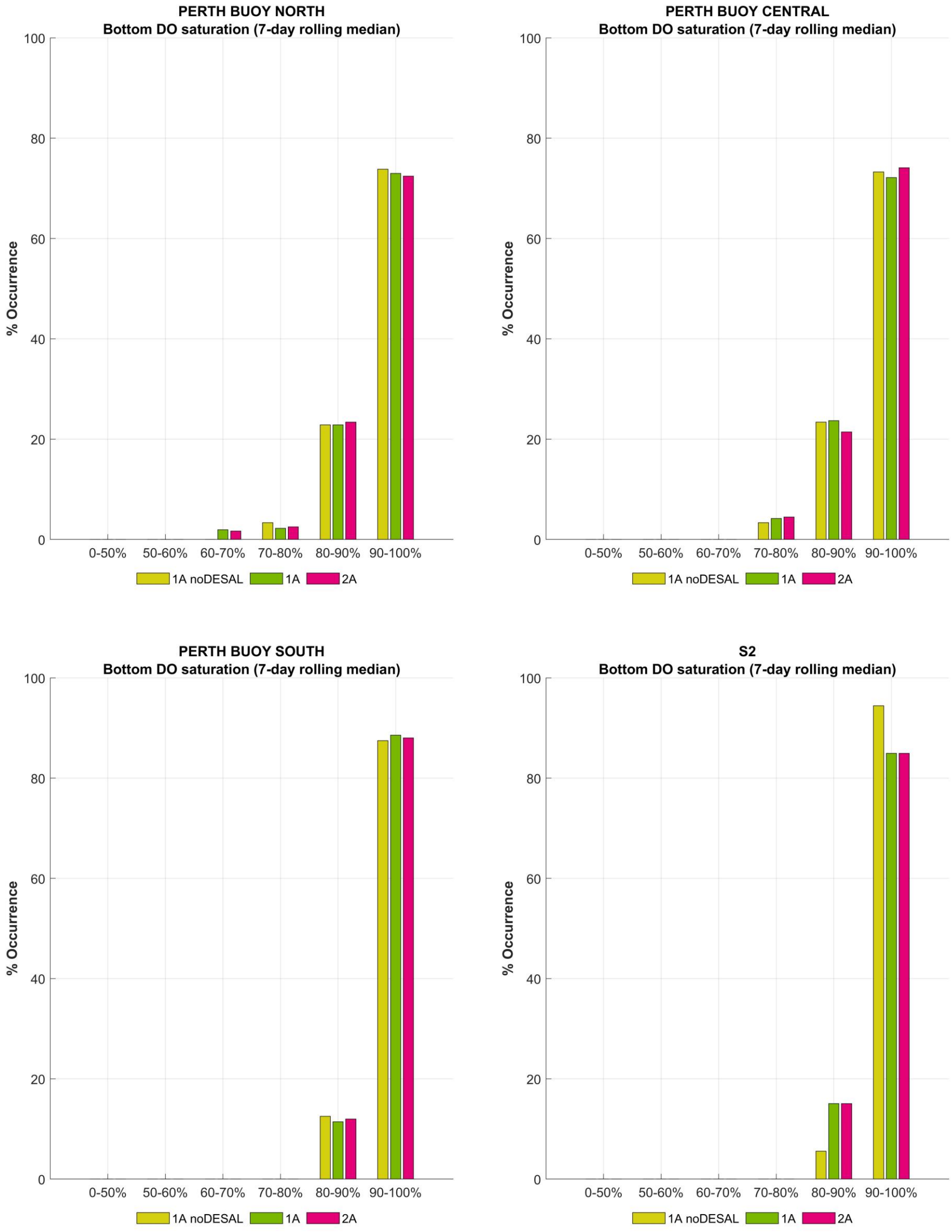

Figure 3-83 Histograms of median DO saturation occurrence across different DO saturation bands in Mar 2008 – Mar 2009

The DO saturation occurrence histograms reflect the occurrence maps, with the more frequent low DO occurring over the Apr 2013 and Autumn 2008 periods. Apr 2103 was the only case to present median DO saturations in the bands 50-60%. At Perth Buoy North and Central, conditions were below 70% DO saturation for more than approximately 50% of the time (all scenarios), whilst at South Buoy, occurrences on this band were just under 35% of the time. The discharge cases presented marginally more occurrences of low DO in those saturation bands (i.e. 50-60% and 60-70% bands).

At S2 in Apr 2013, the saturated discharge was sufficient to keep more oxygenated conditions for scenarios 1A, 2A and 2C in comparison to the baseline scenario.

With the exception of the Apr 2013 period, the median DO saturation occurrences were more frequently in the bands higher than 80%, owing to the more favourable mixing conditions and, for winter and spring, lower sediment oxygen demand associated with the lower temperatures.

For the end of summer and autumn simulations (i.e. Feb-Mar 2008, Autumn 2008 and Apr 2013), the median DO saturation was more frequently low in comparison to the other seasons. Interestingly, the baseline scenario in Apr 2013 at S2 had more occurrences of lower DO than the discharge scenarios (scenarios 1A, 2A and 2C). Also, more frequent low DO saturation occurrences were simulated for Perth Buoy North and Central in comparison to Perth Buoy South and S2. The reason for lower concentrations at those deep basin stations was likely the naturally-occurring stronger stratification as lower density waters enter the Sound through the northern entrance, reducing the potential of surface re-aeration (see BMT 2018a).

To highlight the relationship between lower density water incursions through the northern Sound entrance, the near bed DO saturation (in this case not the medians) for the conditions in Feb-Mar 2008 was plotted in conjunction with near surface and near bed density differences (Figure 3-84 to Figure 3-85, see also Appendix E for the seasonal and year-long simulation results). The density differences were also subdivided into density differences due to salinity alone, and due to temperature alone.

3.3.4.6 Density difference and near bead DO saturation

The near bed and near surface density difference and near bed DO saturation are presented in Figure 3-84 and Figure 3-85, with seasonal simulation presented in Appendix E. The figures show the density difference for all scenarios (1A noDESAL, 1A, 2A, and 2C, noting scenario 2C is only available for Apr 2013 and Autumn 2008 simulations) and the components of the density difference that relate to temperature and salinity.

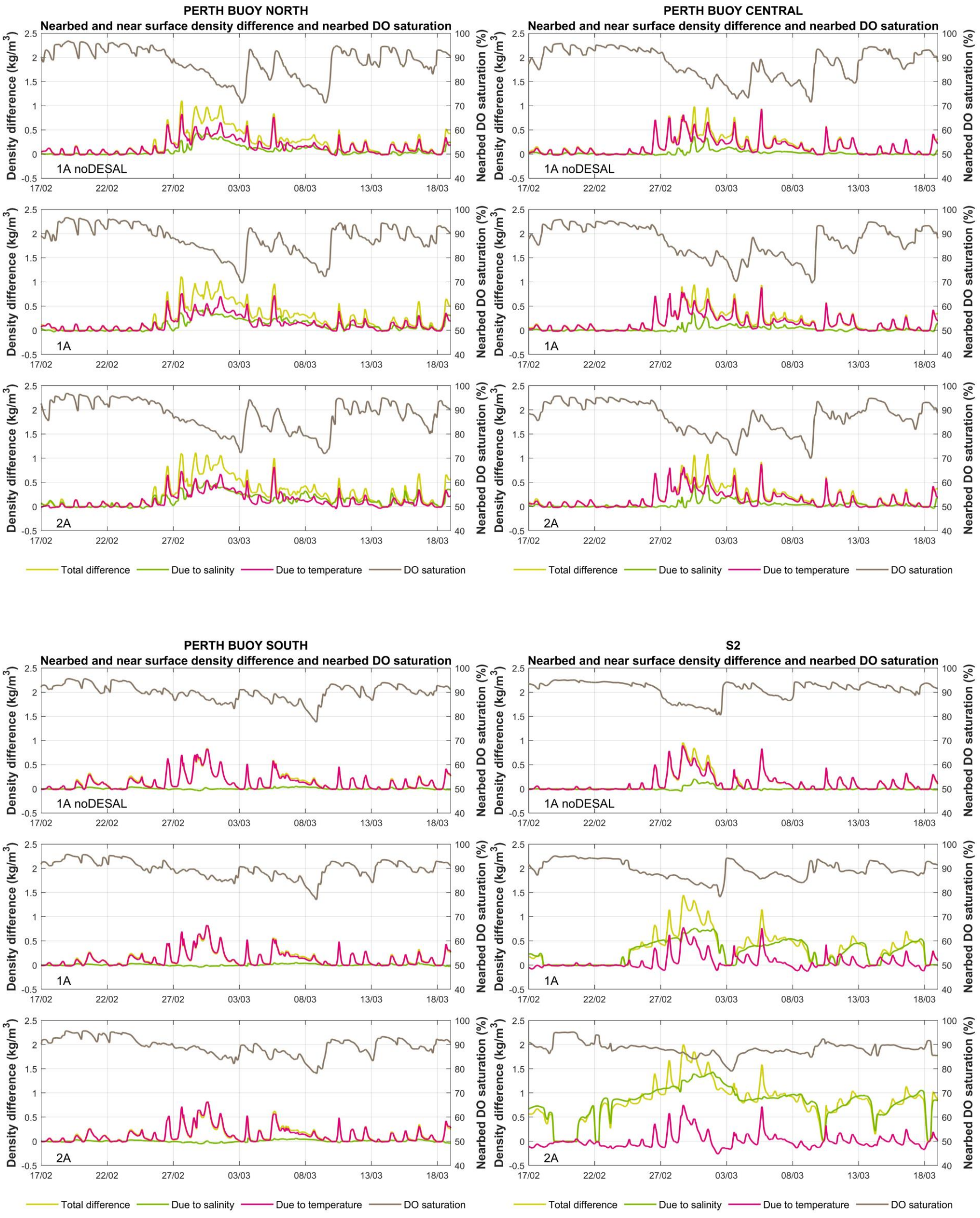

Figure 3-84 Near surface and near bed density differences in conjunction with near bed DO saturation for the ambient conditions in Feb-Mar 2008. Top panel: Scenario 1A noDESAL. Middle panel: Scenario 1A. Lower panel: Scenario 2A.

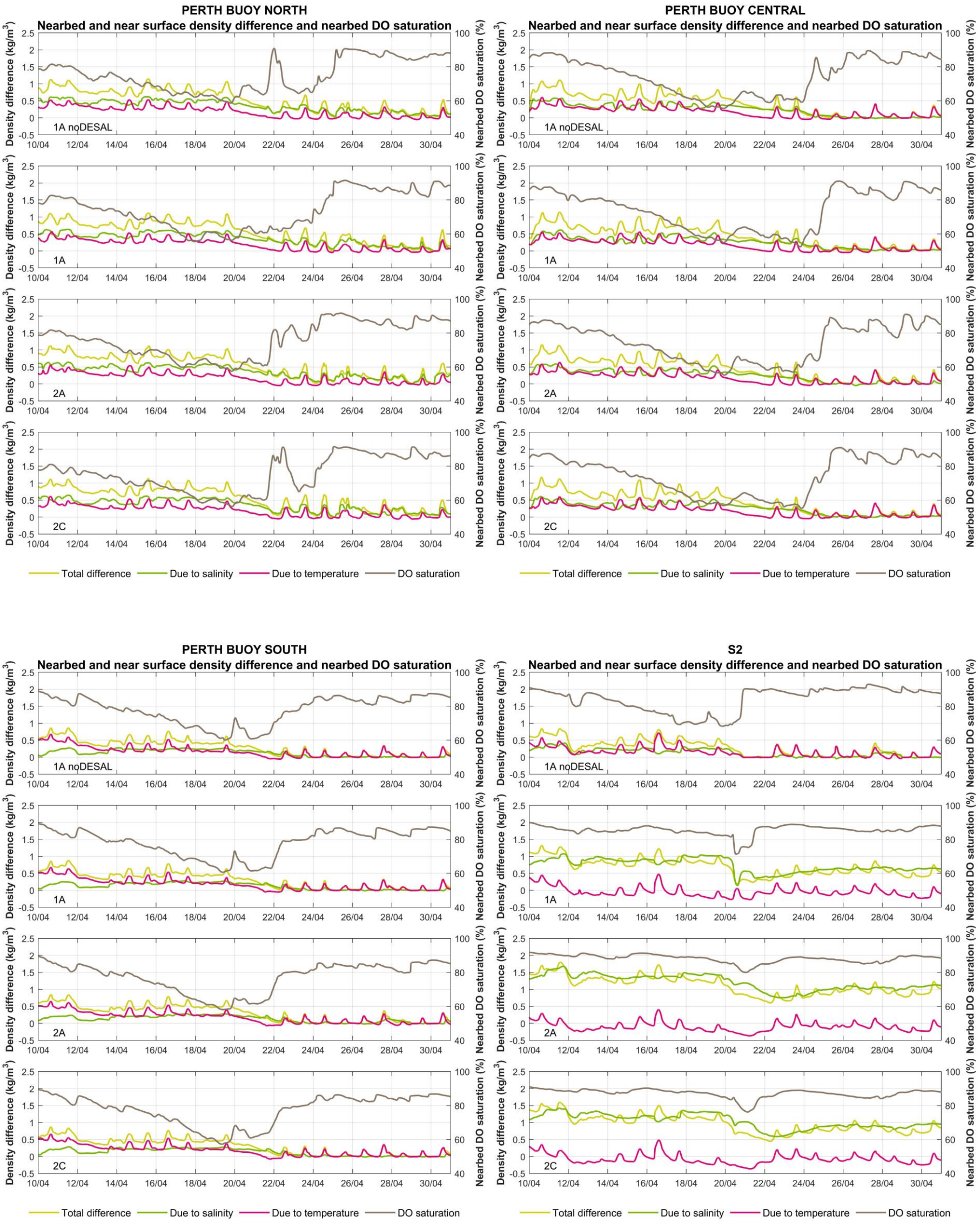

Figure 3-85 Near bed and near surface density difference and near bed DO saturation timeseries comparisons for ambient conditions in Apr 2013. Top panel: Scenario 1A noDESAL. Top middle panel: Scenario 1A. Lower middle panel: Scenario 2A. Lower panel: Scenario 2C.

For all locations, all scenarios show that the decrease in DO and increase in density difference are coincident. At S2, however, despite the larger density differences in the discharge scenarios, DO saturation was not as low as the baseline scenario. Again, as explained earlier, this was a manifestation of the high DO in the discharges themselves.

In the deep basin, effects of temperature and salinity on density at Perth Buoy North were similar for all scenarios. For the Apr 2013 period, this was also the case for Perth Buoy South and Perth Buoy Central, whereas temperature had a more predominant effect on salinity in Feb-Mar 2008 period. Increases in density difference across scenarios were very modest and were due to the increased near bed salinity. These density difference increases were however smaller than 0.05 kg/m^3 at North Buoy and Central Buoy and practically inexistent at South Buoy.

At S2, however, for the desal scenarios (1A, 2A and 2C), density differences due to salinity were generally larger than due to temperature, particularly for scenarios 2A and 2C. For the baseline scenario, salinity barely had an effect on density. For scenarios 2A and 2C, the warmer discharge had in some instances a contrary effect on density (i.e. reducing density difference). These were however very small in comparison to the salinity effects alone.

4 Intake Assessment

The intake assessment comprises an evaluation of *Pagrus auratus* (snapper fish) eggs and larvae entrainment on the PSDP1 and PSDP2 intakes and its effects on viable larvae (i.e. those that survive and become fish at the end of the larvae life-cycle period). This assessment was undertaken with the combination of TUFLOW FV's particle-tracking module to simulate larvae movement and a stochastic approach to quantify larvae that entrain into the intakes. Details are described below.

4.1 Period

The simulation period was from September 2008 to January 2009 to mirror the spawning season in Cockburn Sound. The intake assessment was undertaken for scenario 2A only.

4.2 Approach

Movement of larvae was simulated using a particle tracking approach. This approach assumes the larvae cannot swim and are dispersed by the action of the currents in Cockburn Sound. The terms particle and larvae will therefore be used interchangeably throughout this section.

TUFLOW FV Particle Tracking Module (PTM) module was adopted for these simulations. PTM is based on a Lagrangian tracking scheme and driven by three-dimensional currents. The Lagrangian PTM approach in TUFLOW FV allows for high resolution meshless representation of particles' advection, dispersion, deposition and resuspension. For the current assessment, deposition and resuspension were not simulated.

The movement of the Lagrangian particles includes a deterministic component derived from modelled currents in TUFLOW FV and a stochastic random walk component to represent vertical and horizontal dispersive processes due to unresolved turbulent scales. The particles remain in suspension throughout the model domain under the influence of tides and currents.

4.3 Initial conditions

4.3.1 Lateral distribution

The temporal and spatial patterns of snapper spawning in Cockburn Sound have been well documented (Wakefield, 2006). Specifically, snapper have been found to aggregate in similar locations during the spawning season, albeit with some interannual variation. Surveys in 2001 to 2004 found that the main spawning aggregations occur during October, November and December and rotate clockwise around Cockburn Sound from Woodman Point in October, to the north-west of James Point in November, and then near the centre of Cockburn Sound and toward Garden Island in December (Figure 4-1). From the aggregation patterns, generalised spawning patterns have been formulated.

This generalised spawning pattern was adopted as release locations for the particles within TUFLOWFV (Figure 4-2). The water depths in these areas range from 4 to 23 m, with the average depth of the October and November sites from 11 to 14 m and the December site averaging 20 m depth.

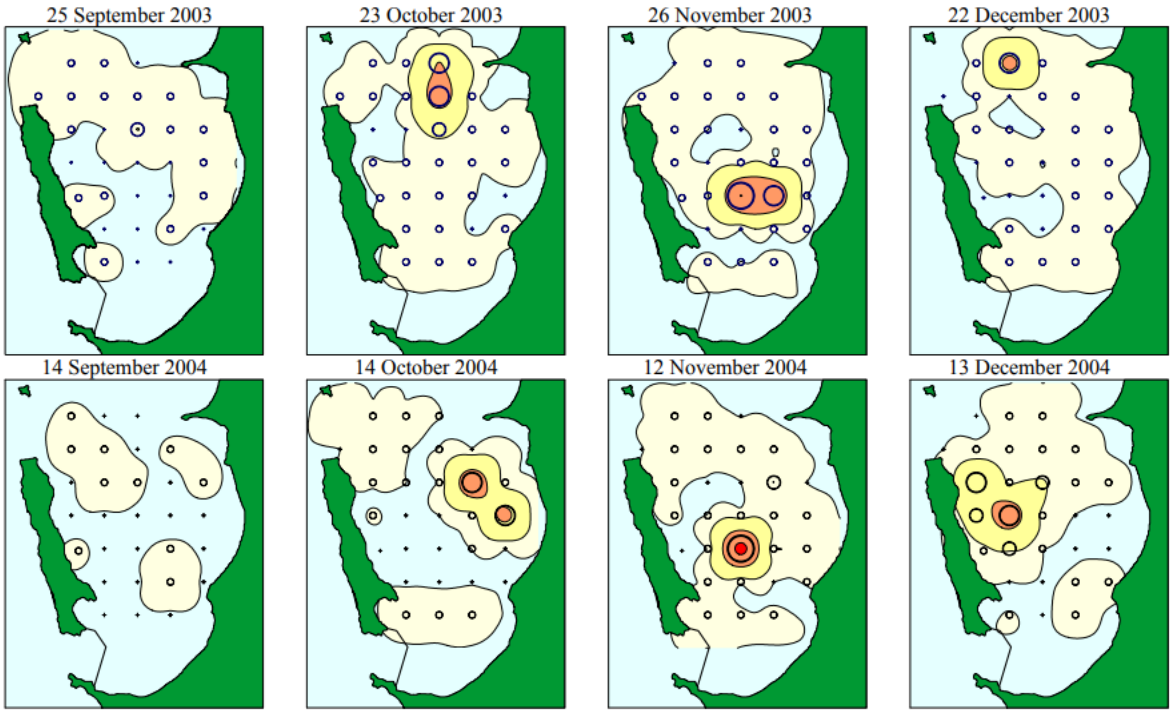

Figure 4-1 Distribution of eggs during the four new moons with the orange areas representing a concentration of 40,000 – 80,000 per m³ and red above 80,000 per m³ (Wakefield, 2006)

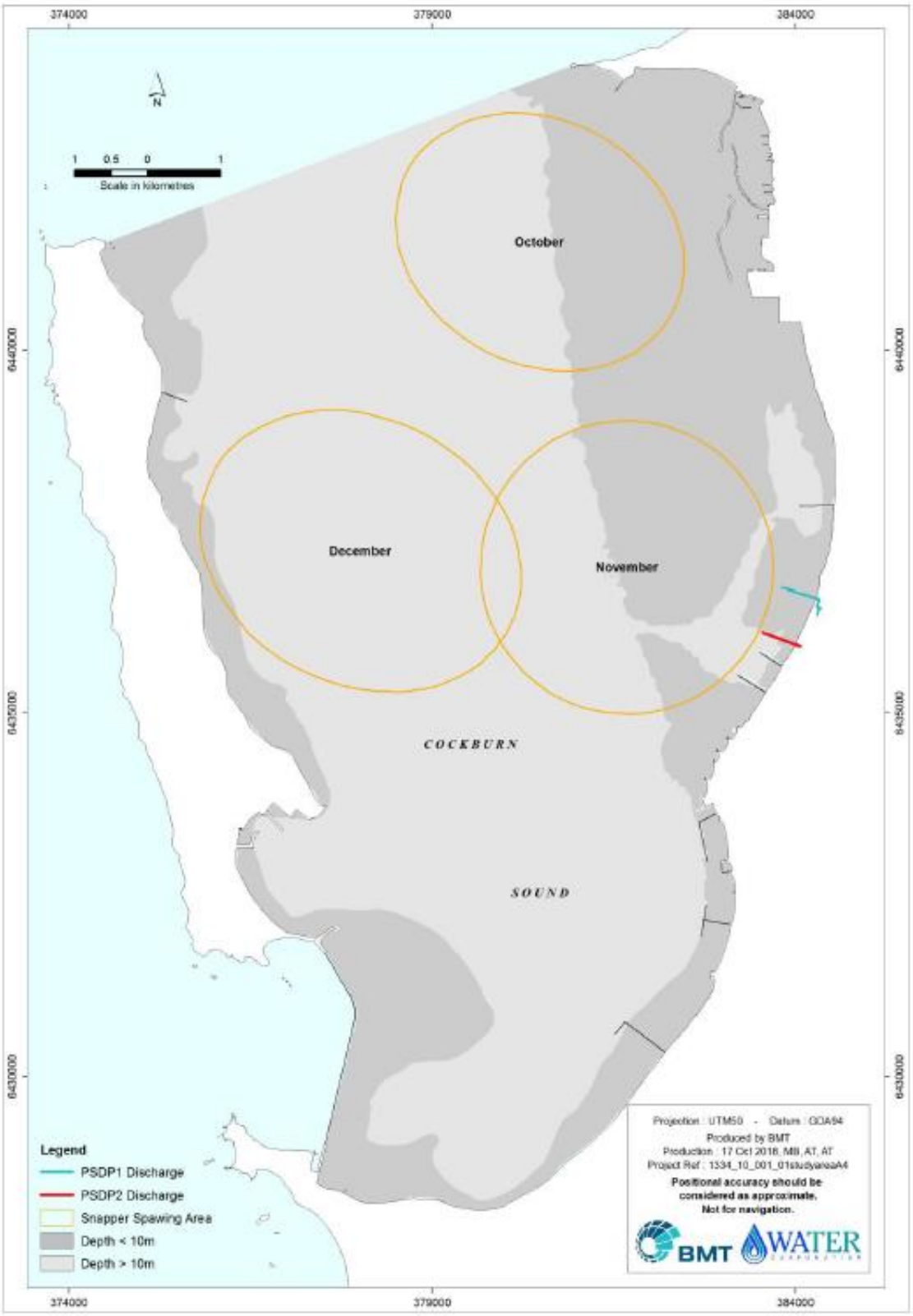

Figure 4-2 Generalised spawning patterns assumed in the modelling

4.3.2 Temporal distribution

The spawning of snapper in Cockburn Sound occurs when average surface water temperatures are 19 to 20^{o}C (Wakefield 2006, Figure 4-3). The average spawning numbers within Cockburn Sound are low in September and January, with peak spawning occurring in the month of November (the exception was 2002 when the peak occurred in December). For modelling purposes, it has been determined that the level of spawning during September and January is generally so low as to be negligible and therefore only simulate the release of eggs over October, November and December.

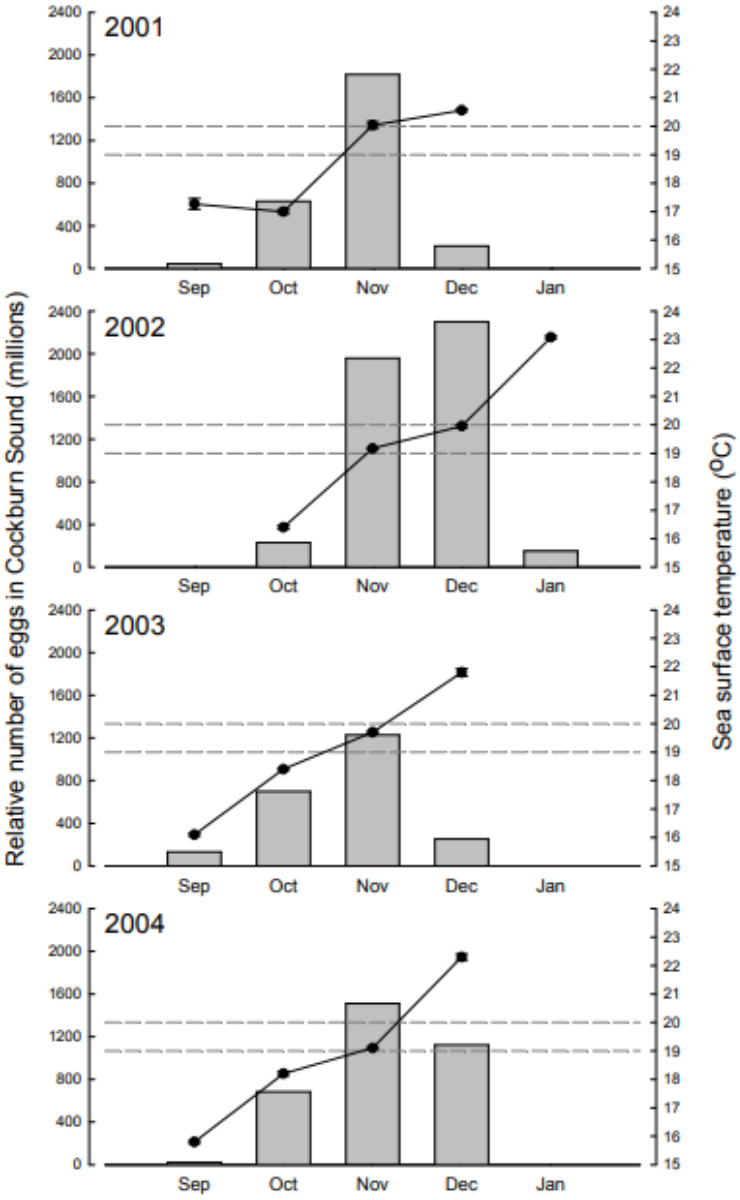

Figure 4-3 Volume estimates of spawn rates per month on the full moon in Cockburn Sound. The mean water temperature on the surface is represented by the black circles (Wakefield 2006).

Snapper spawn bimodally with peak spawning following the new moon, and to a lesser extent, the full moon, during the night in the three hours following high tide (Wakefield 2006) (Figure 4-4). Therefore, the particle modelling included two releases during the month: one at the new moon, and another, less prominent, at the full moon. In both events, spawning was simulated over three hours after high tide at night.

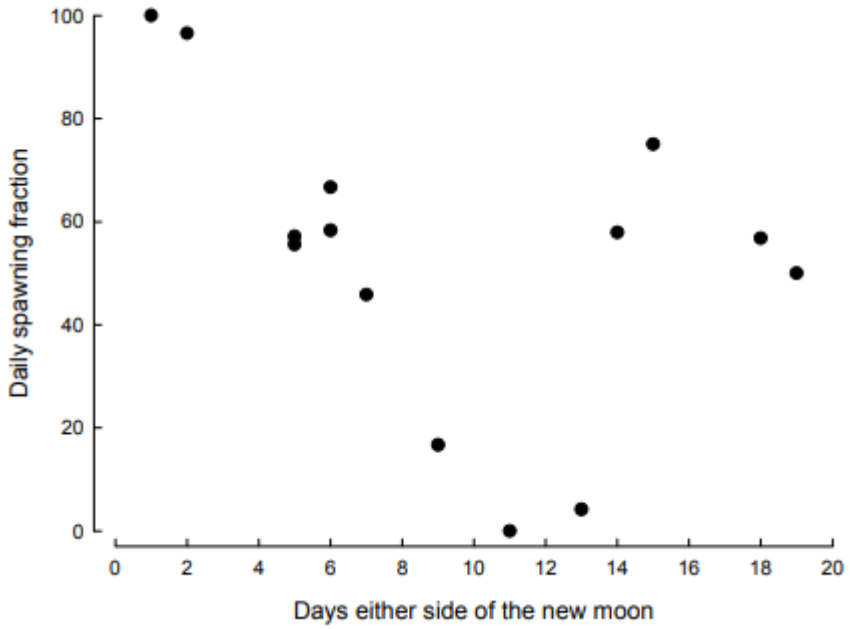

Figure 4-4 Spawning fractions relative to the lunar cycle (Wakefield 2006)

Moon phases in 2008 were determined from data obtained from the Perth Observatory. Table 4-1 shows the new and full moon occurrences during the months of September to December 2008 and therefore the starting times for the spawning events assumed in the modelling.

Flow conditions at the start of the TUFLOW FV PTM simulations were well established (i.e. they were not from cold starts) as they were based on re-starts from the seasonal runs presented in Section 3.

Table 4-1 Occurrences of the new and full moon during the simulation period with the coinciding high tide time

Date	Moon Phases	High Tide	Simulation
29/09/2008 16:12	New Moon	29/09/2008 22:00	October New
15/10/2008 04:02	Full Moon	15/10/2008 21:30	October Full
29/10/2008 07:14	New Moon	29/10/2008 20:30	November New
13/11/2008 13:17	Full Moon	19/11/2008 21:00	November Full
28/11/2008 00:54	New Moon	29/11/2008 21:00	December New
13/12/2008 00:37	Full Moon	13/12/2008 22:00	December Full

4.3.3 Depth distribution

The depth of particles release was based on research and modelling of snapper eggs and larvae in Shark Bay, Western Australia, between 1997 and 2000 (Jackson 2007), which showed that in depths of 10 to 14 m, snapper spawning occurred between 3 and 5 metres below the surface. These release depths were applied across the entire release zones and spawning periods.

4.3.4 Number of released particles

The information above has been used to generate the proportion of eggs released relative to the maximum average reported to occur in November (Wakefield 2010). The average release during November is estimated to be the order of 1,625 million eggs (Wakefield 2010). From Wakefield (2010), a proportional number of eggs released per event was derived for modelling purposes (Table 4-2).

Table 4-2 Generalised abundance of eggs relative to peak average event (November new moon) based on Wakefield (2010)

Moon Phase	September	October	November	December	January
New	0	34%	100%	58%	0
Full	0	25%	75%	44%	0

The numbers in Table 4-3 were then applied for a simulation within each of the spawning periods. Due to number of particles and the limitations in computational power, the total number of particles released in the model were scaled by a factor of 1,000. This meant that each particle in the model represents 1,000 larvae.

Table 4-3 TUFLOW FV Particle Tracking Module release totals for each simulation

Date	Moon Phases	Scale Factor	Total Eggs	Particles
29/09/2008 16:12	New Moon	0.34	552,500,000	552,500
15/10/2008 04:02	Full Moon	0.25	406,250,000	406,250
29/10/2008 07:14	New Moon	1.00	1,625,000,000	1,625,000
13/11/2008 13:17	Full Moon	0.75	1,218,750,000	1,218,750
28/11/2008 00:54	New Moon	0.58	942,500,000	942,500
13/12/2008 00:37	Full Moon	0.44	715,000,000	715,000

4.4 Parameters

Table 4-4 summarises the model parameters adopted for the simulations.

Table 4-4 TUFLOW FV PTM model parameters

Particle scalar mass	0.001kg
Horizontal dispersion	0.1 m^2/s
Vertical dispersion coefficient	1.0
Settling model	None (neutrally buoyant particles)
Erosion model	None (no erodible particles from the bed)

4.5 Mortality

The mortality of snapper eggs and larvae in the wild is affected by a range of variables i.e. predators, temperature, density, visibility. Partridge and Michael (2010) have estimated the daily mortality rate to be 21.3% for snapper eggs and larvae in the wild, before they become motile.

Mortality was not accounted for in the TUFLOW FV PTM simulation. Rather, it was accounted for in the post-processing, using a random selection of particles (the *randperm* function in Matlab®) that were removed at each output time step (15 minutes). This way, using the same mortality rate, several permutations (or replicates, being equally valid given the random selection) of dead particles could be obtained. This provided some statistical bounds to the analysis, rather than reporting a single number only.

It was assumed there were no areas of preferential mortality (i.e. due to predation).

4.6 Entrainment

Entrainment was also accounted for during post-processing following Largier et al. (2007), assuming it is a function of radial distance from the intake locations. This model assumes larvae that pass directly over the intake structure will have a high likelihood of being entrained, whereas larvae passing the intake at a distance have a lower likelihood, and beyond a certain distance there is no chance of entrainment. The probability of entrainment of a particle is given by the distance from the intake r:

$$P(r) = b\left(1 - \frac{r}{r_o}\right)$$

where $P(0) = b$ and $P(r_o) = 0$. A conservative assumption $b = 1$ was adopted in the modelling. r_o can be defined by the following relationship (Largier et al. 2007):

$$r_o = \sqrt{\frac{3\Delta t Q_0}{\pi b h}}$$

where Δt is the time step, Q_0 is each of the intakes flow rates, and h is the thickness of influence of the intake structure, here assumed to be 5.0 m for each of the intakes (2.5 m above and below the centre of the intake). The model configuration for Scenario 2A was assumed in the simulations, leading to r_o = 26.4 m for PSDP1 and r_o = 26.5 m for PSDP2.

For each time step, all particles within r_o and the thickness of influence of the intakes were selected. The particles that effectively entrained into the intakes were calculated from random selection of

those particles assuming a probability given by $P(r)$. These were then removed from the particle population for the next time step calculation. Again, these allowed for several permutations or replicates to be undertaken for each of the spawning events. Simulations assuming entrainment only at PSDP1, only at PSDP2, and at both intakes were run independently to isolate the entrainment of a single intake and the combination of both.

4.7 Lifecycle

After a period of 20-25 days, larvae become more developed and motile and as such, modelling of the particles was restricted to the more conservative period of 25 days. In this case, it was assumed that after 25 days all live particles will amount to the viable larvae (i.e. those that turned into fish). Assuming a larger life span is conservative in the modelling, as it creates a larger effect of mortality on the final population numbers and allows a higher probability of larvae being entrained into the intakes.

4.8 Position in water column and buoyancy

Although others (e.g. Le Port et al. 2014) have found that in deeper waters, snapper larvae may be concentrated at different heights of the water column (hypothesised to be feeding on phytoplankton), Cockburn Sound is relatively shallow and well mixed, and as per Doak (2004) and Nahas et al. (2003), the eggs and larvae will be treated as neutrally buoyant and well mixed through the water column. This is likely a conservative assumption (i.e. produces higher intake entrainment rates), as the motility behaviour is likely to drive the particles away from the zone of intake influence.

4.9 Results

4.9.1 Particle movement

For ease of presentation, the October 2008 full moon event has been chosen to illustrate the general movement of particles, as predicted by the TUFLOW FV PTM model. As such, a series of time stamped contour maps are presented in Figure 4-5.

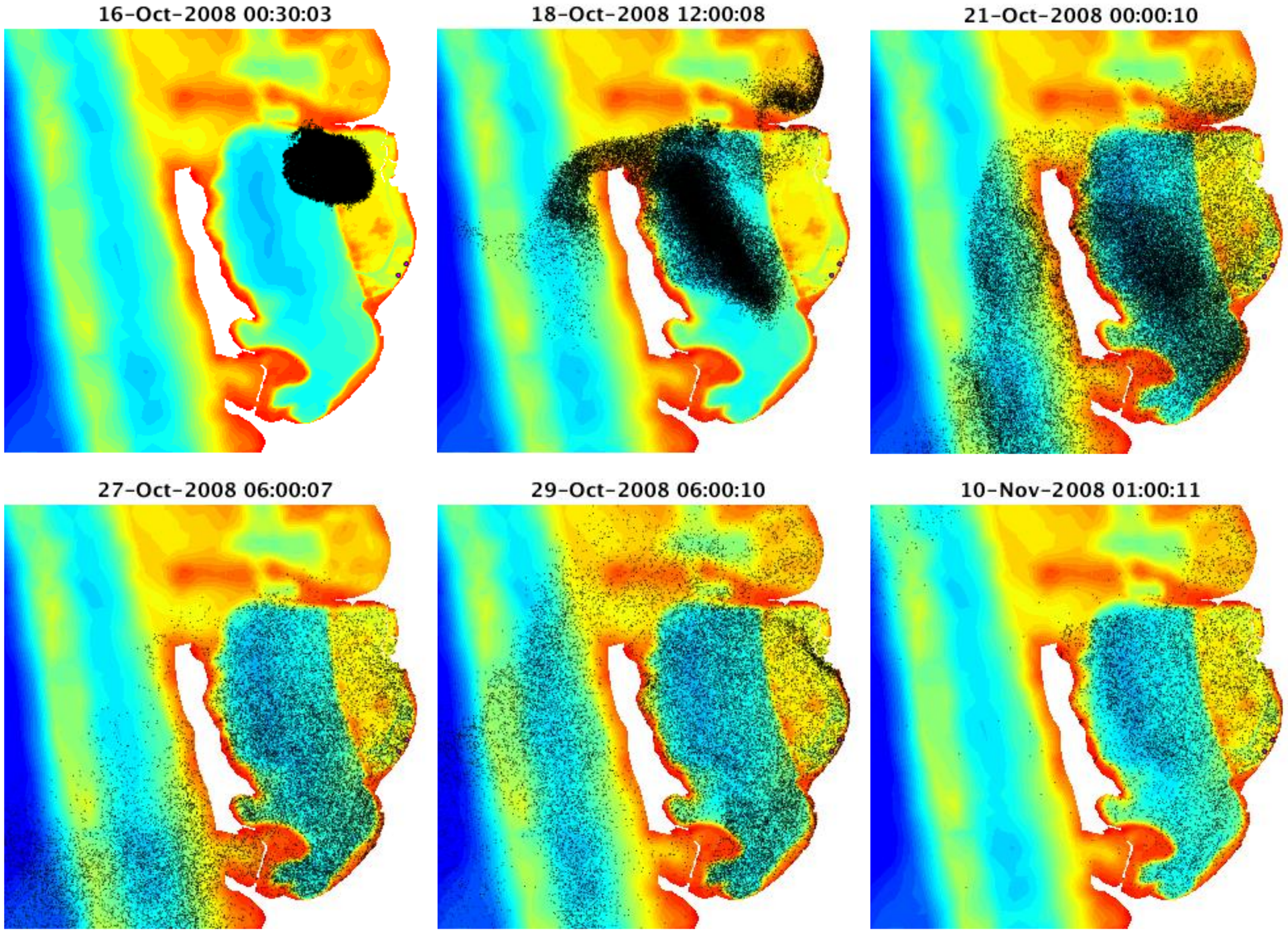

Figure 4-5 Snapshots of a subset of the released particles (approximately 50,000) following the spawning event during full moon of October 2008. Particles are the black dots, whilst the colours represent the model bathymetry. Results from TUFLOW FV PTM without post-processing.

4.9.2 Viable and entrained larvae

The number of entrained and viable larvae following post-processing of the TUFLOW FV PTM results are shown in Table 4-5 under the range of scenarios considered. The “number of surviving larvae at the end of simulation” refer to the larvae that were neither entrained into the intake structures nor died within the 25 days of their release.

The results are consistent across simulations, with the largest proportional difference in viable larvae due to entrainment being the December 2008 full moon spawning event (showing up to 1.3% decline in the number of available larvae). In general, the model predicts a larger proportion of total entrainment occurring at the PSDP1 intake.

Table 4-5 Viable and entrained larvae for each of the spawning events

Spawning Event		Full Moon (October 2008)	New Moon (October 2008)	Full Moon (November 2008)	New Moon (November 2008)	Full Moon (December 2008)	New Moon (December 2008)
Number of larvae released (000's)		406,280	552,745	1,218,100	1,625,560	715,150	942,585
Number of permutations		100	100	100	100	100	100
Number of surviving larvae at the end of simulation (range in 000's)	Without entrainment	1942	2,647	5,826	7,773	3,418	4,510
	With PSDP1 entrainment only (range)	1935 – 1940	2,632 - 2,638	5,785 – 5,797	7,731 - 7,743	3,394 – 3,400	4,481 – 4,487
	With PSDP2 entrainment only (range)	1936 – 1940	2,636 - 2,641	5,798 – 5,805	7,741 - 7,751	3,397 – 3,406	4,484 – 4,494
	With PSDP1 and PSDP2 entrainment (range)	1931 – 1936	2,623 - 2,632	5,758 – 5,774	7,703 - 7,717	3,373 – 3,389	4,460 – 4,472
Number of entrained larvae (in 000's)	With PSDP1 entrainment only (range)	82 – 129	319 – 398	1,298 – 1,458	1,064 – 1,254	817 – 935	1,039 – 1,191
	With PSDP2 entrainment only (range)	96 – 144	237 – 331	1,130 – 1,263	735 – 853	617 – 718	759 - 881
	With PSDP1 and PSDP2 entrainment (range)	200 - 270	594 - 712	2,528 – 2,721	1,904 – 2,064	1,455 – 1,609	1,817 – 2,015
Proportion of surviving larvae in the simulations with entrainment in comparison to simulation without entrainment	With PSDP1 entrainment only (range)	0.10% – 0.36%	0.34% - 0.57%	0.50% - 0.70%	0.39% - 0.54%	0.53% - 0.70%	0.51% - 0.64%
	With PSDP2 entrainment only (range)	0.10% – 0.31%	0.23% - 0.42%	0.36% - 0.48%	0.28% - 0.41%	0.35% - 0.61%	0.36% - 0.58%
	With PSDP1 and PSDP2 entrainment (range)	0.31% – 0.57%	0.57% - 0.91%	0.89% - 1.17%	0.72% - 0.90%	0.85% - 1.32%	0.84% - 1.11%

5 References

BMT (2018a), *Perth Desalination Plant Discharge Modelling: Model Validation*, prepared for Water Corporation, August 2018. Ref: R.B22253.002.04.ModelValidation_PRP.

BMT (2018b), Assessment of impacts of proposed desalination plant on fish stocks in Cockburn Sound, memo dated 16 October 2018 Rev2

BMT WBM (2011). Hydrodynamic and Water Quality Modelling of Spencer Gulf: Model Validation Report. Final Report – Included as Appendix H5.2 of the Olympic Dam Supplementary EIS, available at http://www.bhpbilliton.com/home/aboutus/regulatory/Documents/Olympic%20Dam%20Supplementary%20EIS/Appendices/Appendix%20H5.2_Spencer%20Gulf%20Model%20Validation%20Report.pdf.

BMT WBM (2014). Port Pirie Marine Modelling Assessment of Cooling Water Discharge Modelling: Upgraded Models'Assessments. Report n.R.B20995.001.00.

BMT WBM (2015). Sepia Depression Ocean Outlet Monitoring and Modelling – Nearfield Model Validation. Report n. R.20467.005.00

Botelho, D. A, Barry, M.E., Collecutt,G.C., Brook, J. and Wiltshire, D., 2013. Linking near- and farfield hydrodynamic models for simulation of desalination plant brine discharges. Water Science & Techn., 67, 1194-1207. doi:10.2166/wst.2013.673.

Botelho, D.A., Teakle, I.L., Barnes, M., Barry, M.E., Baheerathan, R., Shiell, G. and Collecut, G.C. (2016). Linking Nearfield CFD Models of Buoyant Discharges to Farfield Dispersion Models. In: Proceedings of the International Symposium on Outfall Systems 2016, Ottawa, ON, Canada.

Centre for Water Research (CWR) (2009) Kwinana Quays: Hydrodynamic Modelling of Cockburn Sound. Final Report. 124 pp.

Cummings, J.A. and Smedstad, O. M., 2013: Variational Data Assimilation for the Global Ocean. Data Assimilation for Atmospheric, Oceanic and Hydrologic Applications vol II, chapter 13, 303-343.

D'Adamo, N. (2002). Exchange and Mixing in Cockburn Sound, Western Australia: A Seasonally Stratified, Micro-tidal, Semi-enclosed Coastal Embayment. PhD Thesis, University of Canterbury, New Zealand. 482 pp.

Department of Environment Protection (DEP), (1996). Southern Metropolitan Coastal Waters Study (1991-1994). Final Report.

Doak, C., (2004). Hydrodynamic modeling of snapper (Pagrus auratus) eggs and larvae in Cockburn Sound. BSc (Hons) thesis, University of Western Australia, Perth

Egbert, G.D. and Erofeeva, S.Y., 2002: Efficient Inverse Modeling of Barotropic Ocean Tides. J. Atmos. Oceanic Technol., 19, 183204. doi: http://dx.doi.org/10.1175/1520-0426(2002)019<0183:EIMOBO>2.0.CO;2

Jackson, G. (2007), Fisheries biology and management of pink snapper, Pagrus auratus, in the inner gulfs of Shark Bay, Western Australia, Murdoch University Western Australia.

Largier, J.L., White, J.W., Clarke, L., and Nichols, K.J. (2007). Assessment of larval entrainment by cooling water intake systems: models of larval dispersal and recruitment incorporating coastal boundary layer flow. Report prepared for California Energy Commission.

Le Port, A., Montgomery, J., and Croucher, A. (2014). Biophysical modelling of snapper *Pagrus auratus* larval dispersal from a temperate MPA. Marine Ecology Progress Series. 515. 203-215.

Nahas EL, Jackson G, Pattiaratchi CB, Gregory IN (2003) Hydrodynamic modelling of snapper *Pagrus auratus* egg and larval dispersal in Shark Bay, Western Australia: reproductive isolation at a fine spatial scale. Marine ecology progress series 265:213–226.

Newgen (2014) Newgen Power Station Kwinana: Marine Environment Temperature Elevation Management Plan (METEMP). Amended September 2014. 26 pp.

Partridge, G J and Michael R J, 2010 Direct and indirect effects of simulated calcareous dredge material on eggs and larvae of pink snapper Pagrus auratus. Journal of Fish Biology 77: 227-240

Riley, J.P., and Skirrow, G. (1974). Chemical Oceanography Academic Press, London.

Roberts, P.J.W., and Abessi, O. (2014) Multiport Diffusers for dense Discharges. Journal of Hydraulic Engineering, 140(8).

Roberts, P.J.W., Ferrier, A. and Daviero, G. (1997) Mixing in Inclined Dense Jets. Journal of Hydraulic Engineering, 123(8).

URS (2014) Summary of compliance monitoring results for process water discharges to Cockburn Sound - July 2013 to June 2014. Report prepared for Synergy. 304 pp.

Wakefield, C.B. (2006). Latitudinal and temporal comparisons of the reproductive biology and growth of snapper, Pagrus auratus (Sparidae), in Western Australia, Murdoch University Australia.

Wakefield, C.B. (2010) Annual lunar and diel reproductive periodicity of a spawning aggregation of sapper Pagurs auratus (Sparidae) in a marine embayment of the lower west coast of Australia, Journal of Fish Biology 77: 1359-1378.

Water Corporation (2013) Perth Seawater Desalination Plant Marine Monitoring & Management Plan. Final Report, August 2013.

Appendix A Salinity Results – Timeseries

Salinity Results – Timeseries

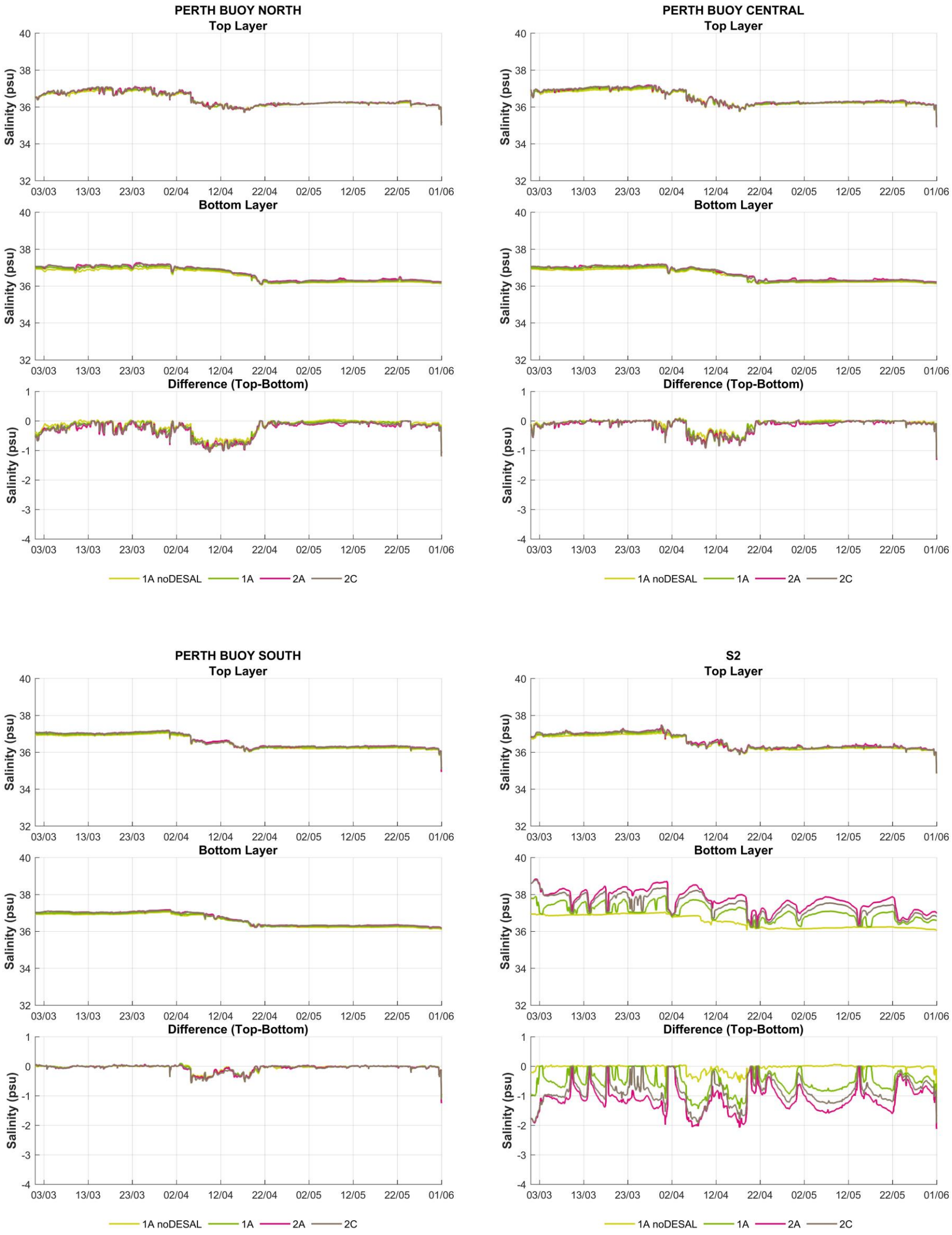

Figure A-1 Salinity timeseries comparisons for top and bottom waters at Perth Buoy North, Perth Buoy Central, Perth Buoy South and S2 (Autumn 2008)

Salinity Results – Timeseries

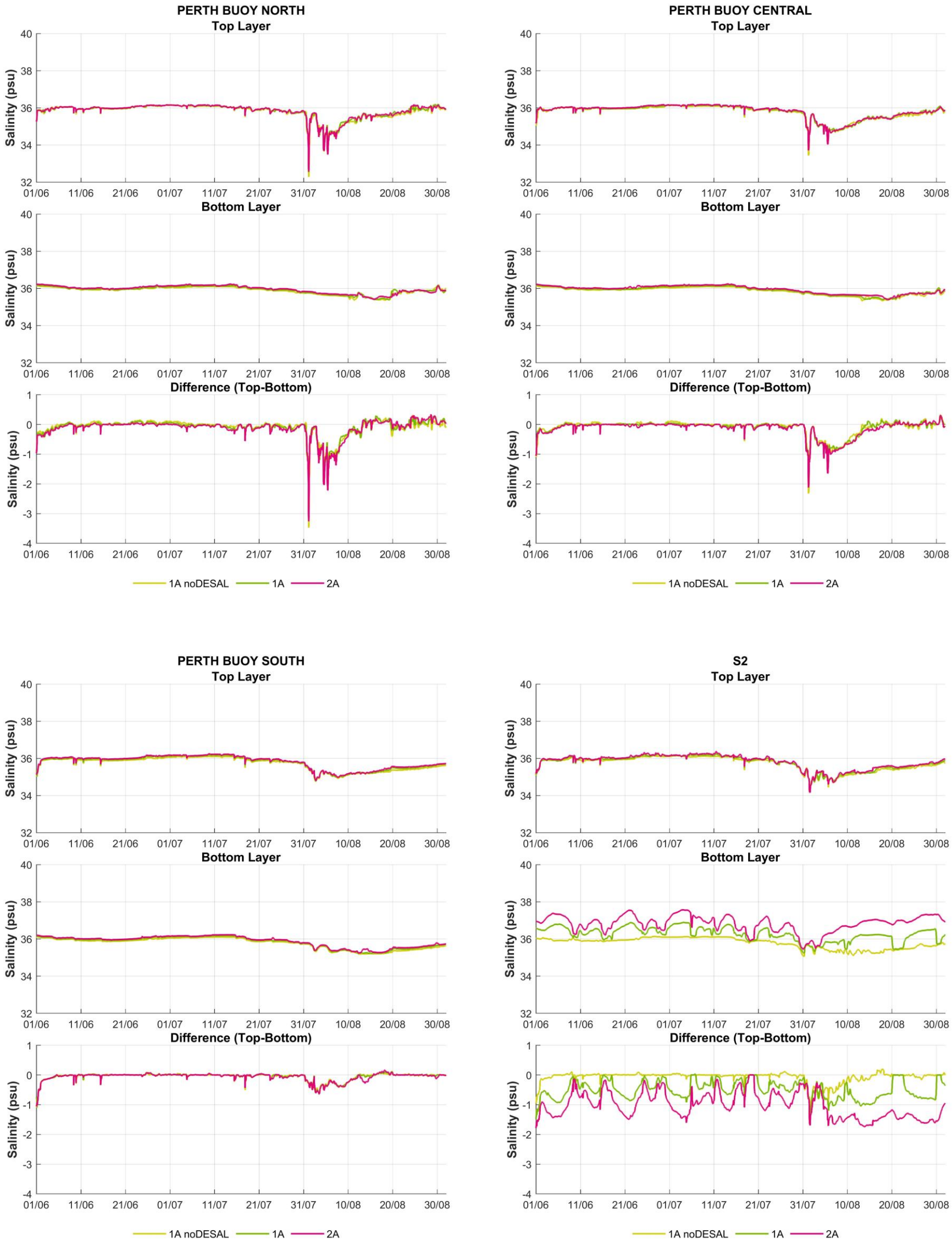

Figure A-2 Salinity timeseries comparisons for top and bottom waters at Perth Buoy North, Perth Buoy Central, Perth Buoy South and S2 (Winter 2008)

Salinity Results – Timeseries

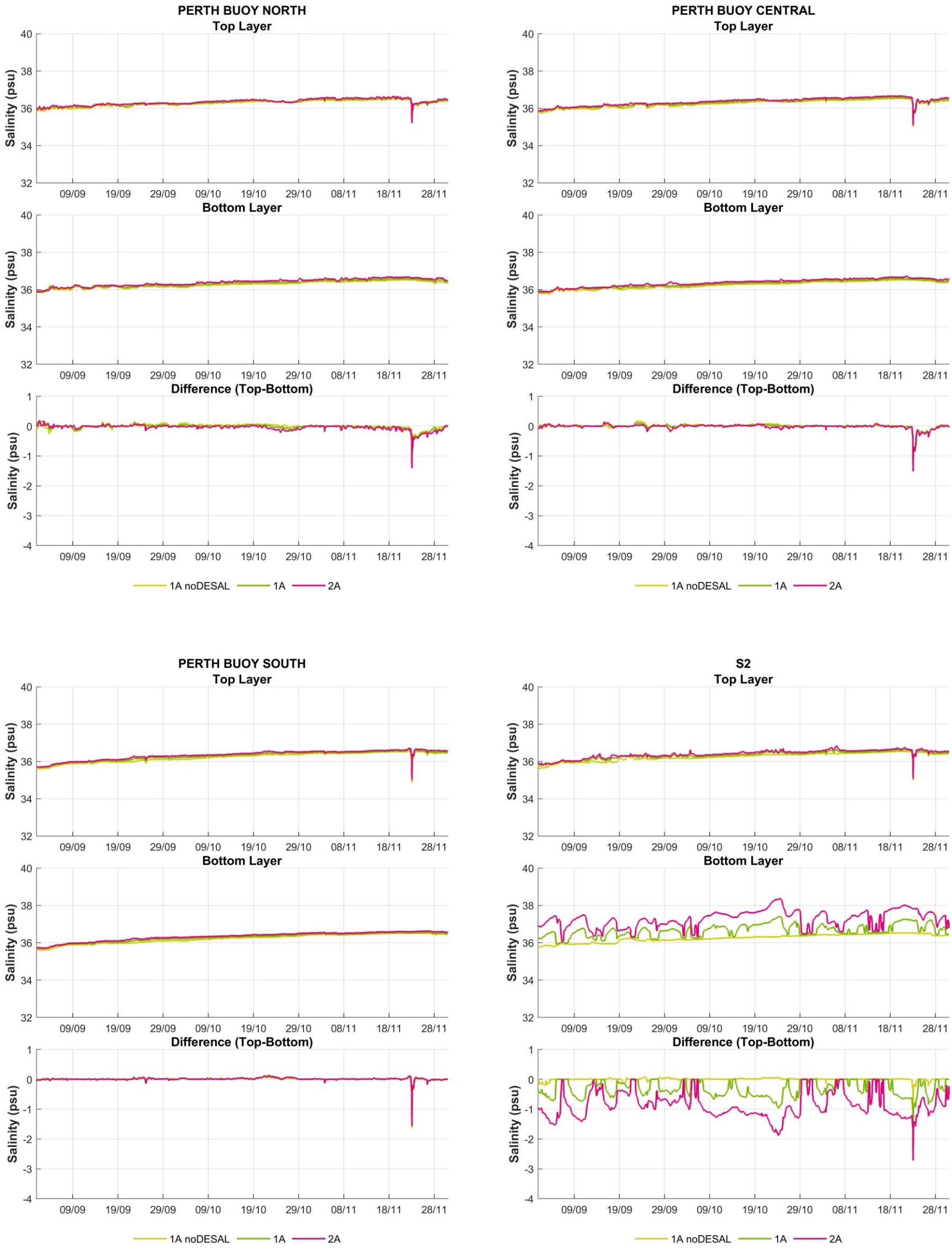

Figure A-3 Salinity timeseries comparisons for top and bottom waters at Perth Buoy North, Perth Buoy Central, Perth Buoy South and S2 (Spring 2008)

Salinity Results – Timeseries

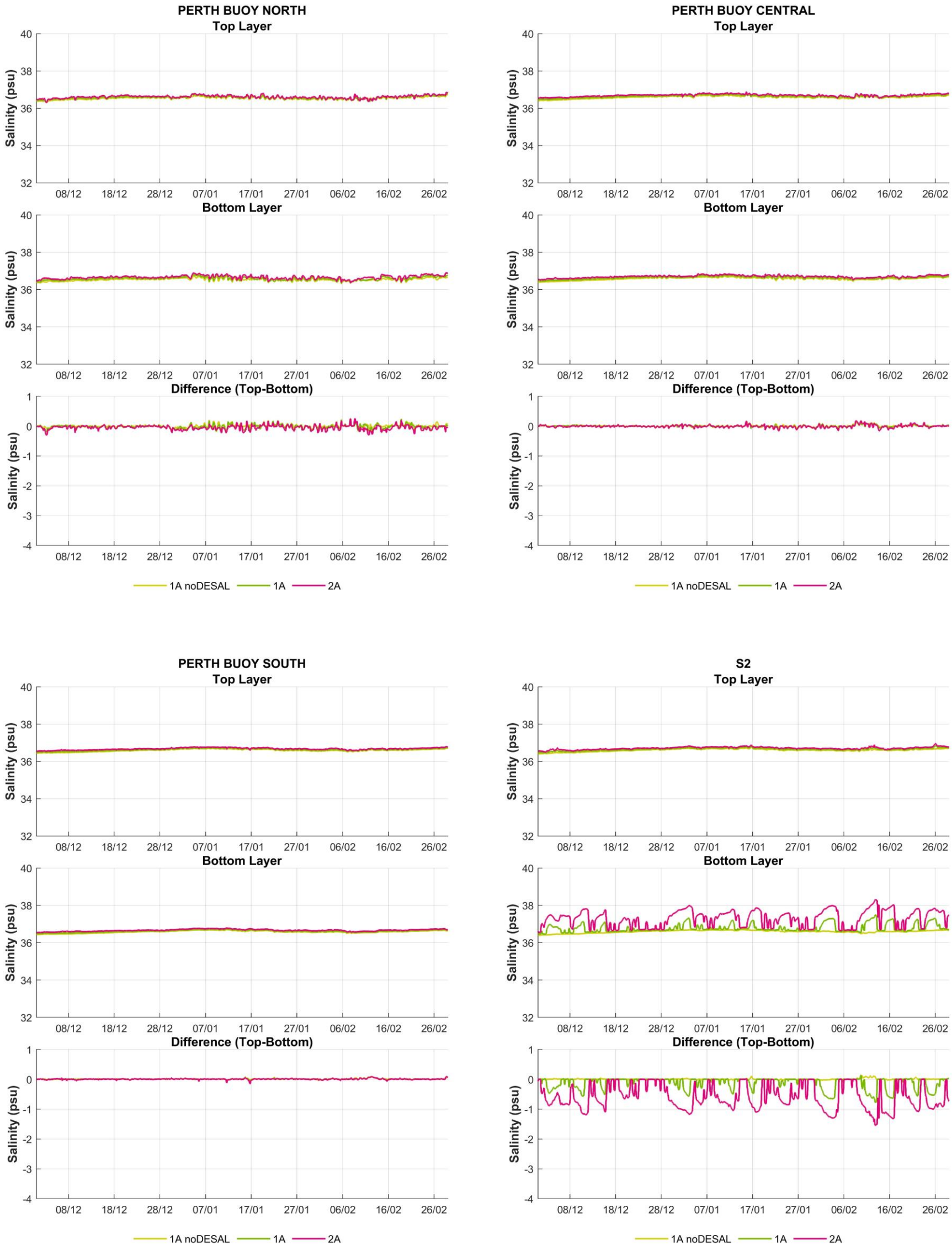

Figure A-4 Salinity timeseries comparisons for top and bottom waters at Perth Buoy North, Perth Buoy Central, Perth Buoy South and S2 (Summer 2008)

Salinity Results – Timeseries

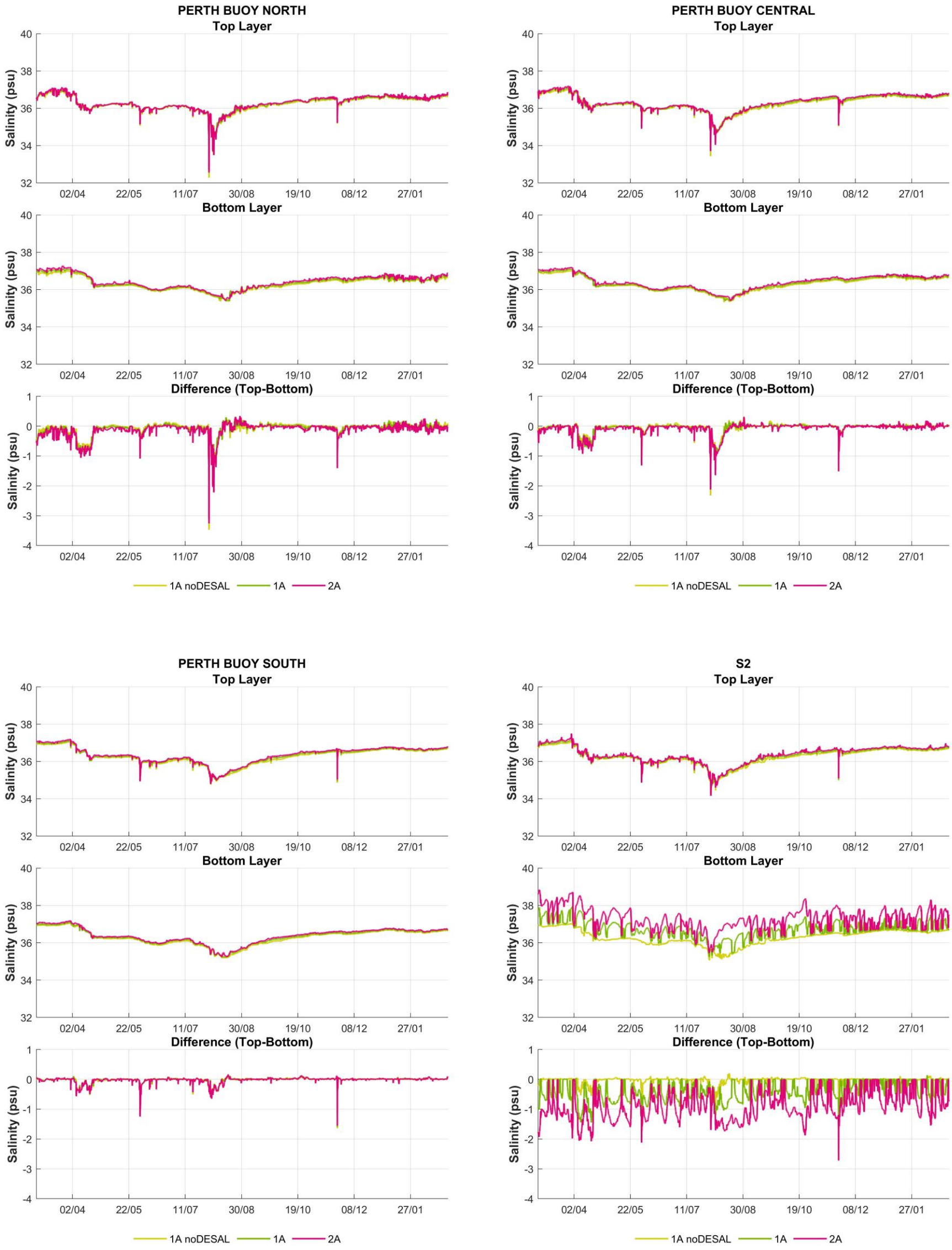

Figure A-5 Salinity timeseries comparisons for top and bottom waters at Perth Buoy North, Perth Buoy Central, Perth Buoy South and S2 in Mar 2008 – Mar 2009

Appendix B Temperature Results – Timeseries

Temperature Results – Timeseries

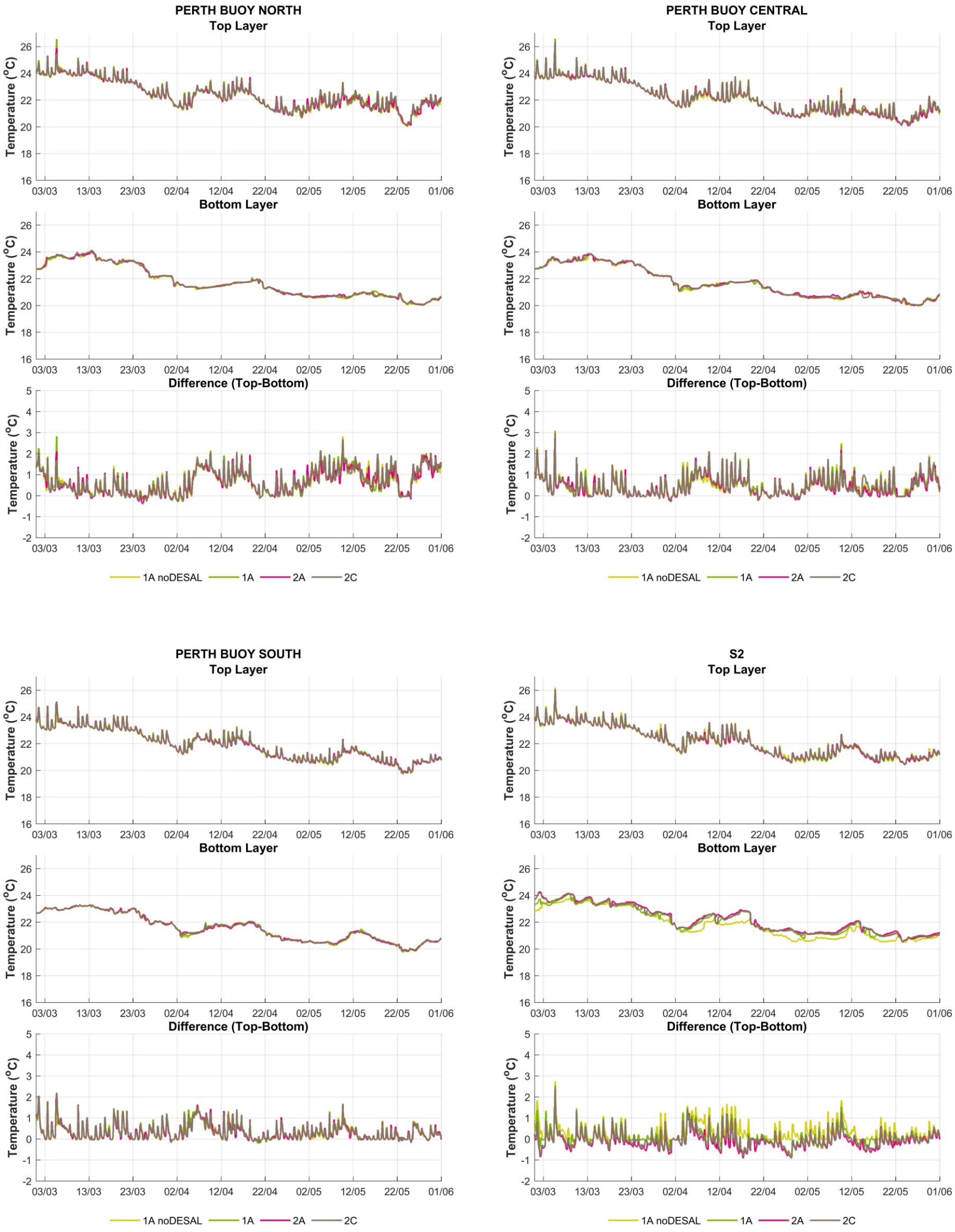

Figure B-1 Temperature timeseries comparisons for top and bottom waters at Perth Buoy North, Perth Buoy Central, Perth Buoy South and S2 (Autumn 2008).

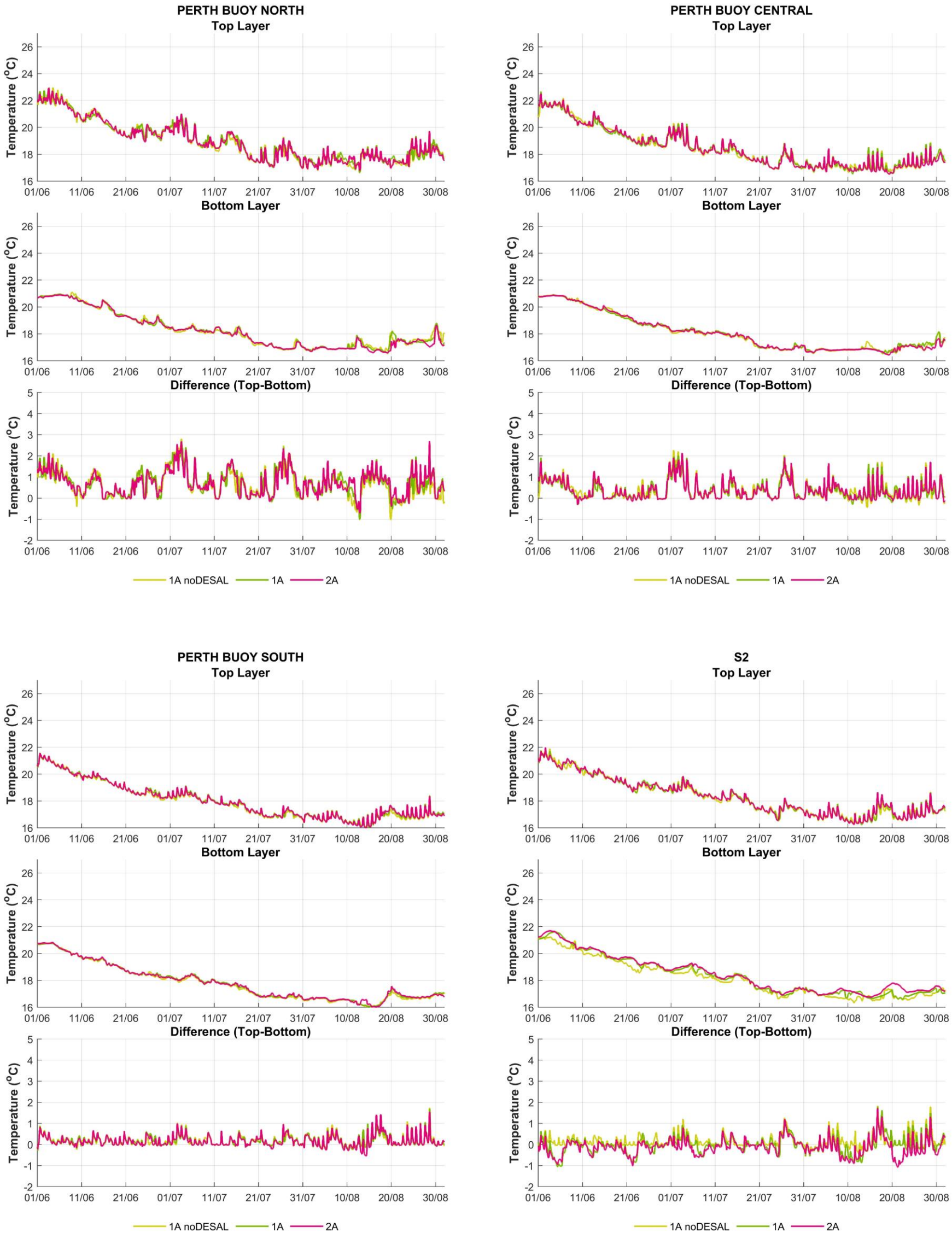

Figure B-2 Temperature timeseries comparisons for top and bottom waters at Perth Buoy North, Perth Buoy Central, Perth Buoy South and S2 (Winter 2008).

Temperature Results – Timeseries

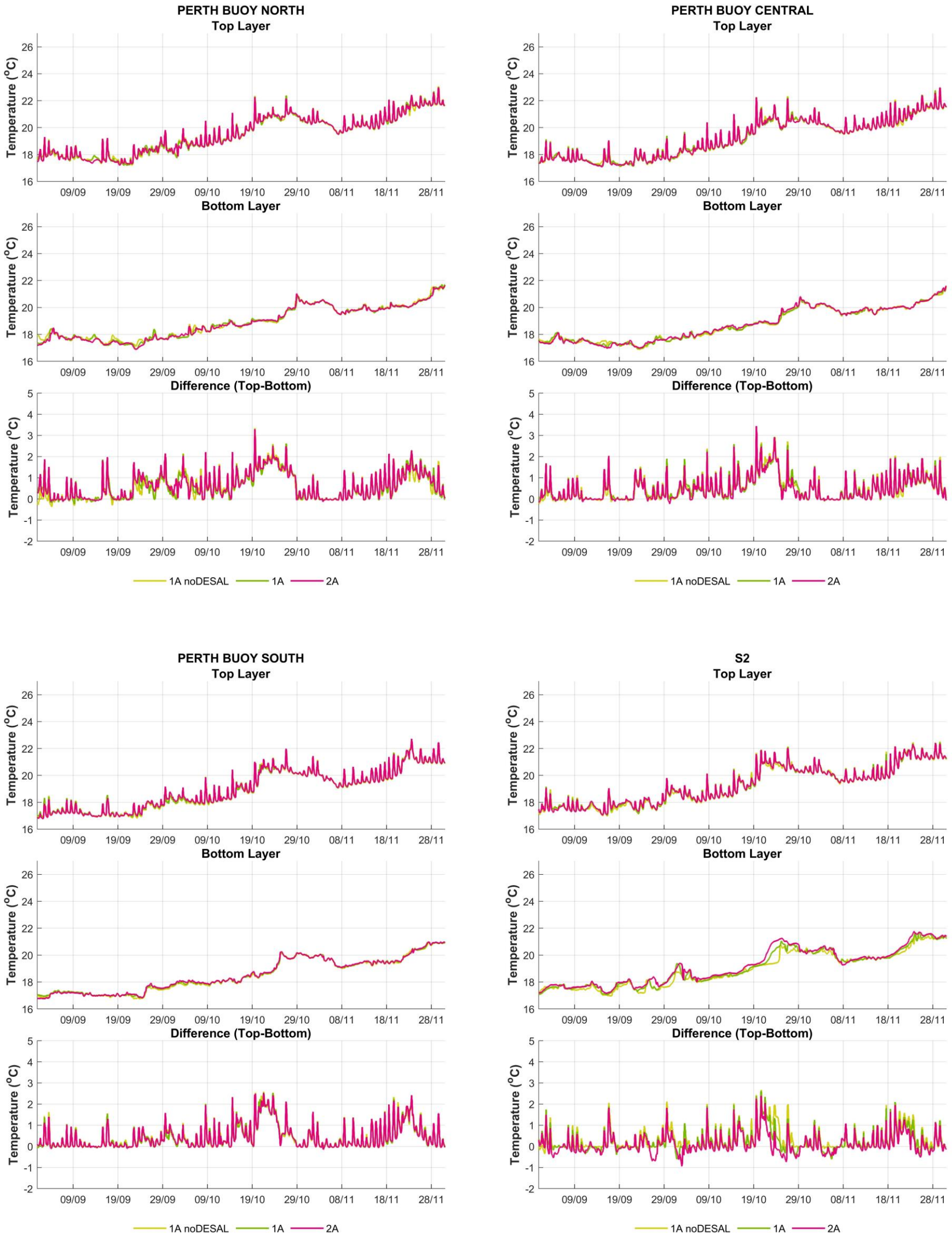

Figure B-3 Temperature timeseries comparisons for top and bottom waters at Perth Buoy North, Perth Buoy Central, Perth Buoy South and S2 (Spring 2008).

Temperature Results – Timeseries

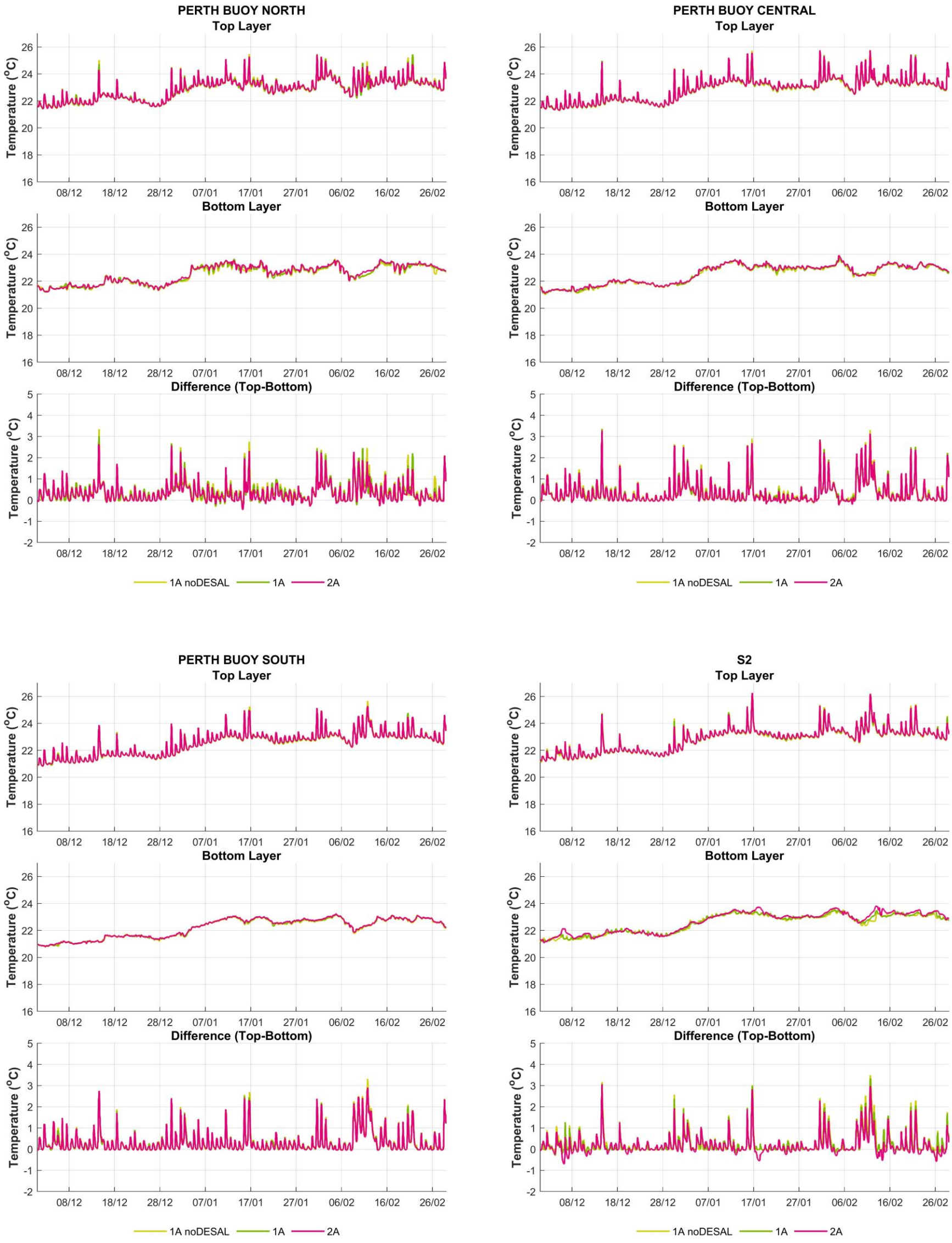

Figure B-4 Temperature timeseries comparisons for top and bottom waters at Perth Buoy North, Perth Buoy Central, Perth Buoy South and S2 (Summer 2008/09).

Appendix C Dissolved Oxygen Concentration – Timeseries

Dissolved Oxygen Concentration – Timeseries

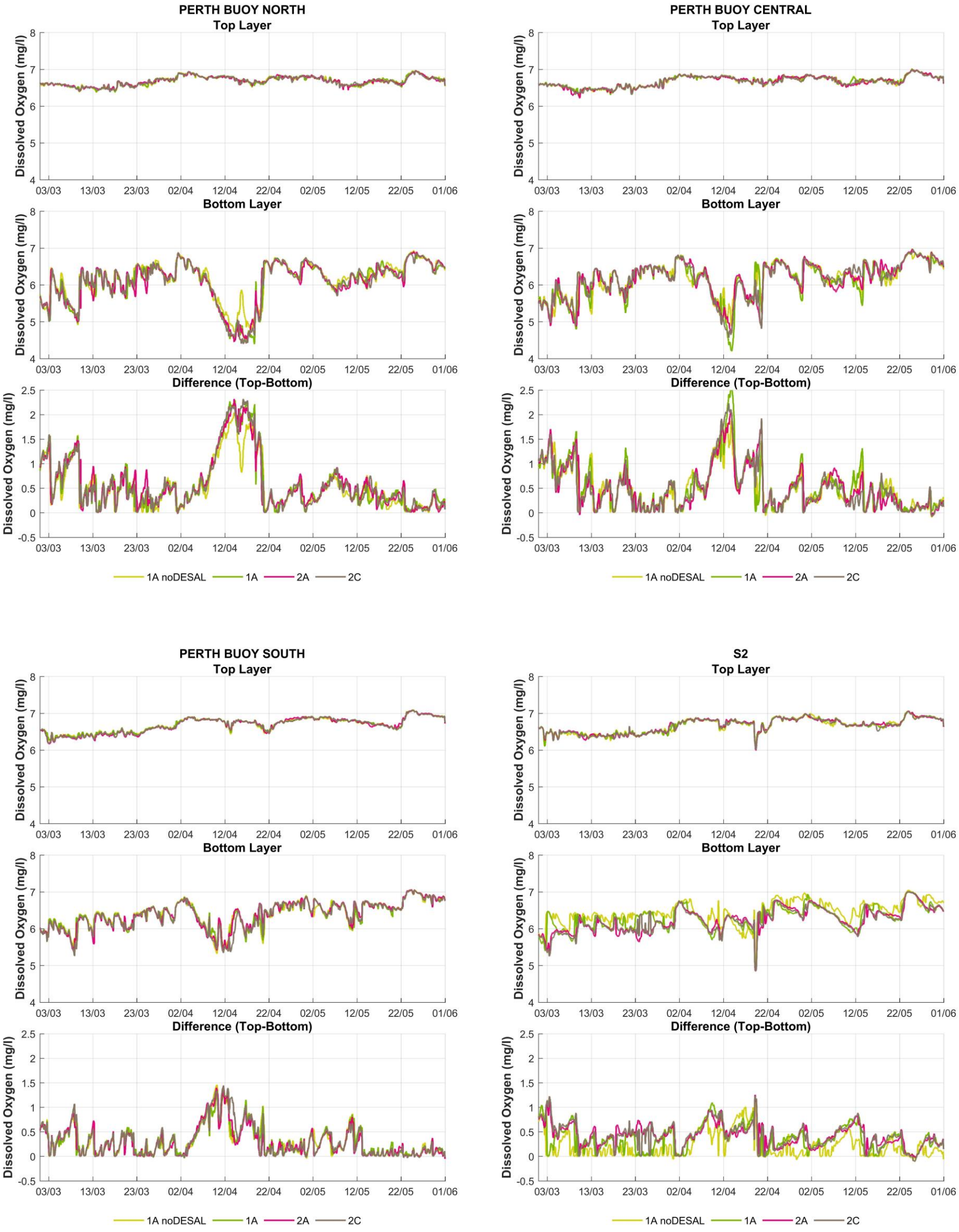

Figure C-1 Dissolved Oxygen concentration timeseries comparisons for top and bottom waters at Perth Buoy North, Perth Buoy Central, Perth Buoy South and S2 (Autumn 2008).

Dissolved Oxygen Concentration – Timeseries

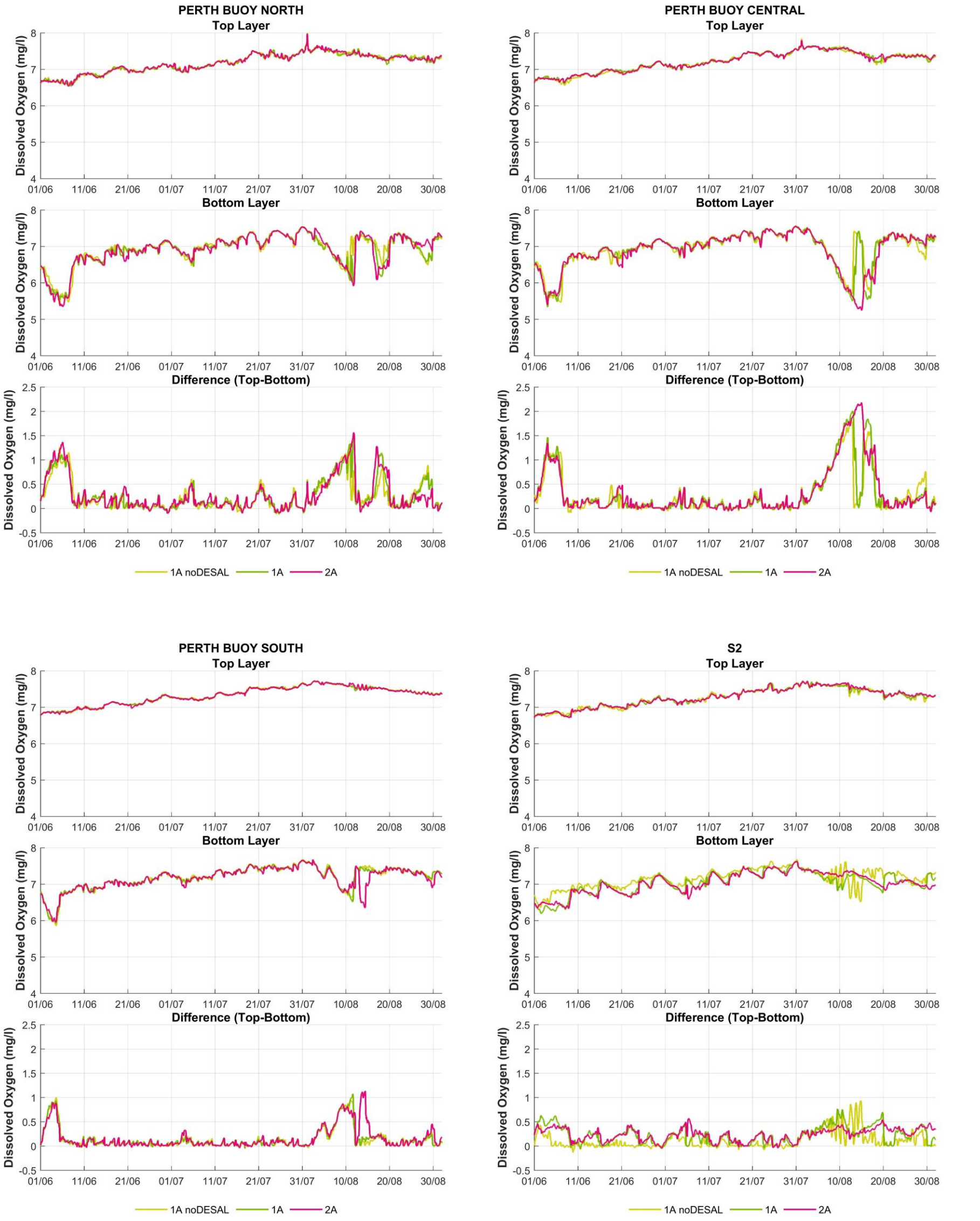

Figure C-2 Dissolved Oxygen concentration timeseries comparisons for top and bottom waters at Perth Buoy North, Perth Buoy Central, Perth Buoy South and S2 (Winter 2008).

Dissolved Oxygen Concentration – Timeseries

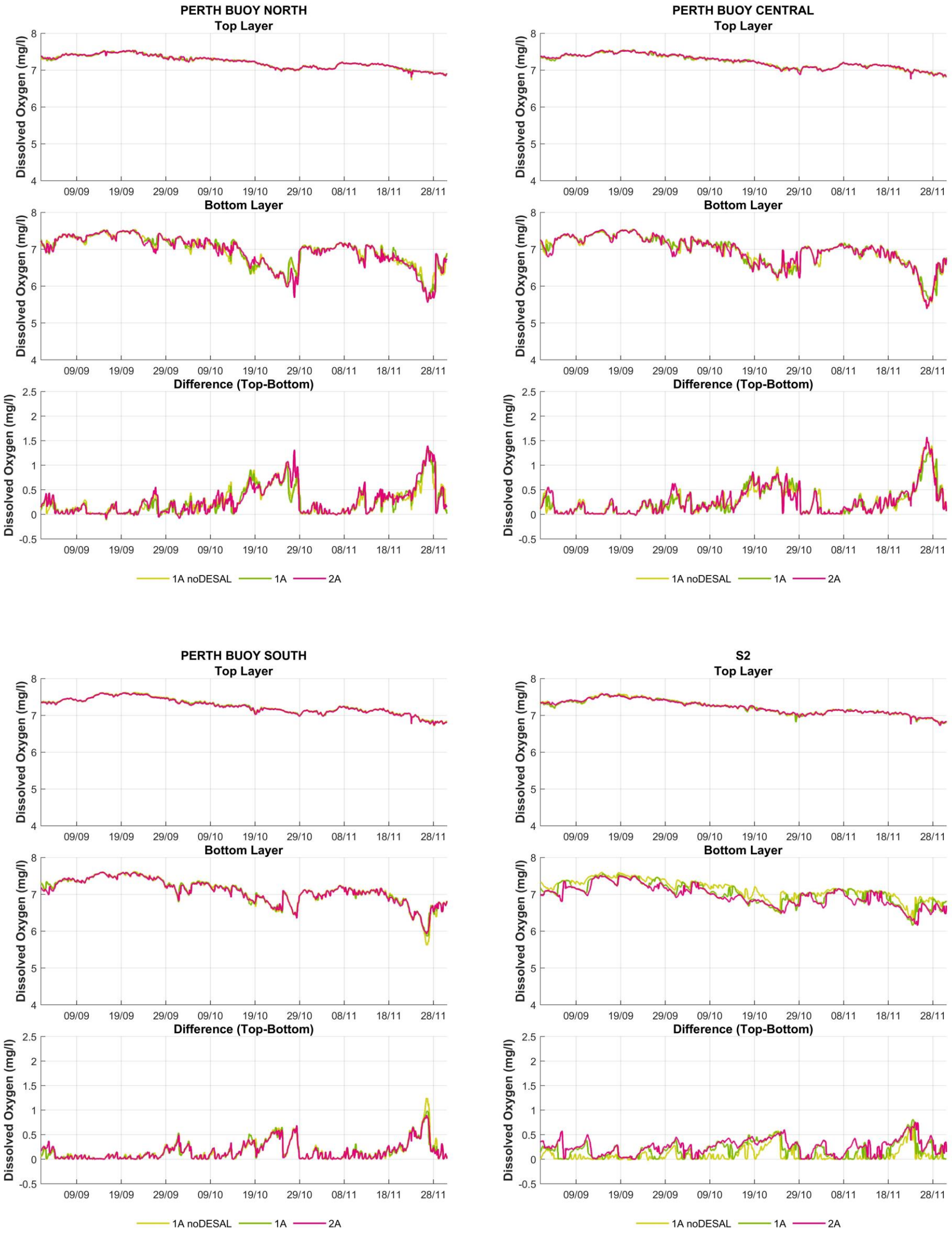

Figure C-3 Dissolved Oxygen concentration timeseries comparisons for top and bottom waters at Perth Buoy North, Perth Buoy Central, Perth Buoy South and S2 (Spring 2008).

Dissolved Oxygen Concentration – Timeseries

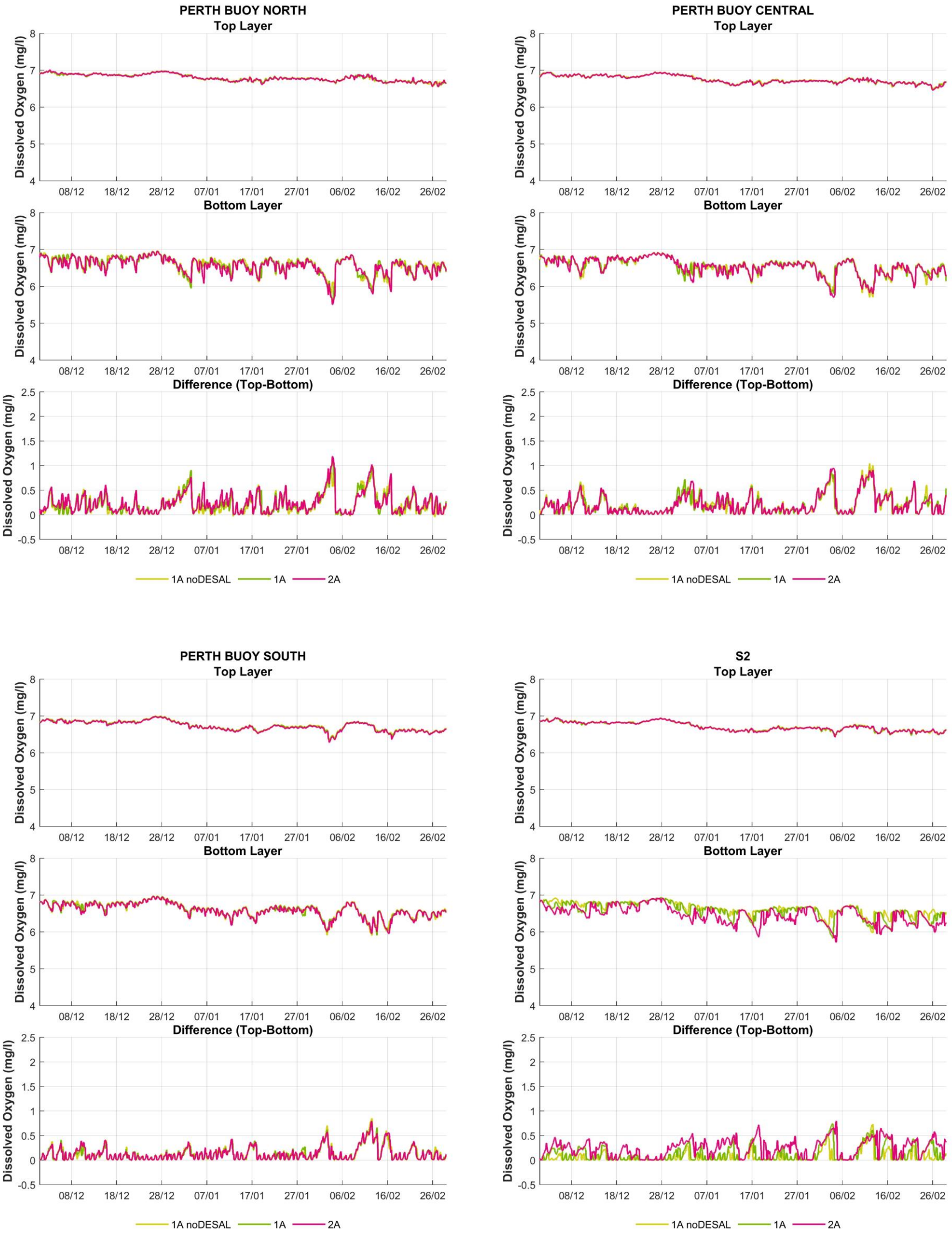

Figure C-4 Dissolved Oxygen concentration timeseries comparisons for top and bottom waters at Perth Buoy North, Perth Buoy Central, Perth Buoy South and S2 (Summer 2008/09).

Appendix D Dissolved Oxygen Saturation – Timeseries

Dissolved Oxygen Saturation – Timeseries

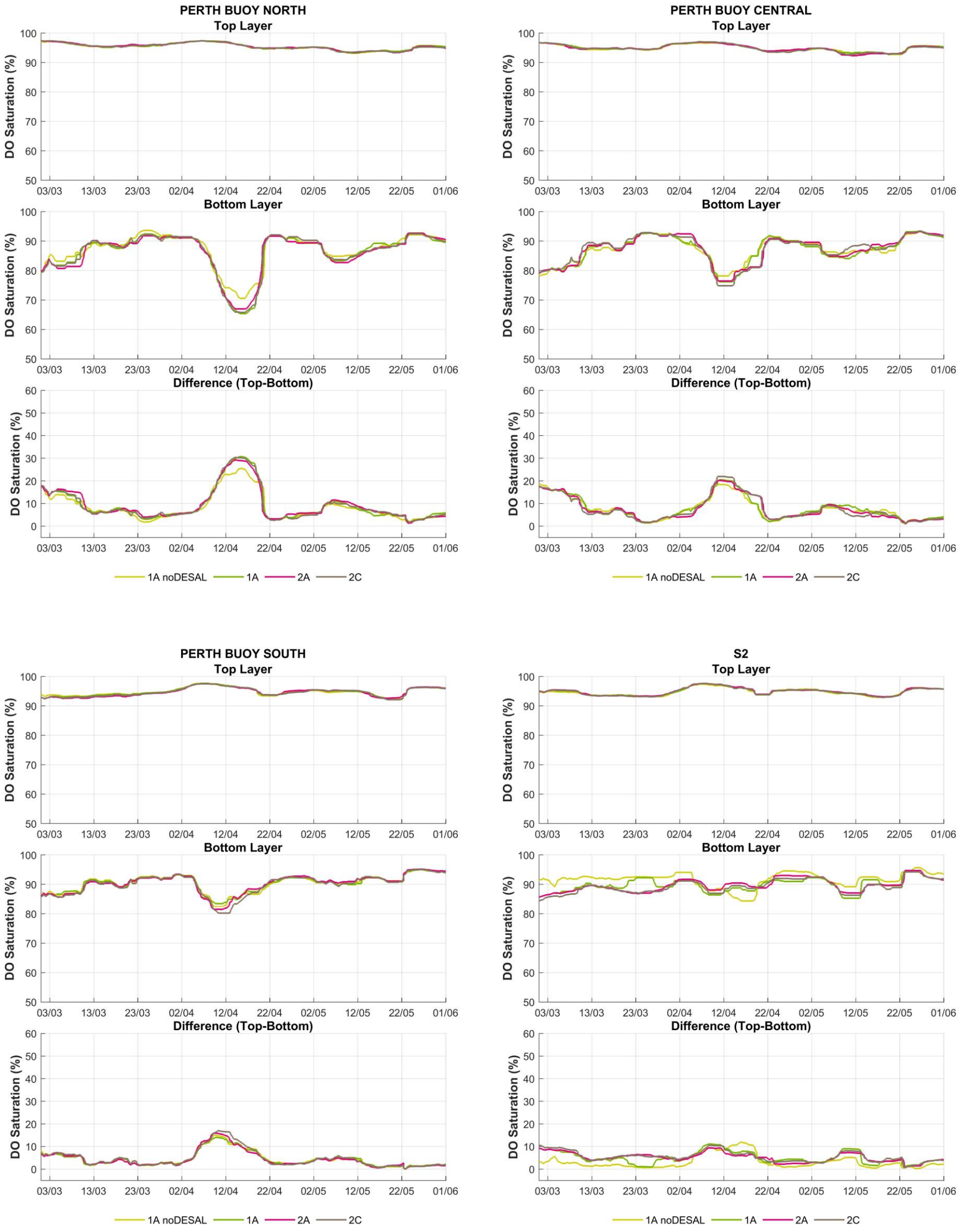

Figure D-1 Dissolved Oxygen saturation timeseries comparisons for top and bottom waters at Perth Buoy North, Perth Buoy Central, Perth Buoy South and S2 (Autumn 2008).

Dissolved Oxygen Saturation – Timeseries

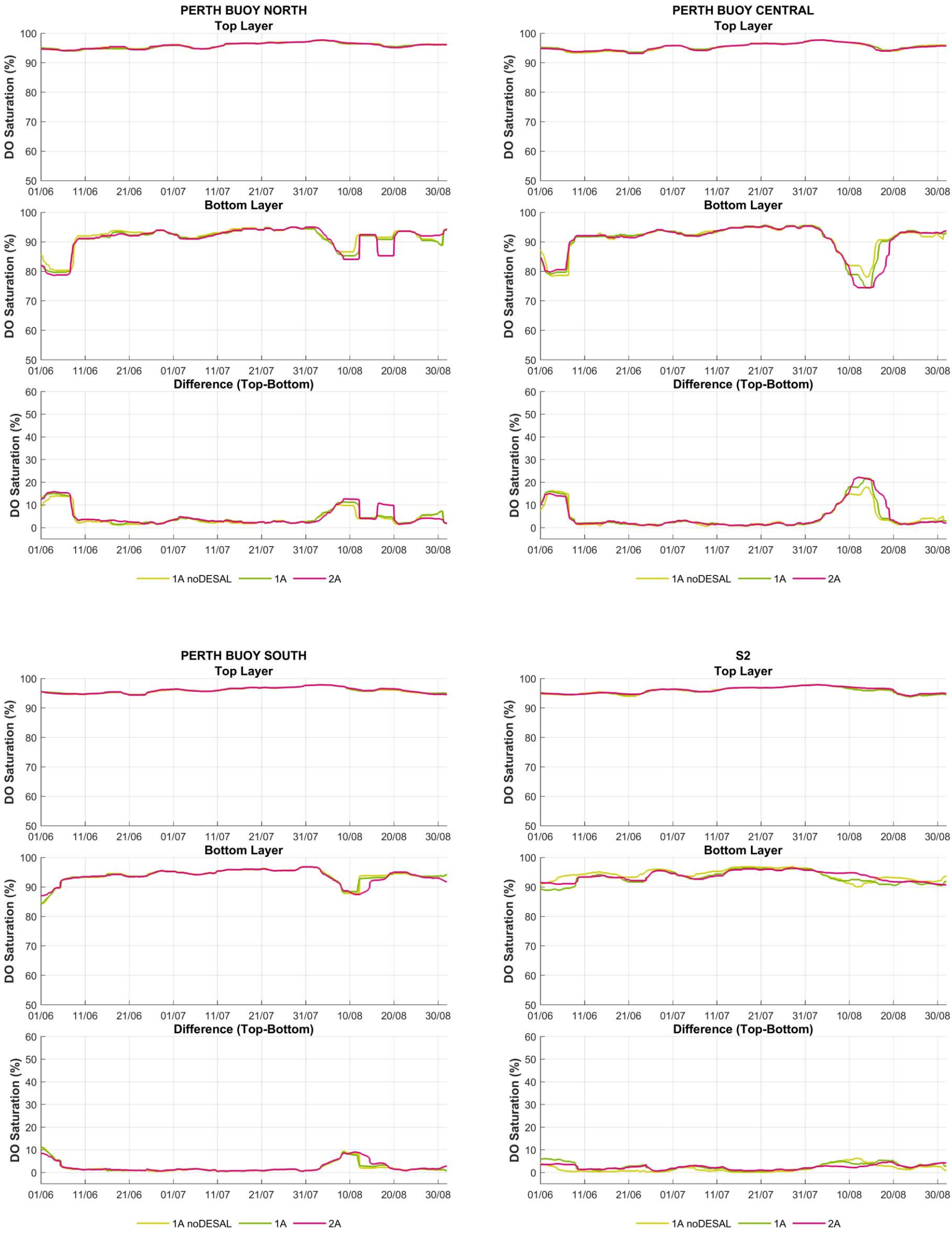

Figure D-2 Dissolved Oxygen saturation timeseries comparisons for top and bottom waters at Perth Buoy North, Perth Buoy Central, Perth Buoy South and S2 (Winter 2008).

Dissolved Oxygen Saturation – Timeseries

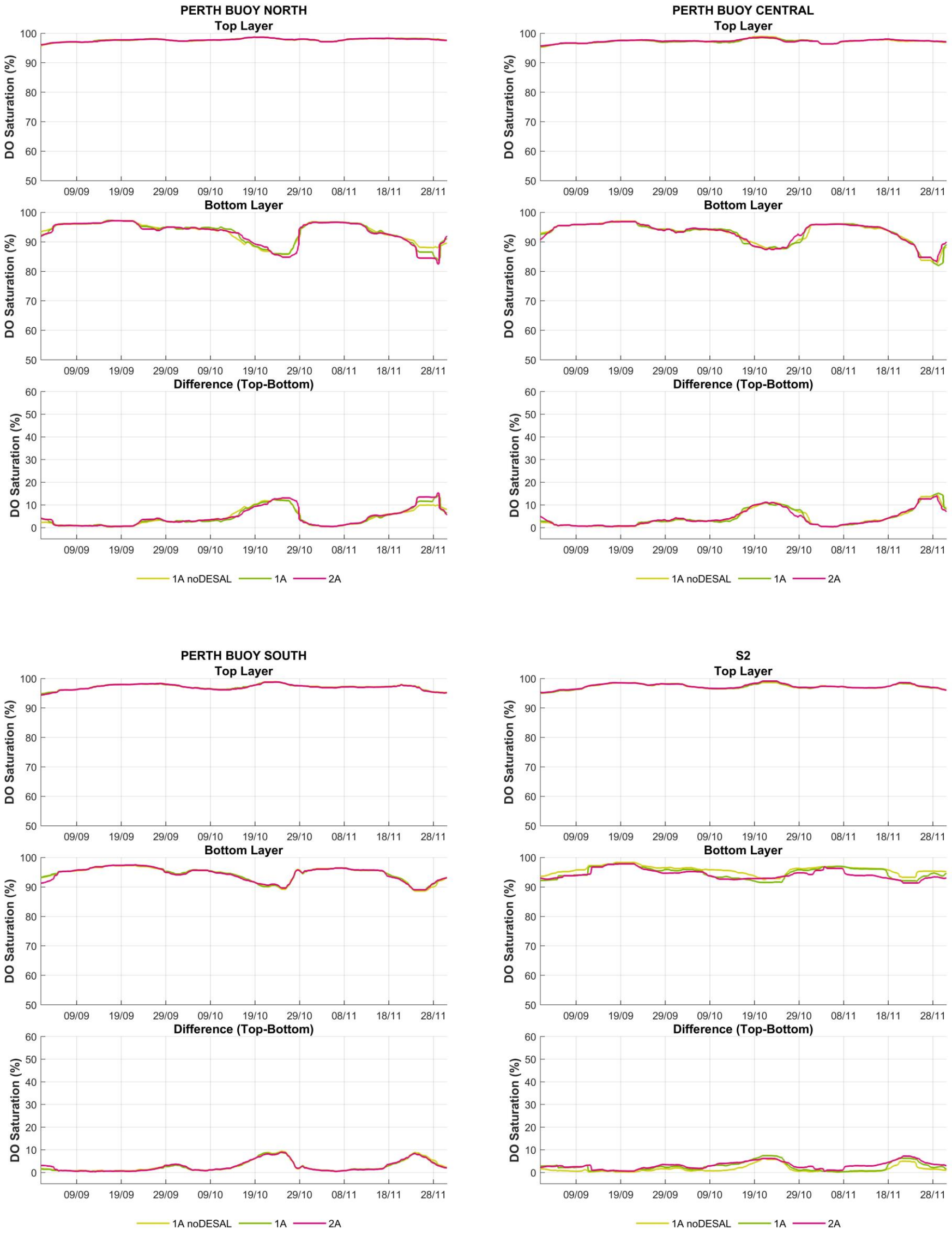

Figure D-3 Dissolved Oxygen saturation timeseries comparisons for top and bottom waters at Perth Buoy North, Perth Buoy Central, Perth Buoy South and S2 (Spring 2008).

Dissolved Oxygen Saturation – Timeseries

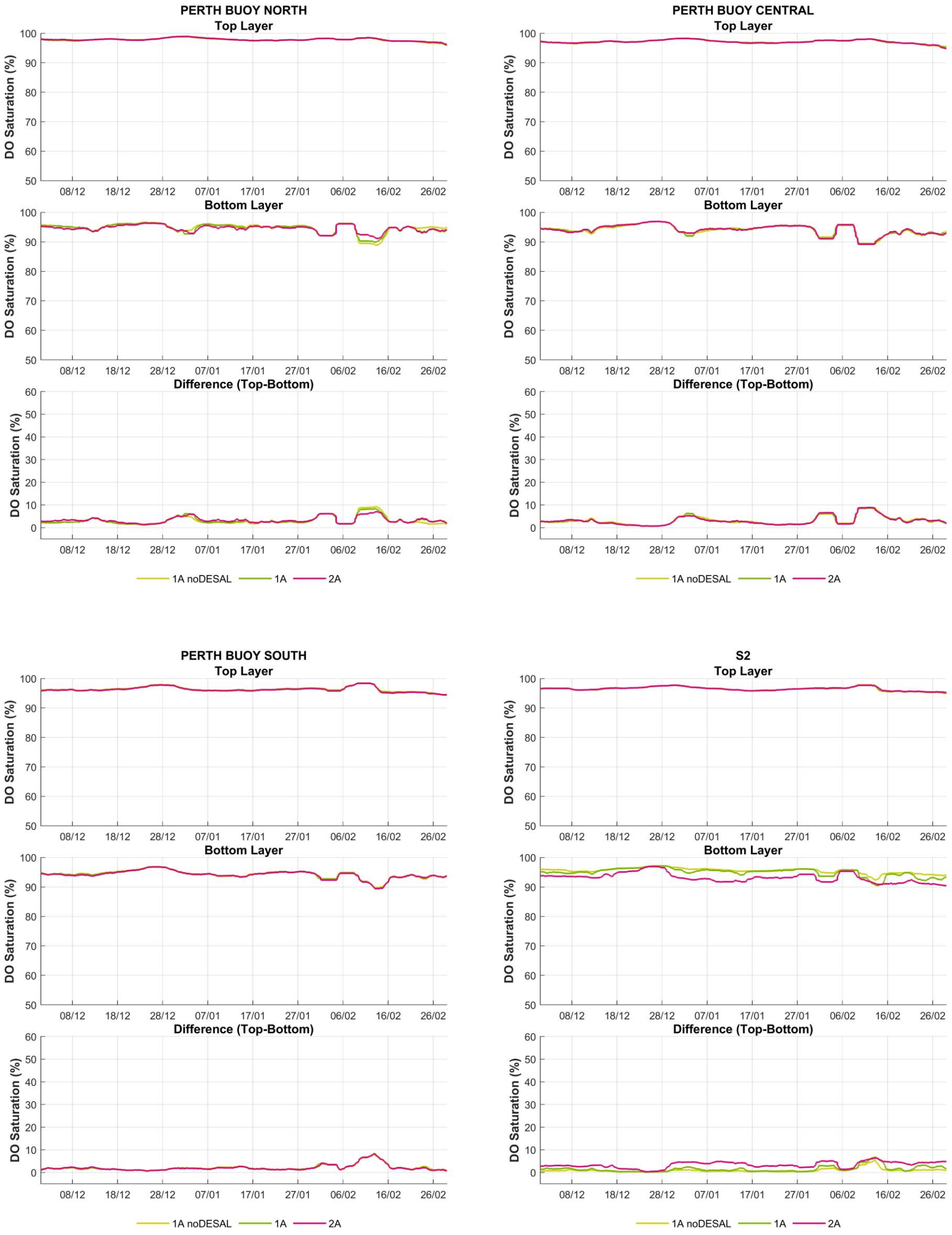

Figure D-4 Dissolved Oxygen saturation timeseries comparisons for top and bottom waters at Perth Buoy North, Perth Buoy Central, Perth Buoy South and S2 (Summer 2008/09).

Dissolved Oxygen Saturation – Timeseries

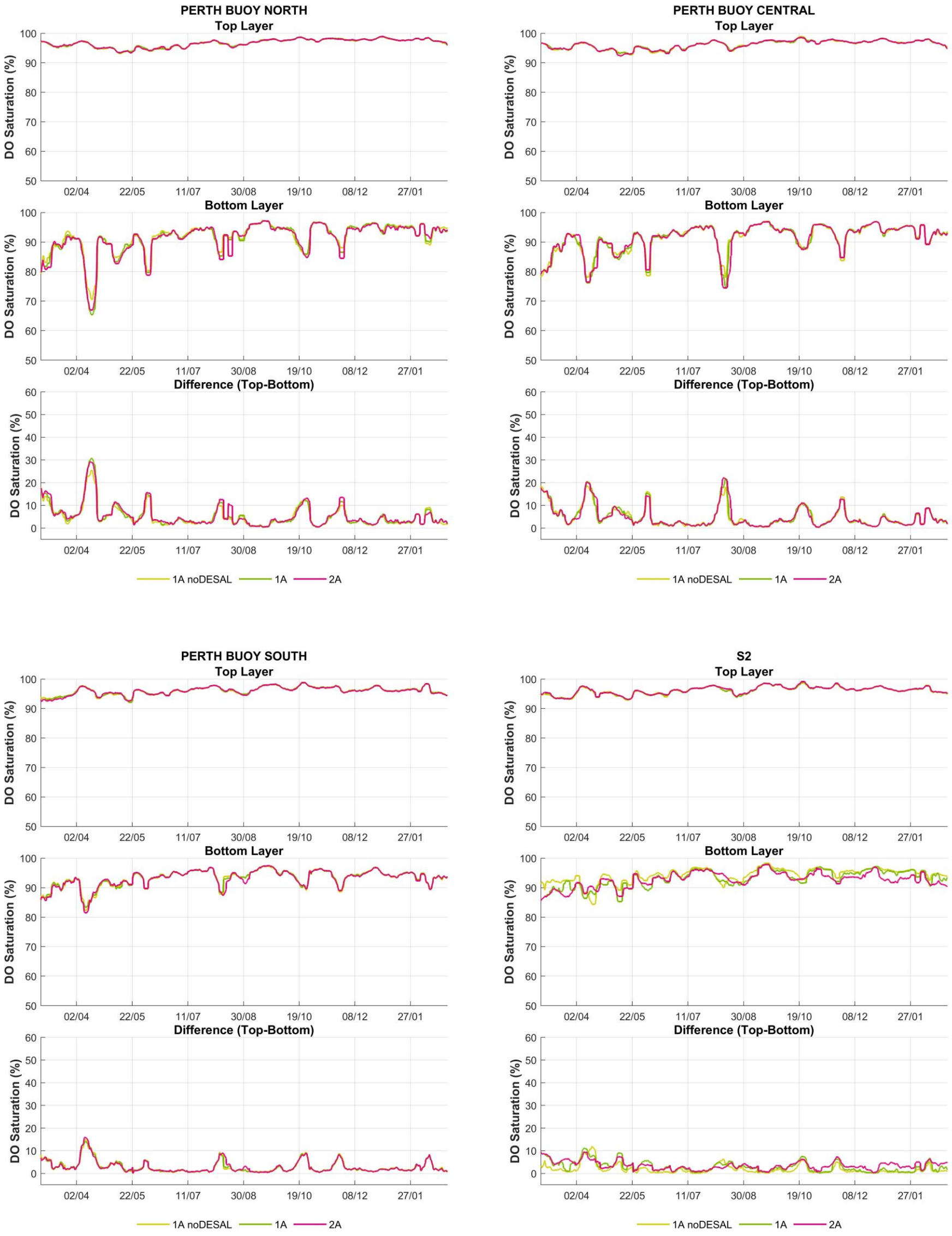

Figure D-5 Dissolved Oxygen saturation timeseries comparisons for top and bottom waters at Perth Buoy North, Perth Buoy Central, Perth Buoy South and S2 in Mar 2008 – Mar 2009

Appendix E Near bed DO Saturation and Density Difference

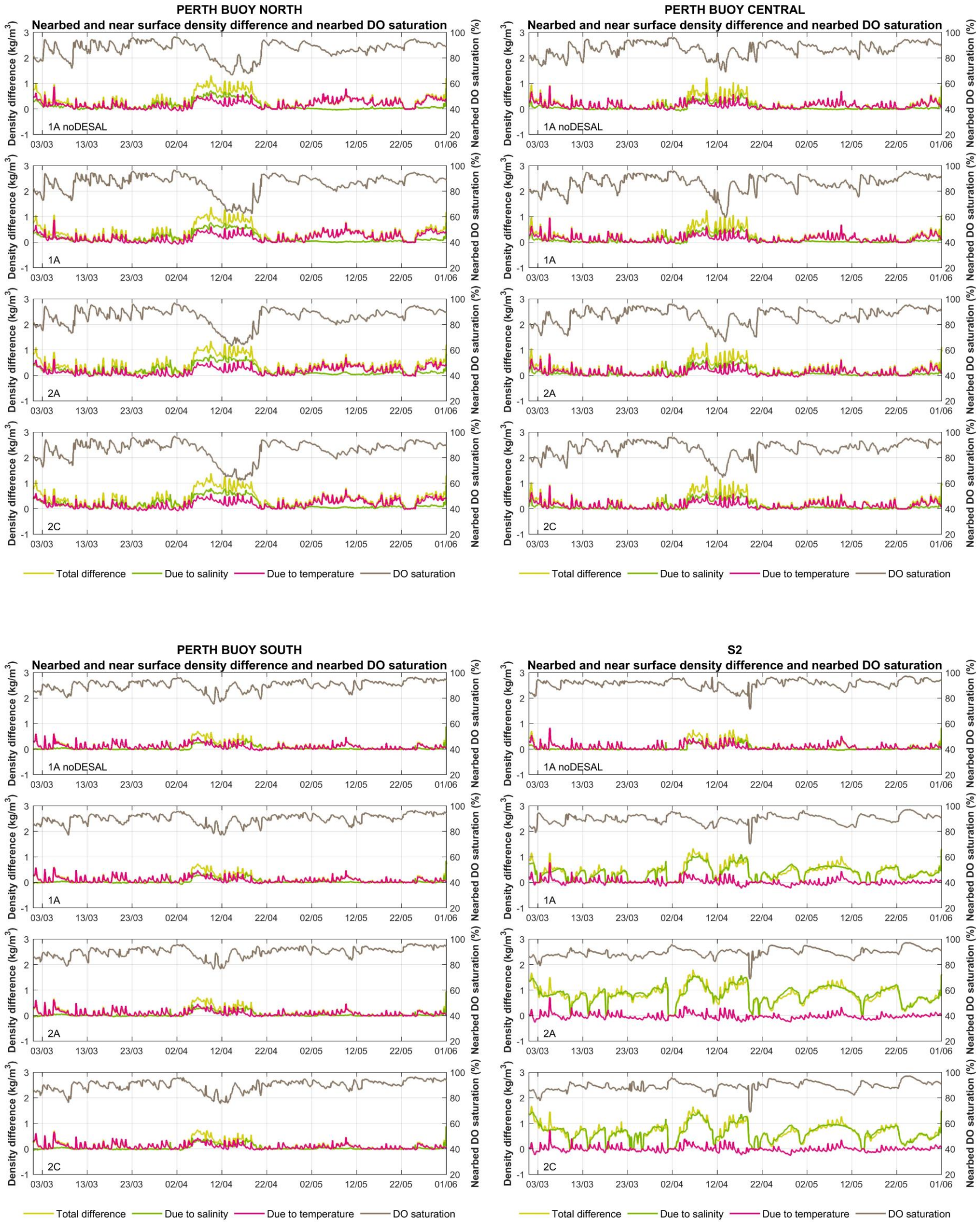

Figure E-1 Near bed and near surface density difference and near bed DO saturation timeseries comparisons at Perth Buoy North, Perth Buoy Central, Perth Buoy South and S2 (Autumn 2008)

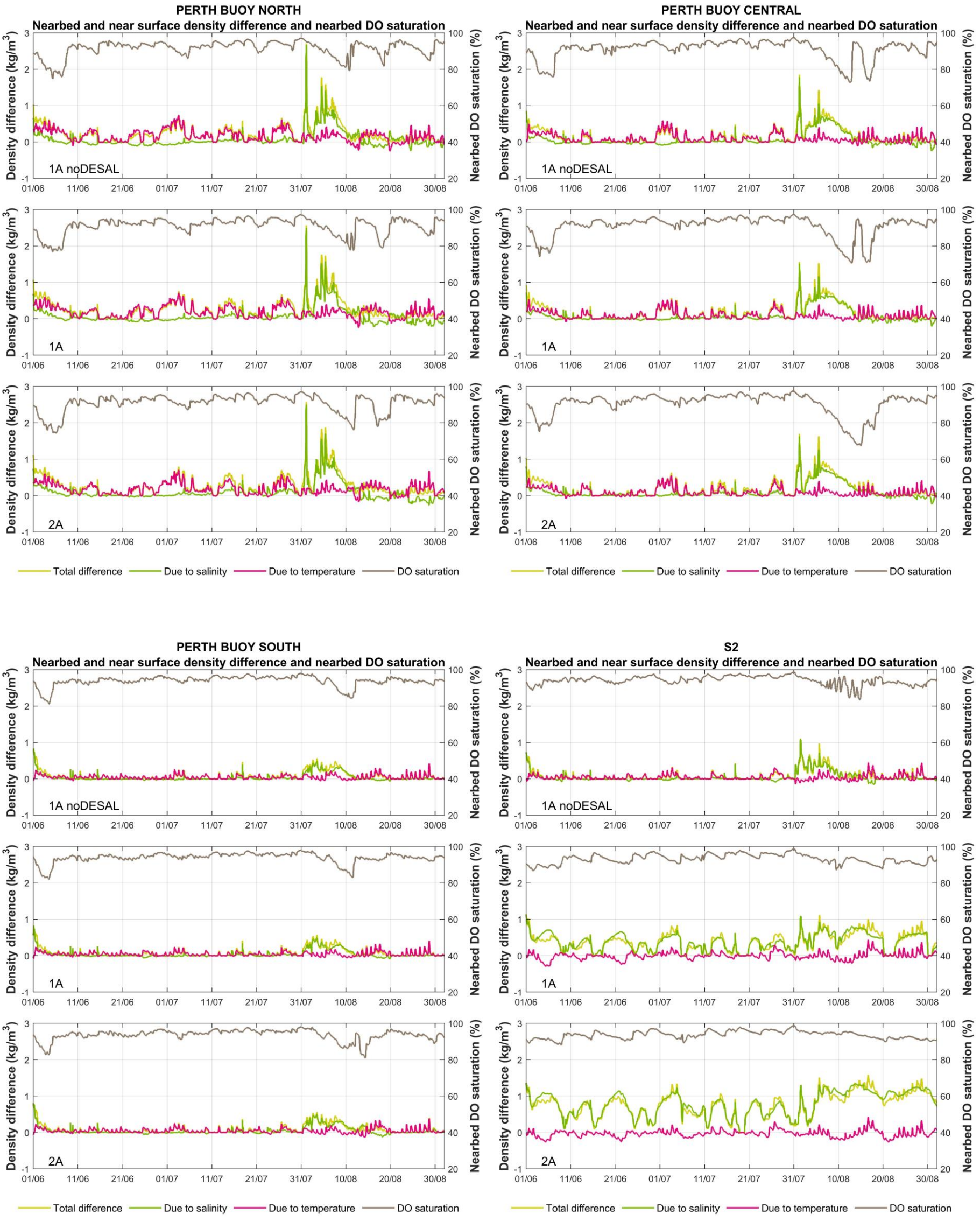

Figure E-2 Near bed and near surface density difference and near bed DO saturation timeseries comparisons at Perth Buoy North, Perth Buoy Central, Perth Buoy South and S2 (Winter 2008)

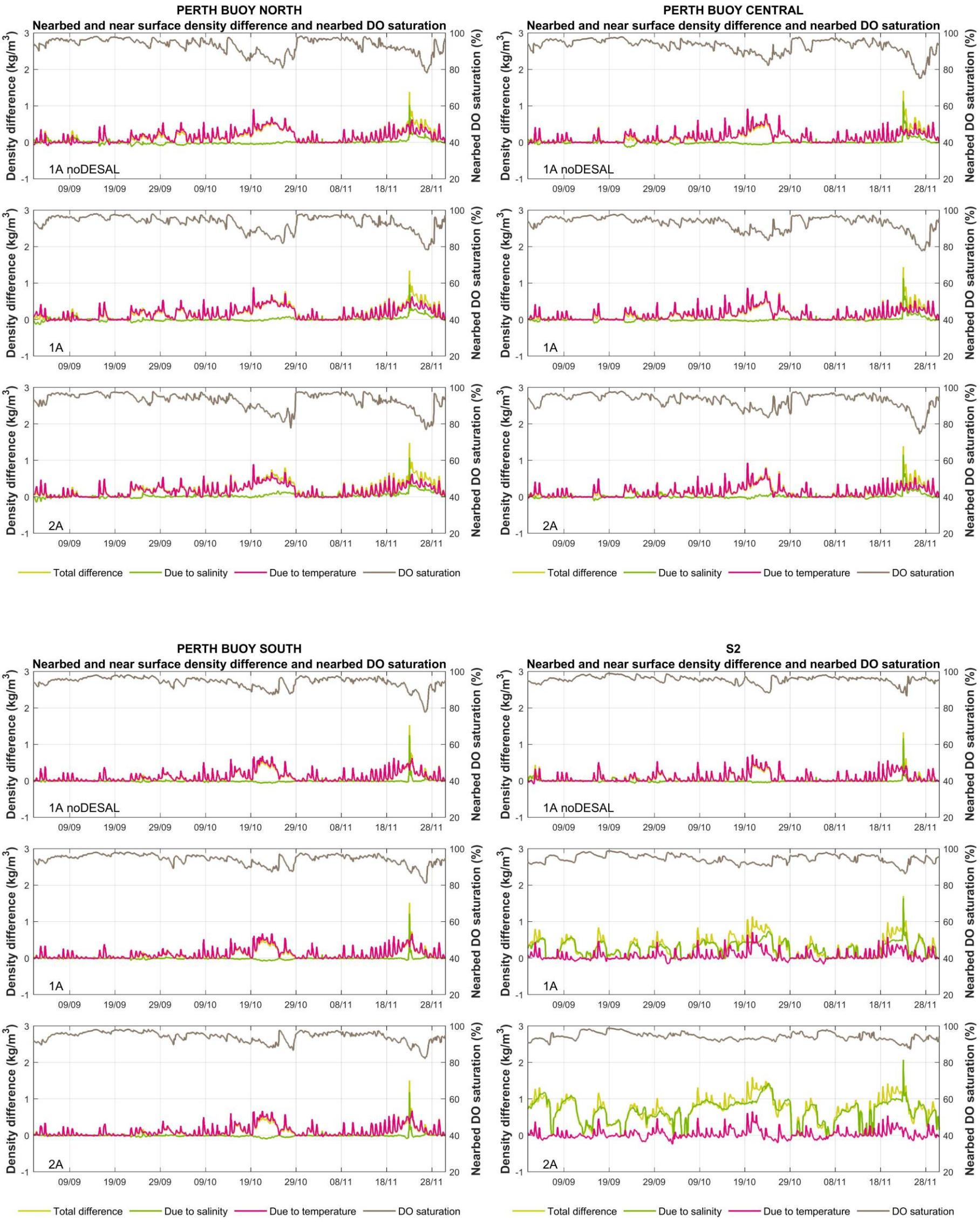

Figure E-3 Near bed and near surface density difference and near bed DO saturation timeseries comparisons at Perth Buoy North, Perth Buoy Central, Perth Buoy South and S2 (Spring 2008)

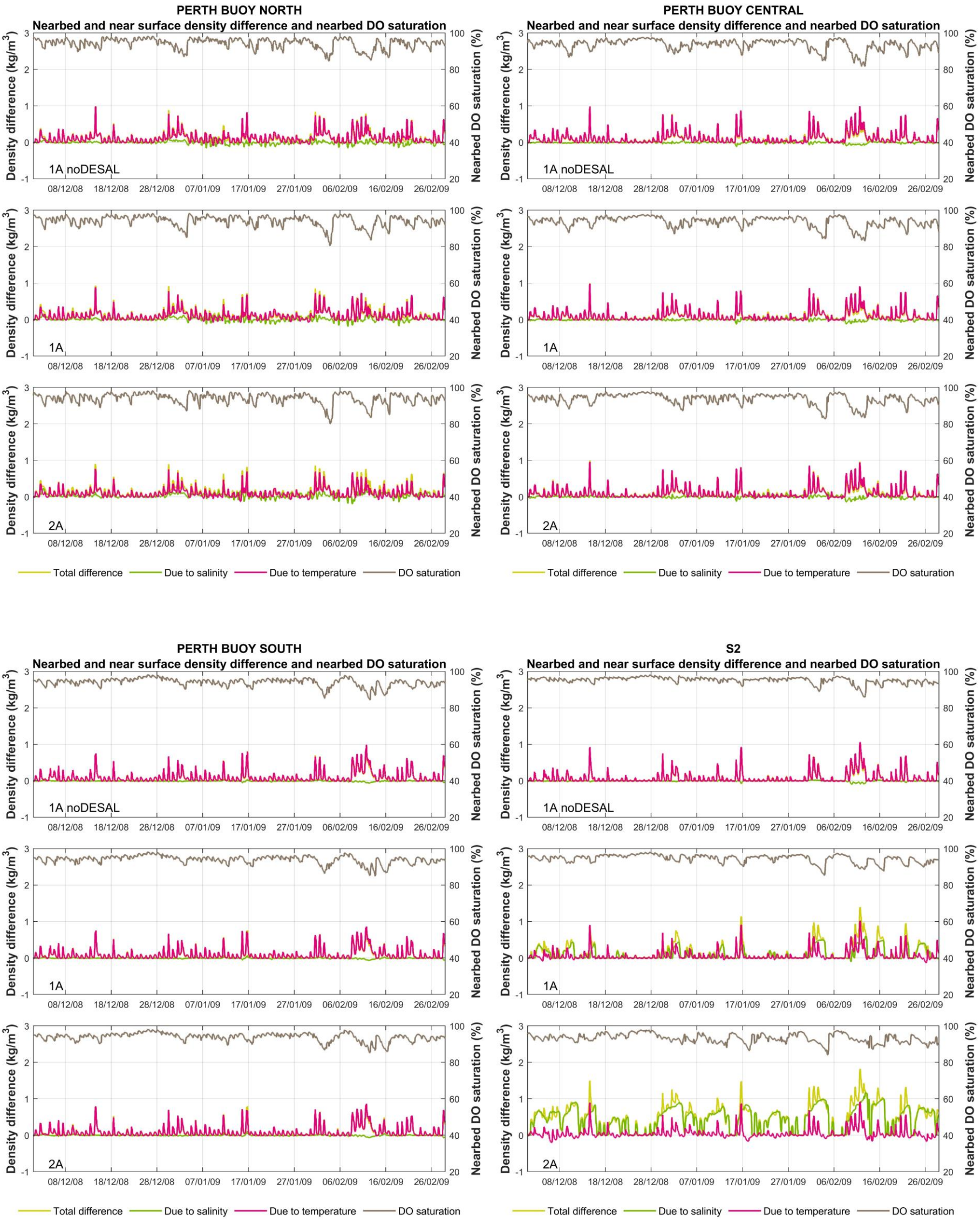

Figure E-4 Near bed and near surface density difference and near bed DO saturation timeseries comparisons at Perth Buoy North, Perth Buoy Central, Perth Buoy South and S2 (Summer 2008/09)

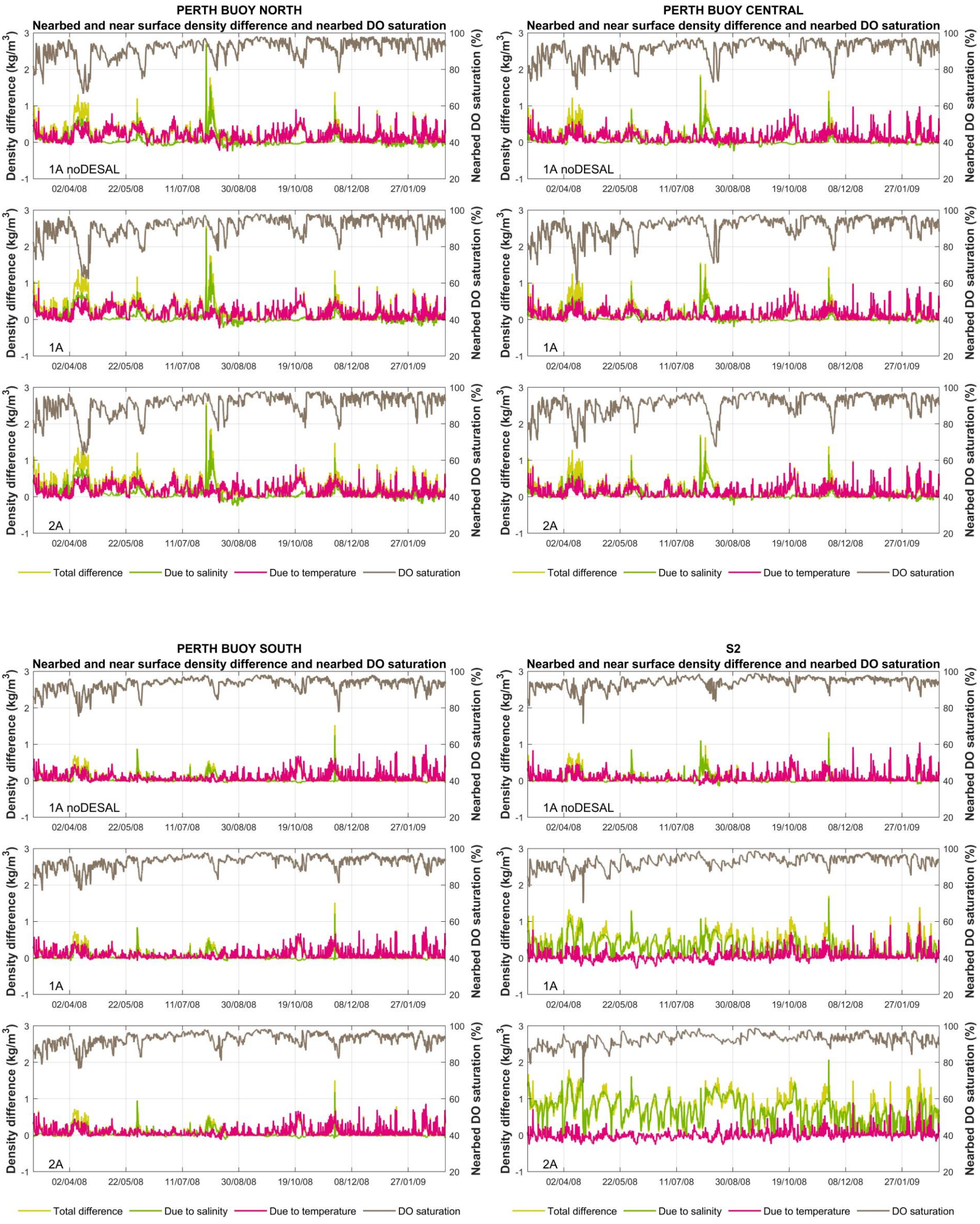

Figure E-5 Near bed and near surface density difference and near bed DO saturation timeseries comparisons at Perth Buoy North, Perth Buoy Central, Perth Buoy South and S2 (Mar 2008 – Mar 2009)

BMT has a proven record in addressing today's engineering and environmental issues.

Our dedication to developing innovative approaches and solutions enhances our ability to meet our client's most challenging needs.

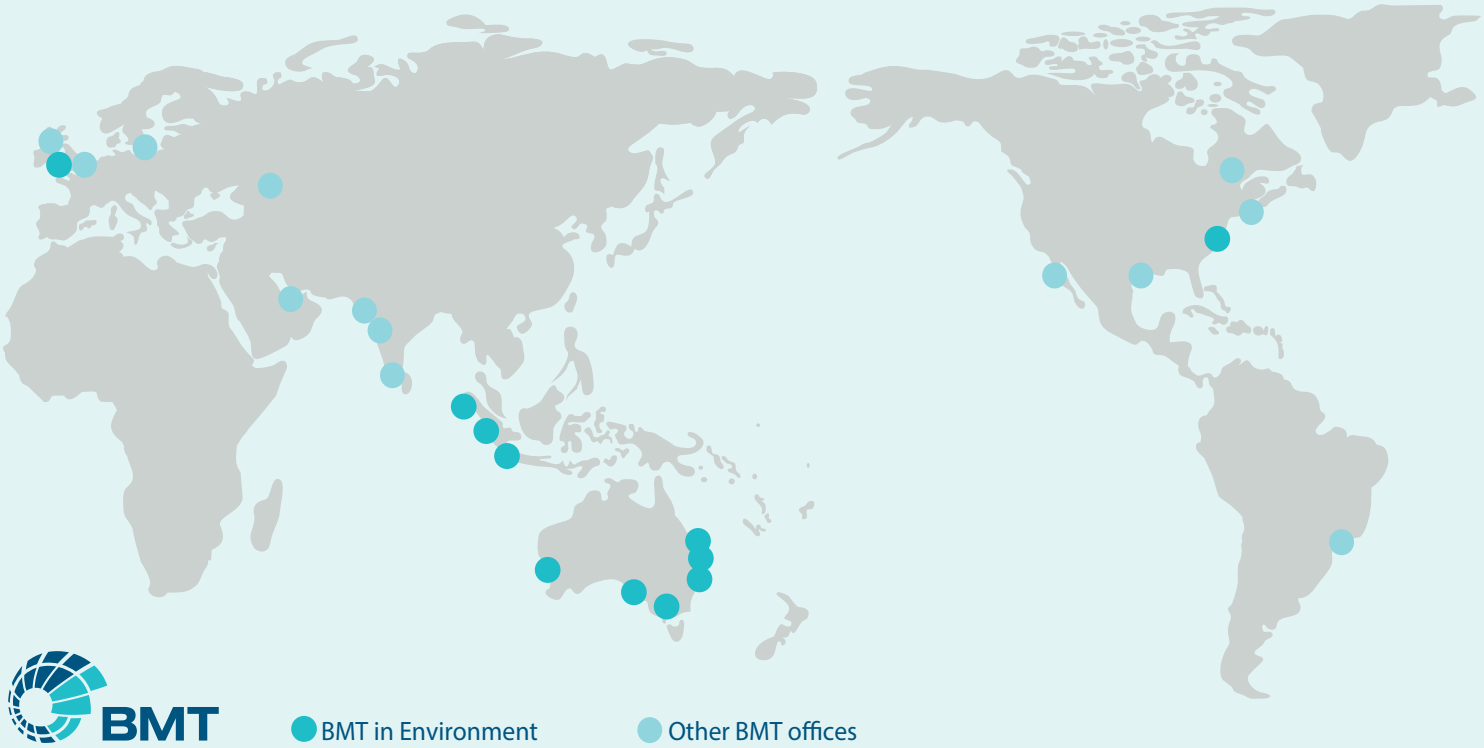

Brisbane
Level 8, 200 Creek Street
Brisbane Queensland 4000
PO Box 203 Spring Hill Queensland 4004
Australia
Tel +61 7 3831 6744
Fax +61 7 3832 3627
Email brisbane@bmtglobal.com

Melbourne
Level 5, 99 King Street
Melbourne Victoria 3000
Australia
Tel +61 3 8620 6100
Fax +61 3 8620 6105
Email melbourne@bmtglobal.com

Newcastle
126 Belford Street
Broadmeadow New South Wales 2292
PO Box 266 Broadmeadow
New South Wales 2292
Australia
Tel +61 2 4940 8882
Fax +61 2 4940 8887
Email newcastle@bmtglobal.com

Adelaide
5 Hackney Road
Hackney Adelaide South Australia 5069
Australia
Tel +61 8 8614 3400
Email info@bmtdt.com.au

Northern Rivers
Suite 5
20 Byron Street
Bangalow New South Wales 2479
Australia
Tel +61 2 6687 0466
Fax +61 2 6687 0422
Email northernrivers@bmtglobal.com

Sydney
Suite G2, 13-15 Smail Street
Ultimo Sydney New South Wales 2007
Australia
Tel +61 2 8960 7755
Fax +61 2 8960 7745
Email sydney@bmtglobal.com

Perth
Level 4
20 Parkland Road
Osborne Park Western Australia 6017
PO Box 2305 Churchlands Western Australia 6018
Australia
Tel +61 8 6163 4900
Email wa@bmtglobal.com

London
1st Floor, International House
St Katharine's Way
London
E1W 1UN
Tel +44 (0) 20 8090 1566
Email london@bmtglobal.com

Aberdeen
Broadfold House
Broadfold Road, Bridge of Don
Aberdeen
AB23 8EE
UK
Tel: +44 (0) 1224 414 200
Fax: +44 (0) 1224 414 250
Email aberdeen@bmtglobal.com

Asia Pacific
Indonesia Office
Perkantoran Hijau Arkadia
Tower C, P Floor
Jl: T.B. Simatupang Kav.88
Jakarta, 12520
Indonesia
Tel: +62 21 782 7639
Fax: +62 21 782 7636
Email asiapacific@bmtglobal.com

Alexandria
4401 Ford Avenue, Suite 1000
Alexandria
VA 22302
USA
Tel: +1 703 920 7070
Fax: +1 703 920 7177
Email inquiries@dandp.com